

# SUPPORTING INFORMATION

## **Solution Structures of Highly Active Molecular Ir Water-Oxidation Catalysts from Density Functional Theory Combined with High-Energy X-Ray Scattering and EXAFS Spectroscopy**

Ke R. Yang,<sup>†</sup> Adam J. Matula,<sup>†</sup> Gihan Kwon,<sup>‡</sup> Jiyun Hong,<sup>§</sup> Stafford W. Sheehan,<sup>†</sup> Julianne M. Thomsen,<sup>†</sup> Gary W. Brudvig,<sup>†</sup> Robert H. Crabtree,<sup>†</sup> David M. Tiede,<sup>‡</sup> Lin X. Chen,<sup>‡,§</sup> and Victor S. Batista\*,<sup>†</sup>

<sup>†</sup> Yale Energy Sciences Institute and Department of Chemistry, Yale University, New Haven, Connecticut 06520-8107, United States

<sup>‡</sup> Chemical Sciences and Engineering Division, Argonne National Laboratory, Argonne, Illinois 60439, United States

<sup>§</sup> Department of Chemistry, Northwestern University, 2145 Sheridan Road, Evanston, Illinois 60208-3113, United States

## **Contents**

<b>1. Experimental Details .....</b>	S-3
<b>1.1. Sample preparation .....</b>	S-3
<b>1.2. High-Energy X-ray Scattering (HEXS) and Data Analysis .....</b>	S-3
<b>1.3. Extended X-ray Absorption Fine Structure (EXAFS) and Data Analysis .....</b>	S-5
<b>2. Computational Details .....</b>	S-10
<b>3. Complexes Considered .....</b>	S-16
<b>3.1 Bi-dentate Binding of Acetate .....</b>	S-22
<b>3.2 Bi-dentate Binding of Macac .....</b>	S-34
<b>3.3 Bi-dentate Binding of Iodate .....</b>	S-45
<b>3.4 Mono-dentate and Bi-dentate Binding of Acetate .....</b>	S-53
<b>3.5 Bi-dentate Binding of Sulfate .....</b>	S-63
<b>3.6 Possible Degradation Pathways of Cp* .....</b>	S-68
<b>3.7 Ligand Bond Lengths in Ir<sup>III</sup> and Ir<sup>IV</sup> Complexes .....</b>	S-72
<b>3.8 Comparison of Experimental Derived and DFT Optimized Structural Parameters .....</b>	S-74
<b>4. Cartesian Coordinates .....</b>	S-77
<b>5. References .....</b>	S-113

## **1. Experimental Details**

### **1.1. Sample preparation**

All chemicals were purchased from major commercial suppliers and were used as received. Organic solvents were purified by passing over activated alumina with dry N<sub>2</sub>. 18 MΩ • cm water was supplied by a Milli-Q purification system. Syntheses reported below were performed using Schlenk techniques under argon, and analyses were performed in air. NaIO<sub>4</sub> was purchased from Acros Organics and used as received. Synthesis of the precatalyst **1** [Cp\*Ir(pyalc)OH] was performed using a published procedures.<sup>1</sup>

**Preparation of 2.** Samples for chemically activated Ir blue solution were prepared by adding the precatalyst **1**, [Cp\*Ir(pyalc)OH], to a final concentration of 20 mM in a solution containing 0.4 M NaIO<sub>4</sub>. The reaction mixture was transferred to 1.5 mm ID thin-walled glass capillaries (Charles Supper Company), and measured within 2-6 hours of mixing.

**Preparation of 3.** Samples for electrochemically activated Ir blue solution were prepared by adding the precatalyst **1**, [Cp\*Ir(pyalc)OH], to a final concentration of 2.6 mM in a solution containing 0.25 M Na<sub>2</sub>SO<sub>4</sub>. The mixture was bulky electrolyzed for 36 hours with an applied potential of 1.45 V at pH = 2.4.

### **1.2. High-Energy X-ray Scattering (HEXS) and Data Analysis**

High-energy X-ray (58.66 keV,  $\lambda = 0.2114 \text{ \AA}$ ) scattering patterns for the active blue solution samples, capillaries, and backgrounds, were measured as a function of the scattered wave vector  $q$ , where  $q = 4\pi \sin \theta / \lambda$  and  $2\theta$  is the scattered angle, in the  $q$  range  $0.4 \text{ \AA}^{-1} < q < 24 \text{ \AA}^{-1}$  at the Advanced Photon Source (APS) of Argonne National

Laboratory at the beamline 11-ID-B.<sup>2-4</sup> The experimental HEXS patterns were used to generate the pair distribution function,  $G(r)$  using the program *PDFgetX2*.<sup>5</sup> In this procedure, the experimental scattering patterns were corrected for solvent, container, and instrument background scatterings, X-ray polarization, sample absorption, and Compton scattering to yield the total scattering for the solute,  $I(q)$ . The reduced scattering structure function  $F(q)$  was calculated from  $I(q)$  according to

$$F(q) = \left[ \frac{I(q)}{f(q)^2} - 1 \right] \quad (\text{S1})$$

where  $f(q)$  is the sum of the composite atomic form factors,  $f(q) = \sum_i^N f_i(q)$ . The real space pair distribution function,  $G(r)$ , was obtained by direct Fourier transform of the oscillatory  $F(q)$ :

$$G(r) = \frac{2}{\pi} \int_0^{q_{\max}} F(q) \sin(qr) dq \quad (\text{S2})$$

with  $F(q)$  extrapolated to  $F(0)$  below the experimental  $q$  range  $< 0.4 \text{ \AA}^{-1}$  and using  $q_{\max} = 24 \text{ \AA}^{-1}$  and a Lorch dampening function to remove truncation effects.<sup>5</sup>  $G(r)$  is related to the real space electron density distribution function according to:

$$G(r) = 4\pi[\rho(r) - \rho_0] \quad (\text{S3})$$

where  $\rho(r)$  is the spherical average of the real space electron density distribution function,  $\rho(\mathbf{r})$ , and  $\rho_0$  is the average electron density of the sample.<sup>5-8</sup>  $G(r)$  can be expressed in terms of the radial distribution function,  $J(r) = 4\pi r^2 \rho(r)$ ,<sup>9,10</sup>

$$G(r) = (1/r)[J(r) - 4\pi r^2 \rho_0] \quad (\text{S4})$$

The pair distribution function (PDF) obtained from the high-energy X-ray scattering experimental of the chemically activated Ir blue solution is shown in Figure S1. We are

able to fit it with a mono- $\mu$ -oxo Ir dimer and can tentatively assign the four peaks at 2.06, 2.84, 3.40, and 4.47 Å to Ir–N/O (first-coordination shell), Ir–C, Ir–Ir, and Ir–C/N/O distances.

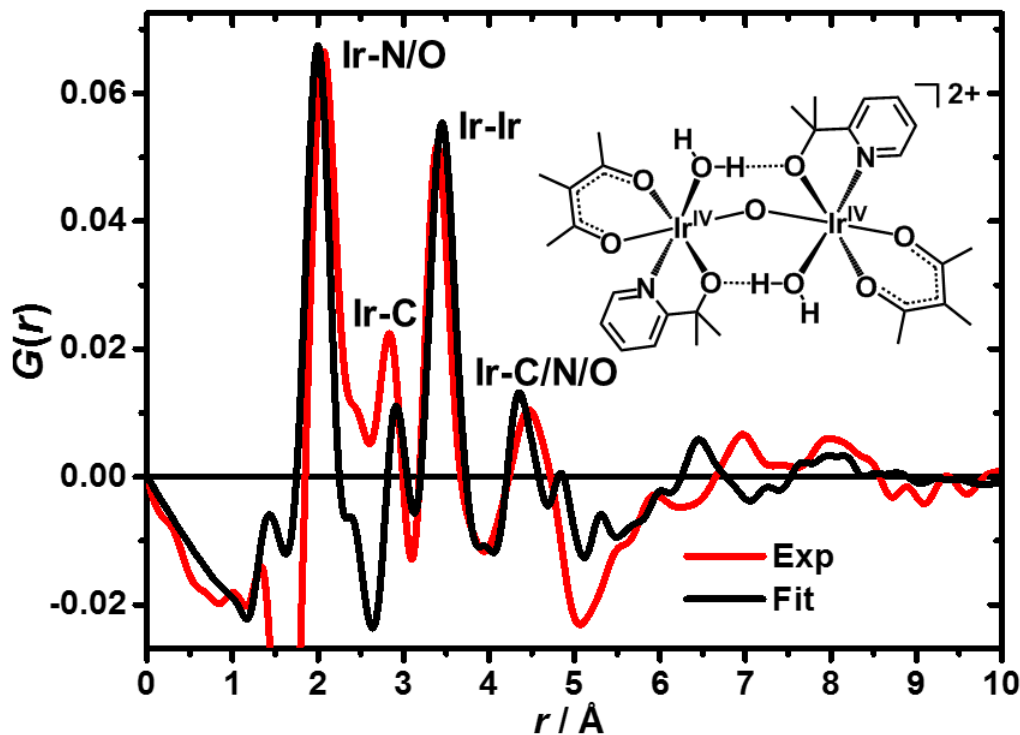


Figure S1. Experimental pair distribution function  $G(r)$  of chemically activated Ir blue solution and Fit  $G(r)$  with a mono- $\mu$ -oxo Ir dimer.

### 1.3. Extended X-ray Absorption Fine Structure (EXAFS) and Data Analysis

X-ray absorption spectroscopy (XANES and EXAFS) measurements at Ir L<sub>III</sub>-edge (11.215 keV) were carried out at Beamline 12BM of the Advanced Photon Source at Argonne National Laboratory. The Si (111) crystals were used for the X-ray monochromator, giving  $10^4$  energy resolution and  $\sim 2 \times 10^{11}$  photons was at the sample. The focused beam size was 0.5 mm (vertical)  $\times$  1 mm (horizontal). The powder samples

were grinded and sandwiched between two Kepton tapes, and the solution samples were placed in home-made liquid cell with about  $40\text{-}\mu\text{L}$  volume. The X-ray fluorescence signals were collected by a 13-element solid-state germanium array detector (Canberra) with the detection energy window set for the total fluorescence from Ir. Data analysis program ATHENA, ARTEMIS, HEPHAESTUS and IFEFFIT<sup>11</sup> were used to process the experimental EXAFS data of Ir complexes.

The experimental EXAFS spectra of precursor, chemically and electrochemically activated Ir blue solutions are shown in Figure S2-S4 (in both  $k$  space and reduced distance space). We use shell-model to extract structural parameters by fitting experimental EXAFS spectra with Artemis program.<sup>11</sup> The fitted EXAFS spectra are also shown in Figure S2-S4. The structural parameters extracted from the fits of experimental EXAFS spectra are listed in Table S1-S3.

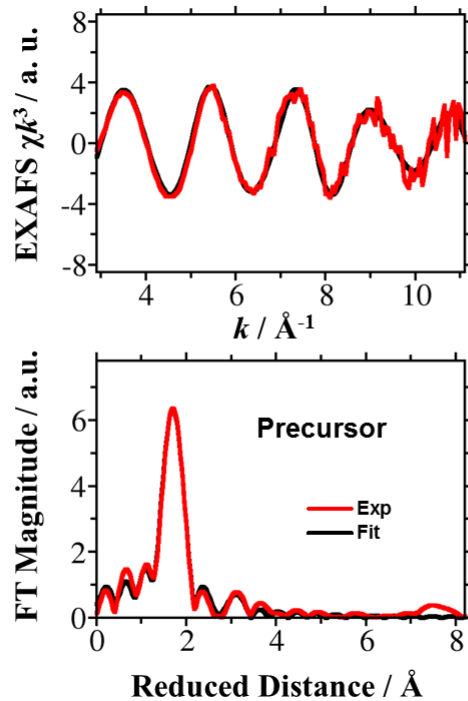


Figure S2. Experimental EXAFS spectra of precursor 1 and fitted EXAFS spectra in  $k$  space (top) and reduced distance  $R$  space (bottom).

Table S1. Structural Parameters Obtained from the Fit of the EXAFS Spectrum of Precursor 1<sup>a</sup>

Scattering Path	EXAFS		
	CN <sup>b</sup>	$R$ ( $\text{\AA}$ )	$\sigma^2$ ( $\text{\AA}^2$ )
Ir–O	2	2.01	0.007
Ir–N	1	2.05	0.007
Ir–C <sub>A</sub>	5	2.15	0.002
Ir–C <sub>B</sub>	2	2.93	0.009
Ir–C <sub>C</sub>	5	3.29	0.009

<sup>a</sup> Goodness of fit value,  $\mathcal{R}=0.001$ ; Fit parameters:  $\Delta k = 3.0\text{--}10.3 \text{\AA}^{-1}$ ,  $dk = 0.2 \text{\AA}^{-1}$ ,  $\Delta R = 1.25\text{--}3.40 \text{\AA}$ ,  $\Delta E_0 = 5.83 \text{ eV}$ ,  $S_0^2 = 0.60$ .

<sup>b</sup> CN is the coordination number.

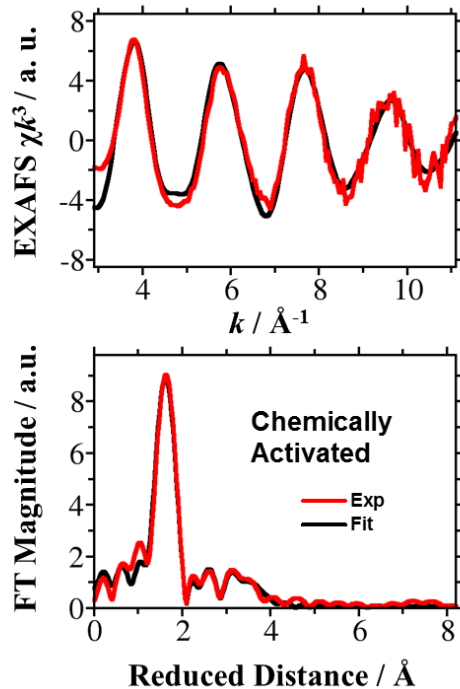


Figure S3. Experimental EXAFS spectra of chemically activated Ir blue solution and fitted EXAFS spectra in  $k$  space (top) and reduced distance  $R$  space (bottom).

Table S2. Structural Parameters Obtained from the Fit of the EXAFS Spectrum of Chemically Activated Ir Blue Solution<sup>a</sup>

Scattering Path	EXAFS		
	CN <sup>b</sup>	$R$ (Å)	$\sigma^2$ (Å <sup>2</sup> )
Ir–O/N	6	2.00	0.006
Ir–C <sub>A</sub>	2	2.93	0.002
Ir–C <sub>B</sub>	4	3.11	0.009
Ir–Ir	1	3.36	0.005

<sup>a</sup> Goodness of fit value,  $\mathcal{R}=0.004$ ; Fit parameters:  $\Delta k = 3.4\text{--}10.9 \text{ \AA}^{-1}$ ,  $dk = 0.2 \text{ \AA}^{-1}$ ,  $\Delta R = 1.12\text{--}4.0 \text{ \AA}$ ,  $\Delta E_0 = 14.39 \text{ eV}$ ,  $S_0^2 = 0.77$ .

<sup>b</sup> CN is the coordination number.

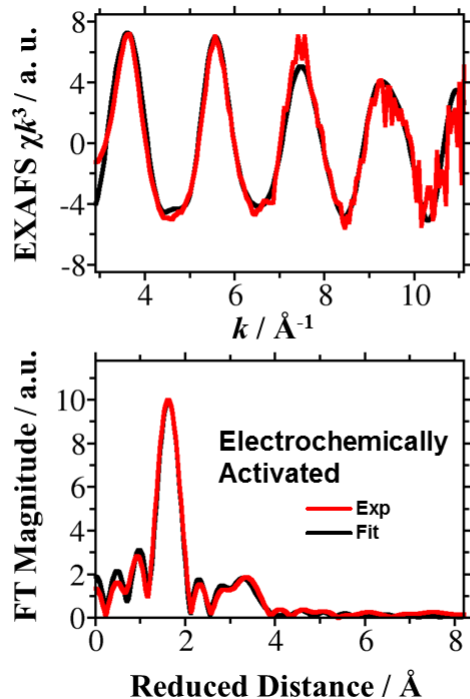


Figure S4. Experimental EXAFS spectra of electrochemically activated Ir blue solution and fitted EXAFS spectra in  $k$  space (top) and reduced distance  $R$  space (bottom).

Table S3. Parameters Obtained from the Fit of the EXAFS Spectrum of Electrochemically Activated Ir Blue Solution<sup>a</sup>

Scattering Path	EXAFS		
	CN <sup>b</sup>	$R$ (Å)	$\sigma^2$ (Å <sup>2</sup> )
Ir–O/N	6	2.04	0.004
Ir–C <sub>A</sub>	2	2.81	0.009
Ir–C <sub>B</sub>	3	2.97	0.006
Ir–Ir	1	3.56	0.002

<sup>a</sup> Goodness of fit value,  $\mathcal{R} = 0.005$ ; Fit parameters:  $\Delta k = 3.1\text{--}9.9 \text{ \AA}^{-1}$ ,  $dk = 0.2 \text{ \AA}^{-1}$ ,  $\Delta R = 1.2\text{--}4.0 \text{ \AA}$ ,  $\Delta E_0 = 10.64 \text{ eV}$ ,  $S_0^2 = 0.90$ .

<sup>b</sup> CN is the coordination number (CN).

## 2. Computational Details

**DFT optimization:** All structures were optimized using the B3LYP functional<sup>12</sup> with a mixed basis set (6-31G for C and H atoms,<sup>13</sup> 6-31G(d) for N, O and S atoms,<sup>13,14</sup> the Stuttgart ECP60MWB pseudopotential and [8s7p6d2f|6s5p3d2f] contracted basis set for Ir atoms,<sup>15,16</sup> and the LanL2DZ pseudopotential and basis set<sup>17</sup> augmented with diffuse s and p functions (exponents 0.0569 and 0.0330, respectively) and d and f polarization functions (exponents 0.292 and 0.441, respectively) (denoted LanL2DZspdf + ECP)<sup>18</sup> for I atoms. A pruned (99, 590) grid (called Ultrafine in Gaussian) was used for the numerical integration. Solvent effect was considered with polarized continuum model (PCM).<sup>19</sup> Default cavity, with UFF Coulomb radii scaled by 1.1, was used in all PCM calculations. The dispersion effects were considered with Grimme's D2 correction.<sup>20</sup> The ground states of Ir(IV) dimers were obtained with broken-symmetry approach, in which the  $\alpha$  and  $\beta$  electronic densities are localized on different metal centers with antiferromagnetic coupling.<sup>21</sup> Frequency analysis was performed to confirm the structures we optimized are indeed minimum with all real frequencies.

**TDDFT calculation:** The  $\omega$ B97X-D functional<sup>22</sup> was used for the time-dependent density functional theory (TD-DFT)<sup>23</sup> calculations with 6-31+G(d) for O atoms,<sup>13,14,24</sup> 6-31G(d) for C, H, N atoms,<sup>13,14</sup> and the Stuttgart ECP60MWB pseudopotential and [8s7p6d2f|6s5p3d2f] contracted basis set for Ir atoms.<sup>15,16</sup> The PCM solvent model was used to take account of the solvation effect.

**Pair Distribution Function  $G(r)$  calculation:** The approach for model calculation to simulate the HEXS spectrum has been described in detail previously.<sup>3</sup> The pair

distribution function,  $G(r)$ , was calculated with the DFT optimized model structures using Eq. S2 and  $F(q) = q[S(q) - 1]$ .  $S(q)$  is calculated from:

$$S(q) = \frac{I^{\text{coh}}(q)}{\sum c_i f_i(q)^2}, \quad (\text{S5})$$

where  $I^{\text{coh}}(q)$ , the reduced total coherent scattering, was calculated from the Debye equation:<sup>25</sup>

$$I^{\text{coh}}(q) = \sum_j^N \sum_k^N A_j(q) A_k(q) \frac{\sin(qr_{jk})}{r_{jk}} \quad (\text{S6})$$

In Eq. S6,  $A_i(q)$  are the atomic scattering amplitudes derived from the atomic structure factors that were obtained by fitting atom scattering data in the International Tables<sup>26</sup> for Crystallography to a function  $f_i$ , composed of five Gaussian components:<sup>27,28</sup>

$$A_i(q) = f_i(q) e^{-b_i q^2 / 16\pi^2} - g_i(q) \quad (\text{S7})$$

The atomic solvent excluded volume form factor,  $g_i(q)$ , was used to account for the scattering contribution due to solvent displacement and represented by a Gaussian form function. Eq. S7 also includes the atom-pair disorder factor,  $b_i$ , which is equivalent to the crystallographic Debye-Waller  $B$ -factor,  $B = 8\pi^2 \langle u^2 \rangle$ , where  $\langle u^2 \rangle$  is the average mean-squared atomic displacement, but written here in terms of the variable  $q$  rather than  $\sin \Theta / \lambda$ . In our  $G(r)$  calculations, a mean isotropic displacement  $\langle u^2 \rangle$  of 0.013 Å<sup>2</sup> (crystallographic  $B$ -factor = 1) was used for the two Ir atoms.

**EXAFS simulation:** The classical EXAFS equation is shown below

$$\chi(k) = \sum_j^{\text{paths}} N_j S_0^2 \frac{|f(k)|}{kR_j^2} \sin(2kR_j + 2\delta_c + \phi) e^{-2R_j / \lambda(k)} e^{-2\sigma^2 k^2}, \quad (\text{S8})$$

where  $j$  goes over all scattering paths,  $k$  is the momentum vector,  $2\delta_c + \phi$  is phase shift.

The structural parameters are the interatomic distances  $R_j$ , the coordination number (or number of equivalent scatterers)  $N_j$ , and the temperature-dependent root-mean-square (rms) fluctuation in bond length  $\sigma$ , which also includes effects due to structural disorder.

In addition,  $f(k) = |f^{\text{eff}}(k)|e^{i\phi(k)}$  is the backscattering amplitude,  $\delta_c$  is central-atom partial-wave phase shift of the final state, and  $\lambda(k)$  is the energy-dependent XAFS mean free path.  $S_0^2$  is the overall amplitude factor.

Isotropic Ir L<sub>3</sub>-edge EXAFS spectra of considered complexes were calculated using the ab initio real space Green function approach as implemented in the FEFF program (version 8.30).<sup>29</sup> The experimental EXAFS data  $\chi(E)$ , that is the fractional change in absorption coefficient of Ir atoms induced by neighboring atoms, are converted into

momentum ( $k$ ) space using the transformation  $k = \left[ \frac{2m_e}{(h/2\pi)^2} (E - E_0) \right]^{1/2}$ , where  $m_e$  is

the mass of the electron and  $h$  is the Planck's constant. The calculated EXAFS data are obtained by fitting the energy of the absorption edge ( $E_0$ ) and the reduced factor ( $S_0^2$ ) against the experimental results, using the IFEFFIT code.<sup>30</sup>

A global Debye-Waller factors (DWF)  $\sigma^2 = 0.002 \text{ \AA}^2$  were used in the screening of complexes. All calculations using Feff 8.30 were performed using the following parameters: NLEG 8, and CRITERIA 4.0 3.5. A fractional cosine-square (Hanning) window with  $\Delta k = 1$  was applied to the experimental and calculated EXAFS data. A grid of  $k$  points equally spaced at  $0.05 \text{ \AA}^{-1}$  was used for the Fourier transformation (FT) of in

the  $k$  range of 3.0-10.3 Å<sup>-1</sup> for catalytic precursor, 3.3-10.9 Å<sup>-1</sup> for chemically activated Ir blue species and 3.1-9.9 Å<sup>-1</sup> for the electrochemically activated Ir blue species.

For the final EXAFS simulation, different Debye-Waller factors (DWF)  $\sigma^2$  were used to different scattering paths. The paths we considered are shown in Scheme S1, including the first coordination shell, multiple scattering in the first coordination shell, second coordination shell, and multiple scattering in the second coordination. The final fitting parameters were given in Table S4.

Table S4. Debye-Waller factors ( $\sigma^2$ , in Å<sup>2</sup>) of Various Scattering Paths Used to Calculate the EXAFS Spectra of Complexes **2** and **3**<sup>a</sup>

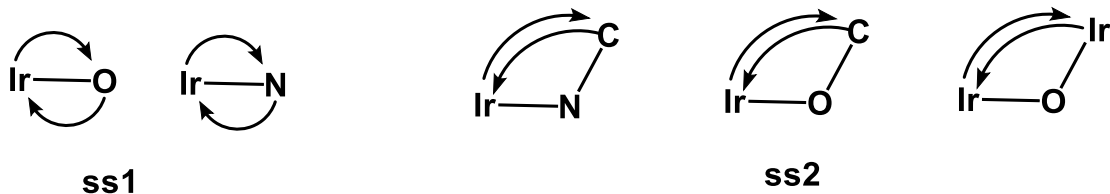
paths	Chemically	Electrochemically
ss1	0.002	0.001
ss2	0.020	0.020
1A	0.010	0.010
1B	0.010	0.006
1C	0.010	0.006
1D	0.010	0.020
2A	0.020	0.025
2B	0.020	0.025

<sup>a</sup> More parameters in the fitting of EXAFS spectra: 1. complex **2**,  $\Delta k = 3.0\text{-}12.0 \text{ Å}^{-1}$ ,  $\Delta R = 0.0\text{-}5.0 \text{ Å}$ ,  $\Delta E_0 = 20.63 \text{ eV}$ ,  $S_0^2 = 0.78$ ; 2. complex **3**,  $\Delta k = 3.0\text{-}11.0 \text{ Å}^{-1}$ ,  $\Delta R = 0.0\text{-}5.0 \text{ Å}$ ,  $\Delta E_0 = 16.58 \text{ eV}$ ,  $S_0^2 = 1.17$ .

**Scheme S1. Main scattering paths contributing to the EXAFS spectra: first and second coordination shell single and multiple scattering.**

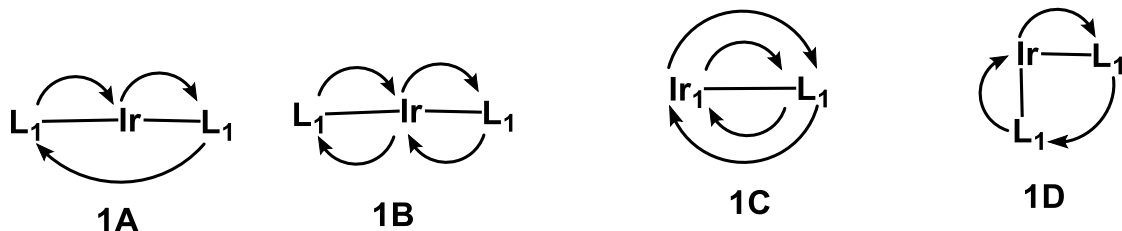
**Scattering Paths:**

**Single Scattering**

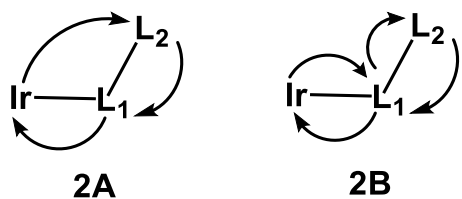


**Multiple Scattering**

$L_1 = N$  or  $O$  in the first coordination shell



$L_2 = C$  or  $Ir$  in the second coordination shell



### 3. Complexes Considered

The catalytic precursor  $[\text{Ir}(\text{OH})(\text{pyalc})(\text{Cp}^*)]$  (pyalc = 2-(2'pyridyl)-2-propanolate),  $\text{Cp}^*$  = pentamethyl-cyclopentadienyl, **1**) can be activated either chemically<sup>31</sup> or electrochemically<sup>32</sup> to yield active catalysts for water oxidation. The calculated and experimental EXAFS spectra of the precursor **1** agree well, as shown in Figure S5. In this section, we presented all complexes we considered as candidates for chemically and electrochemically activated Ir blue species.

For the chemically activated Ir blue species,<sup>31</sup> the  $^1\text{H}$  NMR indicated the pyalc chelating ligand was retained. Analysis of transmission electron microscopy-energy-dispersive X-ray spectroscopy (TEM-EDX) as well as X-ray photoelectron spectroscopy (XPS) data indicated that the ratio of N to Ir in the chemically activated Ir blue solution was 1:1, providing strong evidence of the retention of the chelating ligand. Resonance Raman spectra suggested the presence of the  $\mu$ -O ligand in the species by chemically activation.  $^{17}\text{O}$  NMR suggested the ratio of terminal aqua and  $\mu$ -O ligands to be 2:1. Electrophoresis study suggested a well-defined cation present in the chemically activated Ir blue solution since the blue species moved toward the cathode uniformly.

Matrix-assisted laser desorption ionization time-of-flight mass spectrometry (MALDI-TOF MS) is not a direct measurement of the majority species in the catalytic solution. Under the reducing environment of the matrix, the  $\text{Ir}^{\text{IV}}$  would be reduced to  $\text{Ir}^{\text{III}}$ . Under such conditions, macac might be replaced as a ligand by solvent.<sup>33,34</sup> Based on this, we assigned three groups of peaks to  $[\text{Ir}_2(\text{pyalc})_2(\text{O})(\text{OH})]^+$ ,  $[\text{Ir}_2(\text{pyalc})_2(\text{O})(\text{AcO})]^+$ , and  $[\text{Ir}_2(\text{pyalc})_2(\text{O})(\text{CHC})]^+$  (Figure S6), where CHC =  $\alpha$ -cyano-4-hydroxycinnamate from the  $\alpha$ -cyano-4-hydroxycinnamic acid (CHCA) matrix. The MALDI-TOF MS(+) results

suggest an Ir–O–Ir core structure in the chemically activated Ir blue species, and are more consistent with a mono- $\mu$ -O Ir dimer than the original proposed bis- $\mu$ -O Ir dimer since the incorporation of the  $\text{AcO}^-$  and CHC by replacing of the liable aqua ligands is more feasible than replacing one of the  $\mu$ -O ligands.

The MALDI-TOF MS result indicated a dimer model for the active species in Ir blue solution with metal centers in Ir(III) and/or Ir(IV) oxidation states. Previous X-ray photoelectron spectroscopy (XPS) data<sup>31</sup> suggested iridium is exclusively in the Ir(IV) oxidation state, consistent with the blue color which is the characteristic color of Ir(IV) dimer.<sup>35</sup> The Ir<sup>III</sup>/Ir<sup>III</sup> dimer would be inconsistent with UV-Vis and XPS results. The Ir<sup>III</sup>/Ir<sup>IV</sup> mix-valent dimer would account for the blue color; however, it is inconsistent with XPS results. In addition, previous EPR study<sup>31</sup> suggested the ground state of the active species should be singlet since chemically activated Ir blue species is EPR-silent, in contrast to the doublet ground state of Ir<sup>III</sup>/Ir<sup>IV</sup> mix-valent dimer.

With these experimental results in mind, two different models could be deduced, namely, the mono- $\mu$ -O and bis- $\mu$ -O models. For the mono- $\mu$ -O model, two aqua ligands occupied two sites and left 4 sites to be coordinated by other ligands. In the chemically activated Ir blue solution,  $\text{IO}_3^-$ ,  $\text{AcO}^-$ , and 2-methyl-2-acetyl acetonate are possible ligands. There are three binding modes of those ligands, mono-dentate, bi-dentate chelating and bridging modes. However, mono-dentate binding of iodate, acetate, or macac would require 4 such ligands, resulting in a neutral Ir dimer, inconsistent with electrophoresis results. Thus, only bi-dentate binding modes of acetate, iodate, and macac need to be considered for the chemically activated Ir blue species. For bis- $\mu$ -O, the number of the terminal aqua ligands would be 4; thus, only  $[(\text{pyalc})(\text{H}_2\text{O})_2\text{Ir}^{\text{IV}}(\mu\text{-O})_2]$

$\text{Ir}^{\text{IV}}(\text{OH}_2)_2(\text{pyalc})]^{2+}$  is possible, which is exactly what originally proposed as the active species in chemically activated Ir blue solution.<sup>31</sup>

The bis- $\mu$ -O model  $[(\text{pyalc})(\text{H}_2\text{O})_2\text{Ir}^{\text{IV}}(\mu\text{-O})_2\text{Ir}^{\text{IV}}(\text{OH}_2)_2(\text{pyalc})]^{2+}$  is consistent with the  $^{17}\text{O}$  NMR, resonance Raman spectra, and electrophoresis. However, the calculated EXAFS spectra using the  $[(\text{pyalc})(\text{H}_2\text{O})_2\text{Ir}^{\text{IV}}(\mu\text{-O})_2\text{Ir}^{\text{IV}}(\text{OH}_2)_2(\text{pyalc})]^{2+}$  structure do not agree with the experimental ones (Figure S7). Also, the bis- $\mu$ -O model has an Ir–Ir distance of 3.2 Å, smaller than experimental observed peak at 3.4 Å (Figure S1). Our EXAFS and HEXS results suggest that  $[(\text{pyalc})(\text{H}_2\text{O})_2\text{Ir}^{\text{IV}}(\mu\text{-O})_2\text{Ir}^{\text{IV}}(\text{OH}_2)_2(\text{pyalc})]^{2+}$  is unlikely to be the active species in the chemically activated Ir blue solution.

In this section, we present all complexes we considered, with possible ligands,  $\text{AcO}^-$ ,  $\text{IO}_3^-$ , and 2-methyl-2-acetylacetone (macac) for the chemically activated Ir blue species and  $\text{AcO}^-$ , and  $\text{SO}_4^{2-}$  for the electrochemically activated Ir blue species. The bi-dentate binding of  $\text{AcO}^-$ , macac, and  $\text{IO}_3^-$  to  $\text{Ir}^{\text{IV}}$  centers as candidates for the chemically activated Ir blue species is discussed in sections 3.1, 3.2, and 3.3, respectively; the mono-dentate and bi-dentate binding of  $\text{AcO}^-$  and bi-dentate biding of  $\text{SO}_4^{2-}$  to Ir centers is discussed in sections 3.4 and 3.5. In section 3.6, possible pathways for the degradation of  $\text{Cp}^*$  under chemical and electrochemical activation are discussed. Discussion on ligand Bond Lengths in  $\text{Ir}^{\text{III}}$  and  $\text{Ir}^{\text{IV}}$  Complexes is included in section 3.7. Comparison of experimental derived and DFT optimized structural parameters is included in section 3.8.

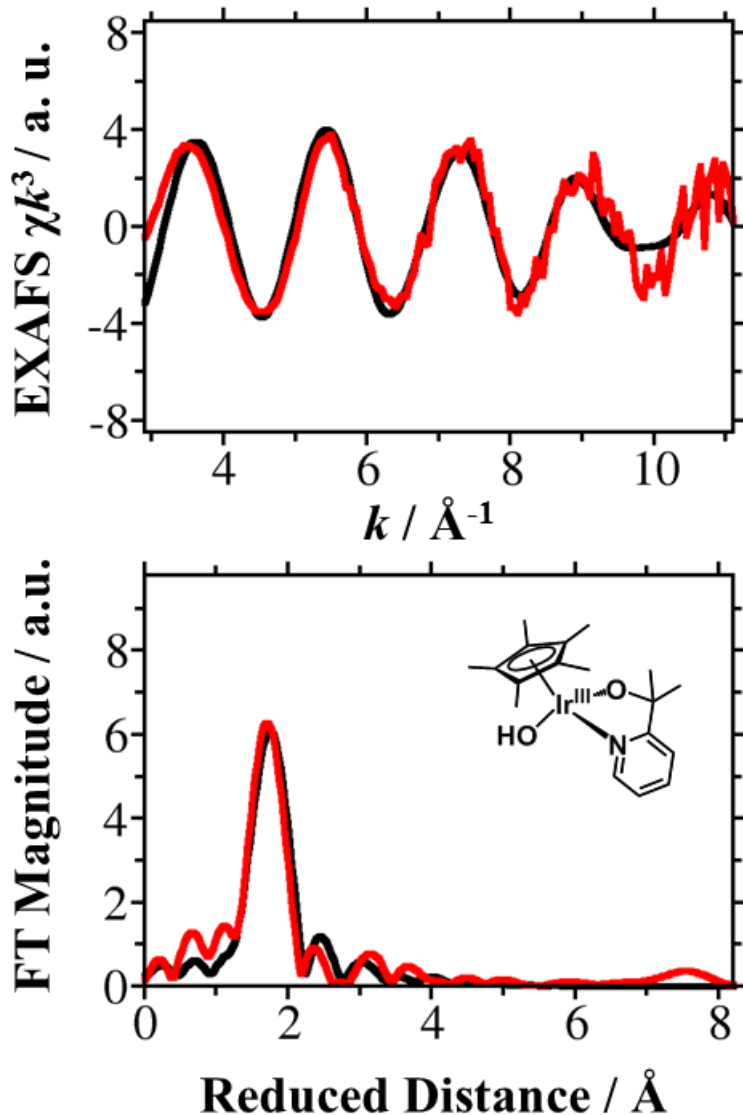


Figure S5. Simulated (black) and experimental (red) EXAFS spectra of catalyst precursor  $[\text{Ir}(\text{OH})(\text{pyalc})(\text{Cp}^*)]$  in  $k$  space (top) and reduced distance  $R$  space (bottom).

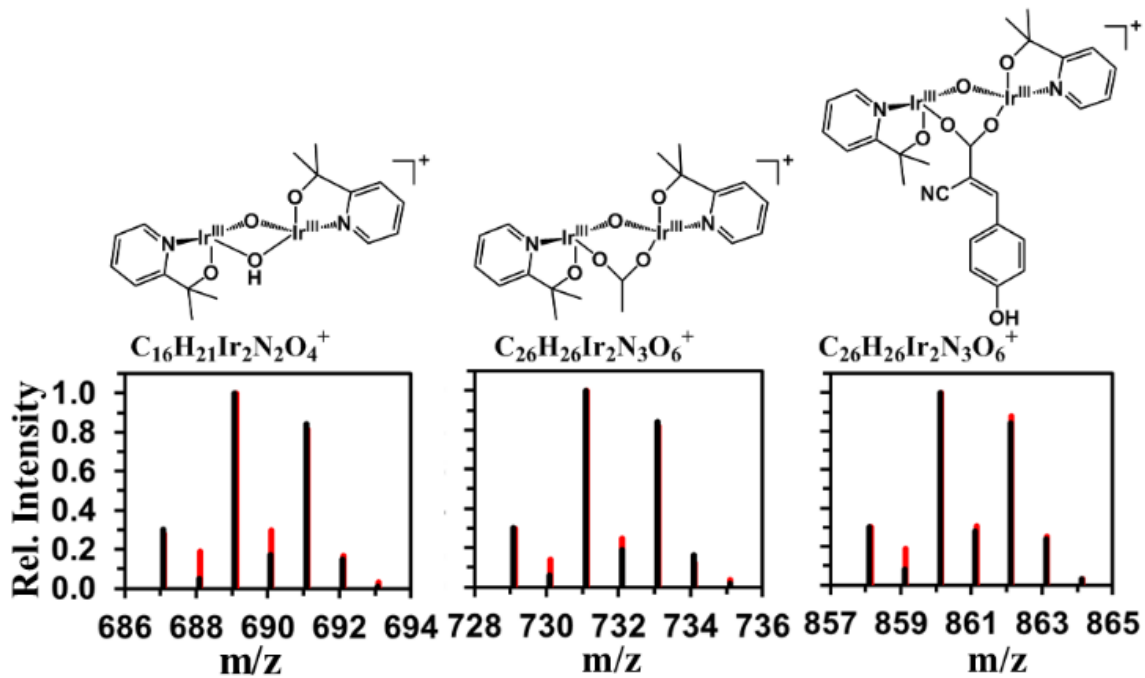


Figure S6. Assignment of the MALDI-TOF-MS(+) of chemically generated active blue species and the experimental (red) and simulated (black) isotope distribution. The experimental MALDI-TOF-MS(+) data are from ref. 31.

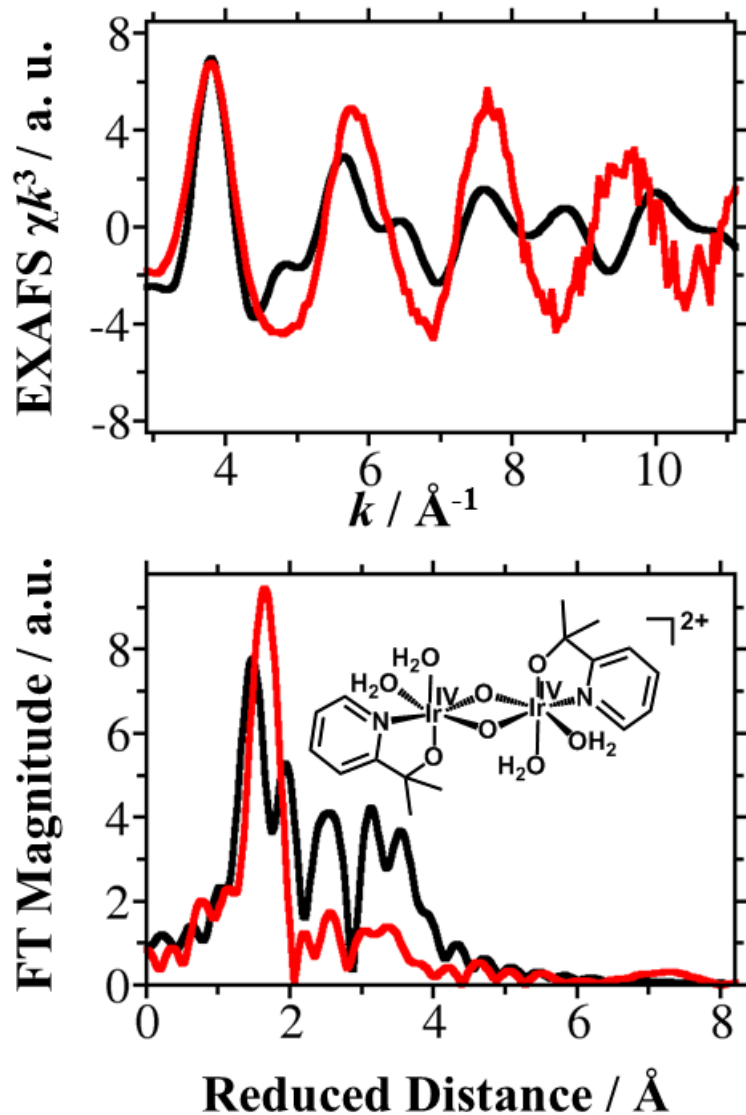


Figure S7. Simulated (black) EXAFS spectra of the originally proposed bis- $\mu$ -O structure ( $[(\text{pyalc})(\text{H}_2\text{O})_2\text{Ir}^{\text{IV}}(\mu\text{-O})_2\text{Ir}^{\text{IV}}(\text{OH}_2)_2(\text{pyalc})]^{2+}$ ) and experimental (red) EXAFS spectra of the chemically activated Ir blue species in  $k$  space (top) and reduced distance  $R$  space (bottom). The geometry of the bis- $\mu$ -O structure was taken from Ref. 31.

### **3.1 Bi-dentate Binding of Acetate**

There are two bi-dentate binding modes of acetate, namely chelating and bridging. For acetate with a chelating binding mode, 36 possible isomers were considered and their structures are shown in Scheme S2 and their relative energetics were shown in Table S5. The relative free energies suggest the isomer S5bb with hydrogen bonds between H atoms in the aqua ligands and O atoms in the pyalc ligands is the most stable isomer. For a bridging bi-dentate binding mode, four possible isomers were considered and their structures are shown in Scheme S3. Two of the bridging isomers, S10ab and S10ba, are mirror images. The three relative energies and free energies, as well as Ir–Ir distances of the bridging isomers (S10aa, S10ab, and S10bb) are presented in Table S6.

All three bridging isomers are more stable than the most stable chelating isomer S5bb indicating  $\text{AcO}^-$  prefers to bind to Ir centers through a bridging bi-dentate mode. The EXAFS and HEXS spectra of S5bb, S10aa, S10ab, and S10bb isomers were simulated and are shown in Figures S8-S15. None of the isomers yields EXAFS spectra that agree well with the experimental EXAFS spectra of the chemically activated Ir blue species. The simulated HEXS spectra of the mono- $\mu$ -O Ir dimers with  $\text{AcO}^-$  chelating show two intense peaks around 2.0 and 3.4 Å which is consistent with experimental HEXS spectrum (Figure S9), indicating the presence of a mono- $\mu$ -O Ir bridge.

**Scheme S2. Possible isomers of mono- $\mu$ -O Ir dimers with  $\text{AcO}^-$  chelating binding mode. (+2 charge of all complexes is omitted for clarity)**

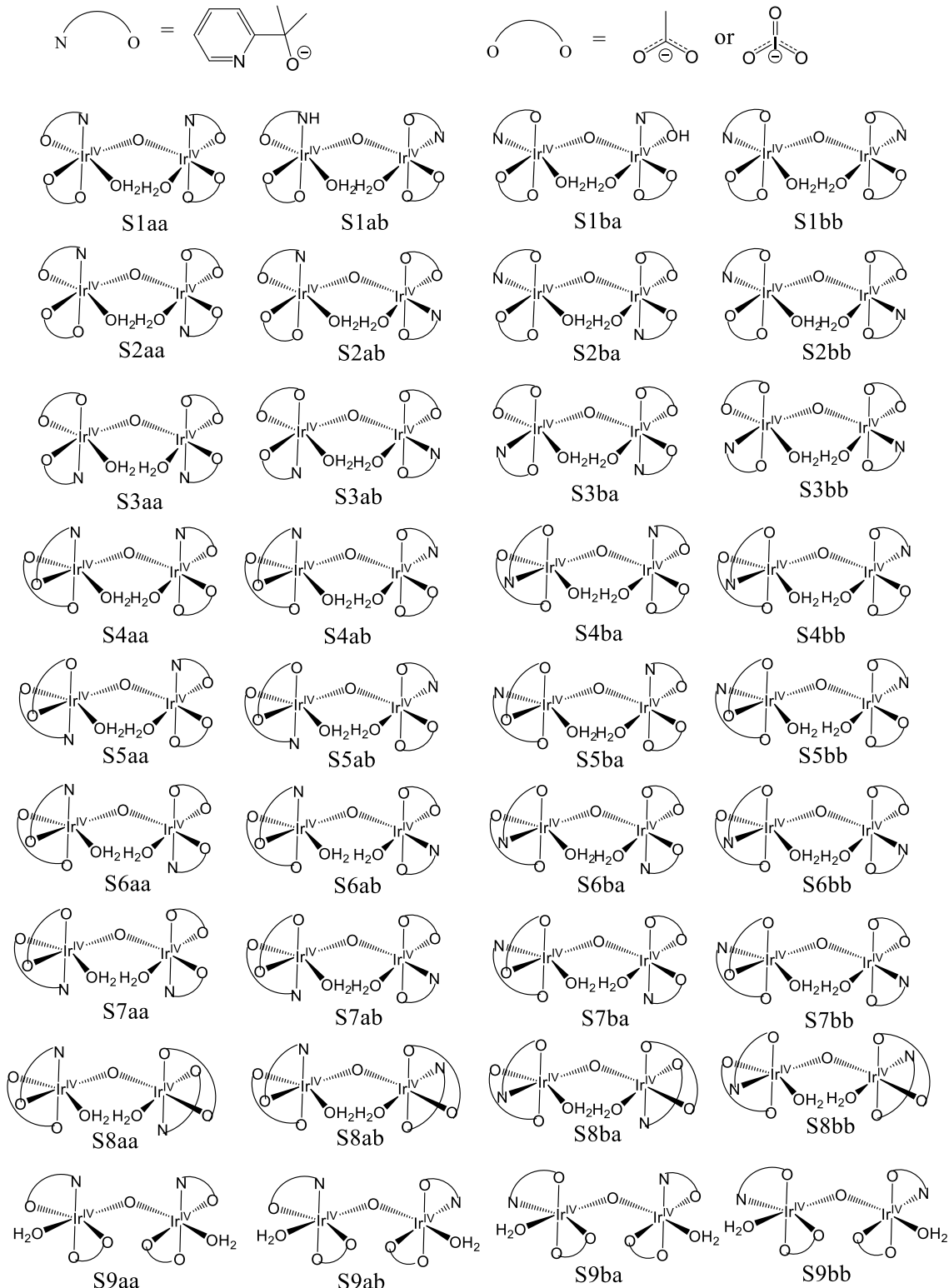
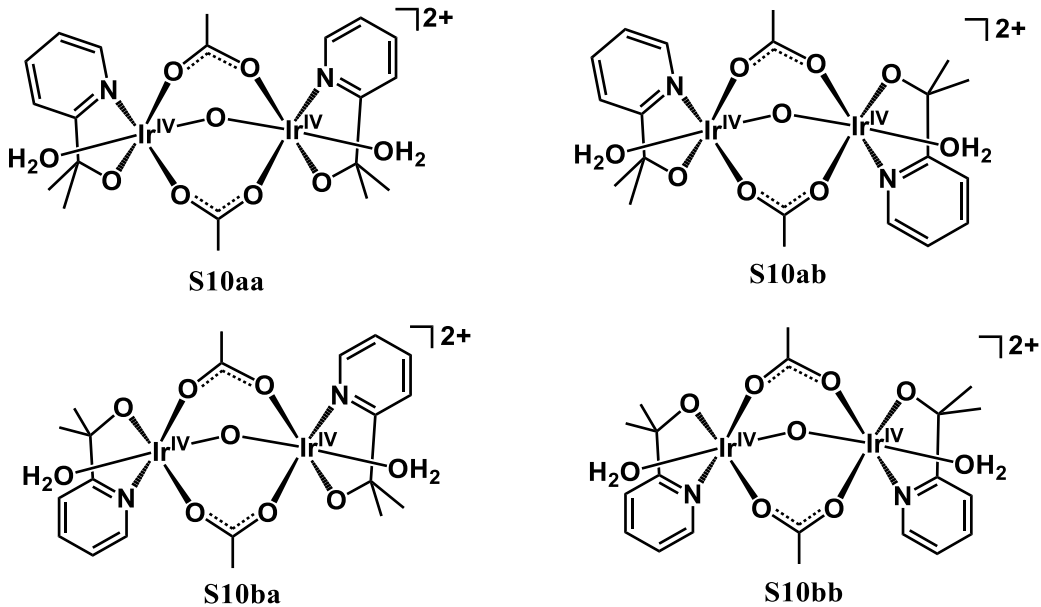


Table S5. Energetics and Ir–Ir Distances of Mono- $\mu$ -O Ir Dimers with  $\text{AcO}^-$  Chelating to Ir Centers.

	$\Delta E$ (kcal/mol)	$\Delta G$ (kcal/mol)	$d_{\text{Ir-Ir}}$ (Å)
S1aa	13.8	14.0	3.48
S1ab	9.8	8.9	3.38
S1ba	7.8	6.4	3.44
S1bb	5.0	3.9	3.43
S2aa	17.8	18.9	3.59
S2ab	25.6	27.9	3.58
S2ba	15.1	15.4	3.49
S2bb	12.3	10.8	3.46
S3aa	24.3	25.1	3.67
S3ab	30.0	30.2	3.57
S3ba	13.5	13.3	3.51
S3bb	18.5	17.9	3.54
S4aa	18.6	19.4	3.58
S4ab	17.6	18.0	3.50
S4ba	12.7	13.6	3.52
S4bb	8.4	9.0	3.44
S5aa	16.9	15.9	3.55
S5ab	11.7	10.6	3.52
S5ba	11.3	10.6	3.40
S5bb	<b>0.0</b>	<b>0.0</b>	<b>3.42</b>
S6aa	25.0	26.2	3.73
S6ab	18.0	16.8	3.57
S6ba	19.2	18.7	3.58
S6bb	14.9	16.0	3.53
S7aa	18.6	18.2	3.54
S7ab	15.5	15.8	3.52
S7ba	15.5	15.9	3.59
S7bb	11.3	9.9	3.47
S8aa	17.9	20.1	3.58
S8ab	15.1	15.4	3.49
S8ba	22.8	21.1	3.41
S8bb	11.3	11.8	3.45
S9aa	13.3	13.1	3.46
S9ab	10.6	10.4	3.40
S9bb	12.4	12.3	3.48

**Scheme S3. Possible isomers of mono- $\mu$ -O Ir dimers with  $\text{AcO}^-$  bridging to Ir centers.**



**Table S6. Energetics and Ir–Ir Distances of Mono- $\mu$ -O Ir Dimers with  $\text{AcO}^-$  Chelating and Bridging to Ir Centers.**

	$\Delta E$ (kcal/mol)	$\Delta G$ (kcal/mol)	$d_{\text{Ir-Ir}}$ (Å)
S5bb	<b>0.0</b>	<b>0.0</b>	<b>3.42</b>
S10aa	-8.9	-11.3	3.31
S10ab	-9.4	-11.0	3.29
S10bb	-8.8	-11.2	3.31

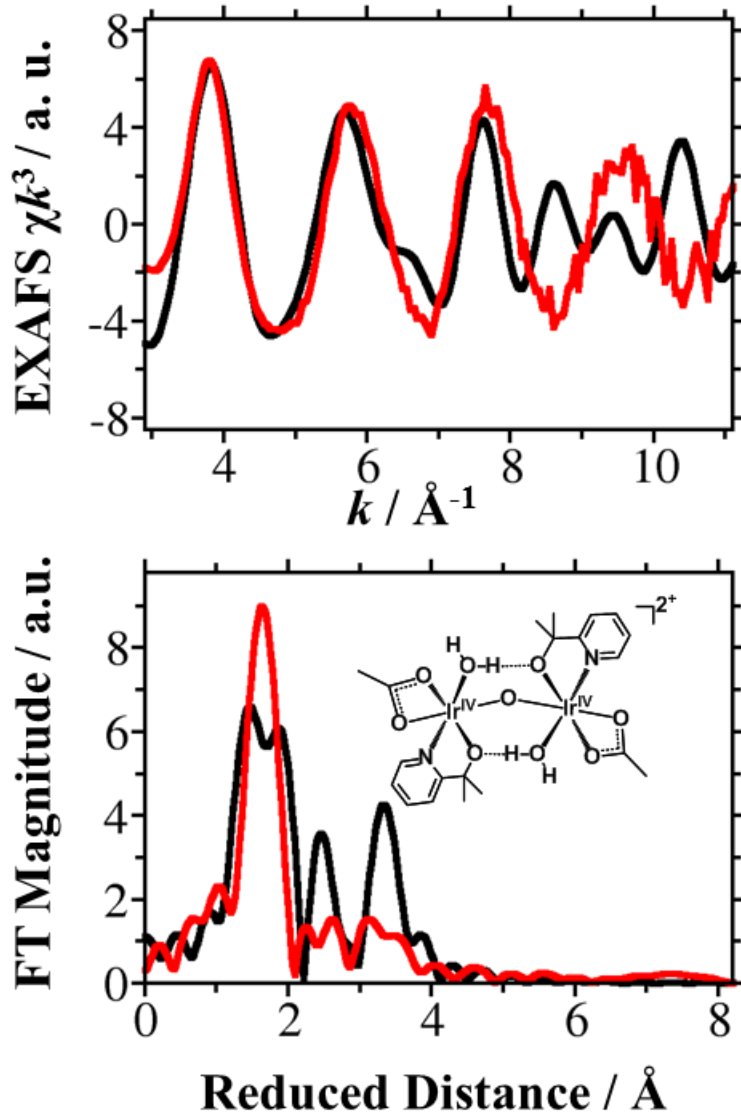


Figure S8. Simulated (black) EXAFS spectra of the most stable mono- $\mu$ -O Ir dimer with AcO<sup>-</sup> chelating to Ir centers (S5bb) and experimental (red) EXAFS spectra of the chemically activated Ir blue species in  $k$  space (top) and reduced distance  $R$  space (bottom).

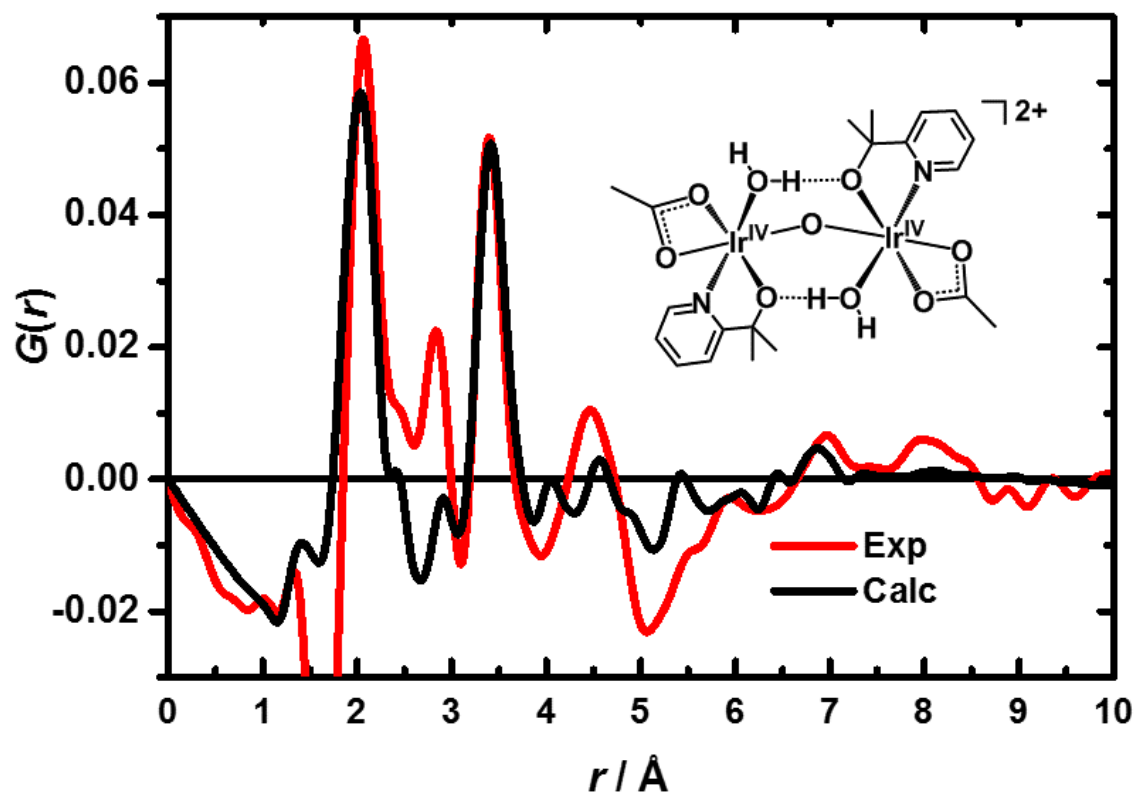


Figure S9. Calculated  $G(r)$  of the most stable mono- $\mu$ -O Ir dimer with  $\text{AcO}^-$  chelating to Ir centers (S5bb) and experimental  $G(r)$  of the chemically activated Ir blue species.

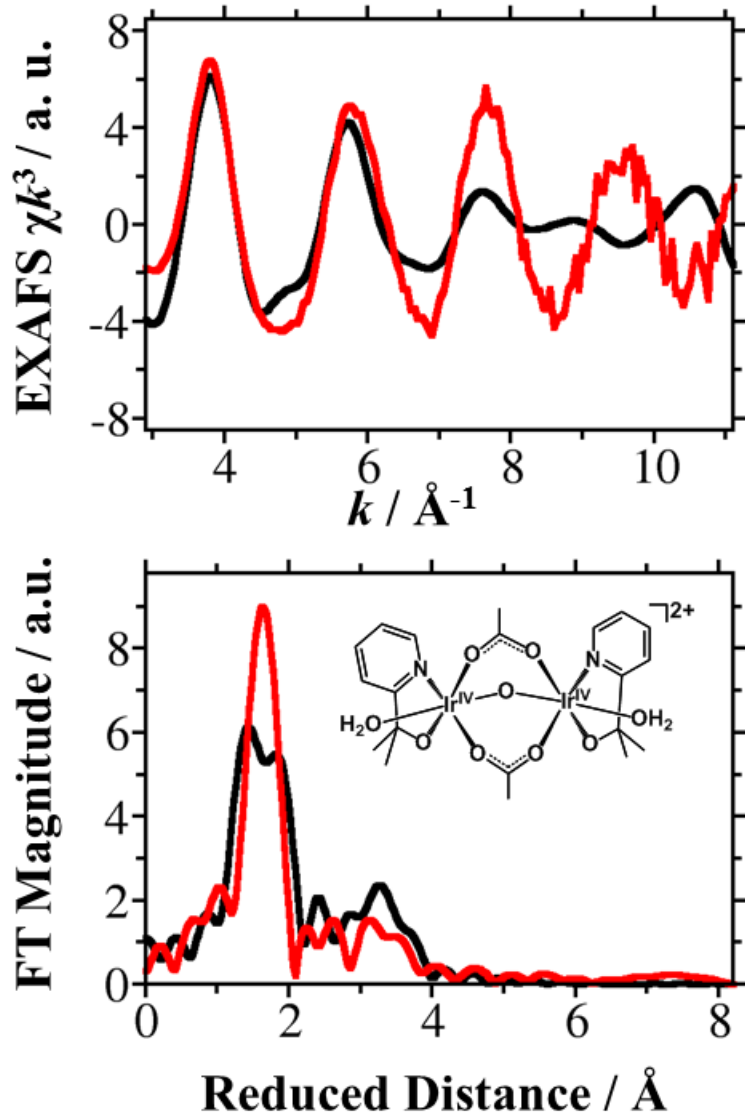


Figure S10. Simulated (black) EXAFS spectra of the mono- $\mu$ -O Ir dimer with  $\text{AcO}^-$  bridging to Ir centers (S10aa) and experimental (red) EXAFS spectra of the chemically activated Ir blue species in  $k$  space (top) and reduced distance  $R$  space (bottom).

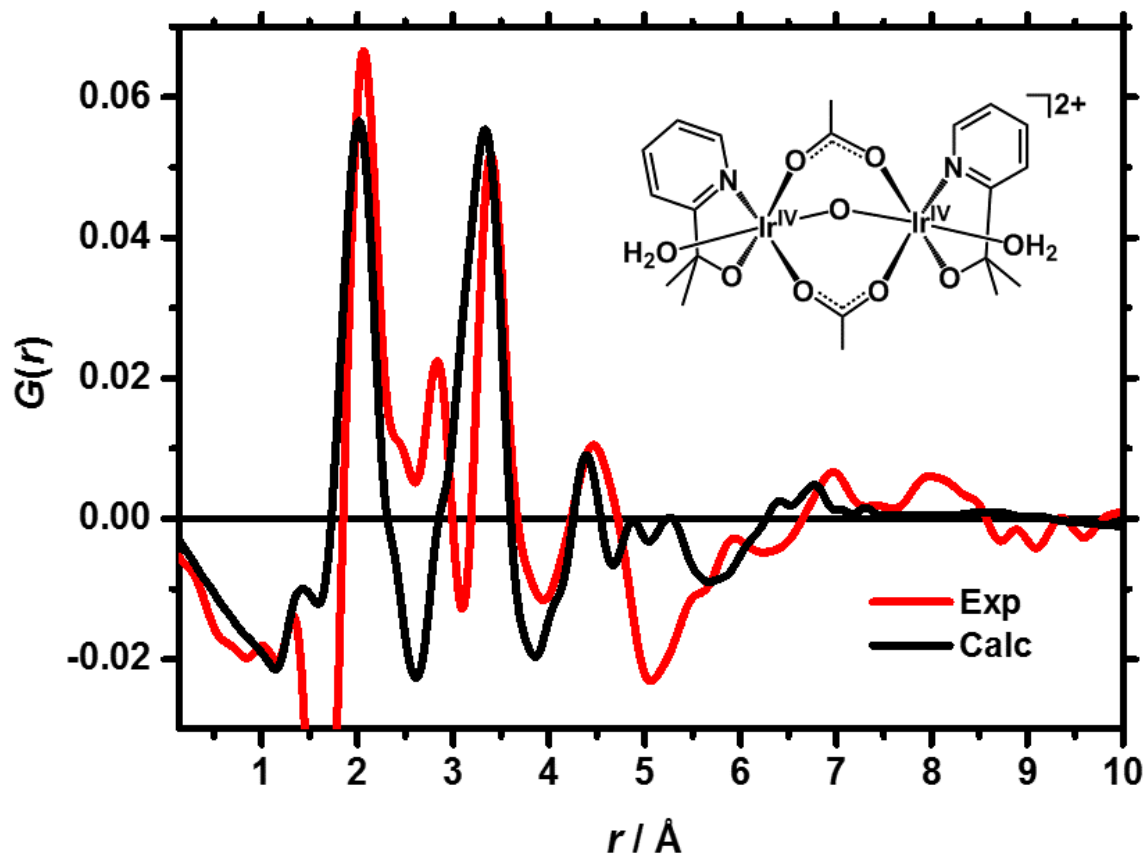


Figure S11. Calculated  $G(r)$  of the mono- $\mu$ -O Ir dimer with  $\text{AcO}^-$  bridging to Ir centers (S10aa) and experimental  $G(r)$  of the chemically activated Ir blue species.

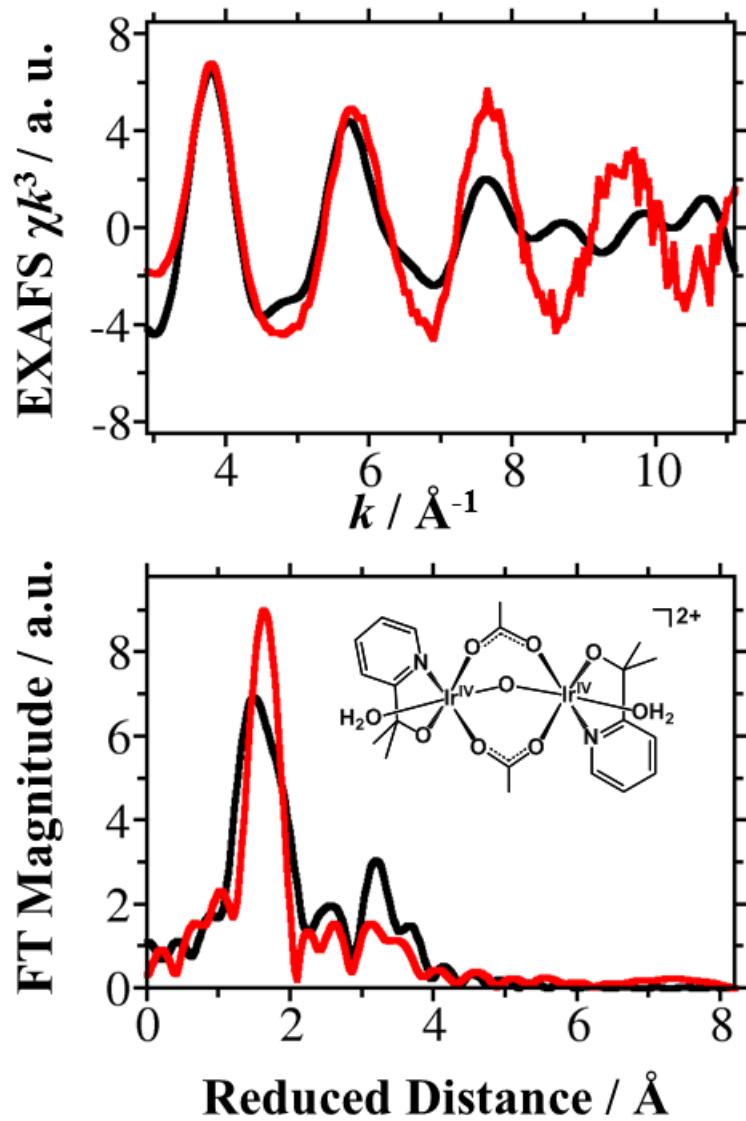


Figure S12. Simulated (black) EXAFS spectra of the mono- $\mu$ -O Ir dimer with AcO<sup>-</sup> bridging to Ir centers (S10ab) and experimental (red) EXAFS spectra of the chemically activated Ir blue species in  $k$  space (top) and reduced distance  $R$  space (bottom).

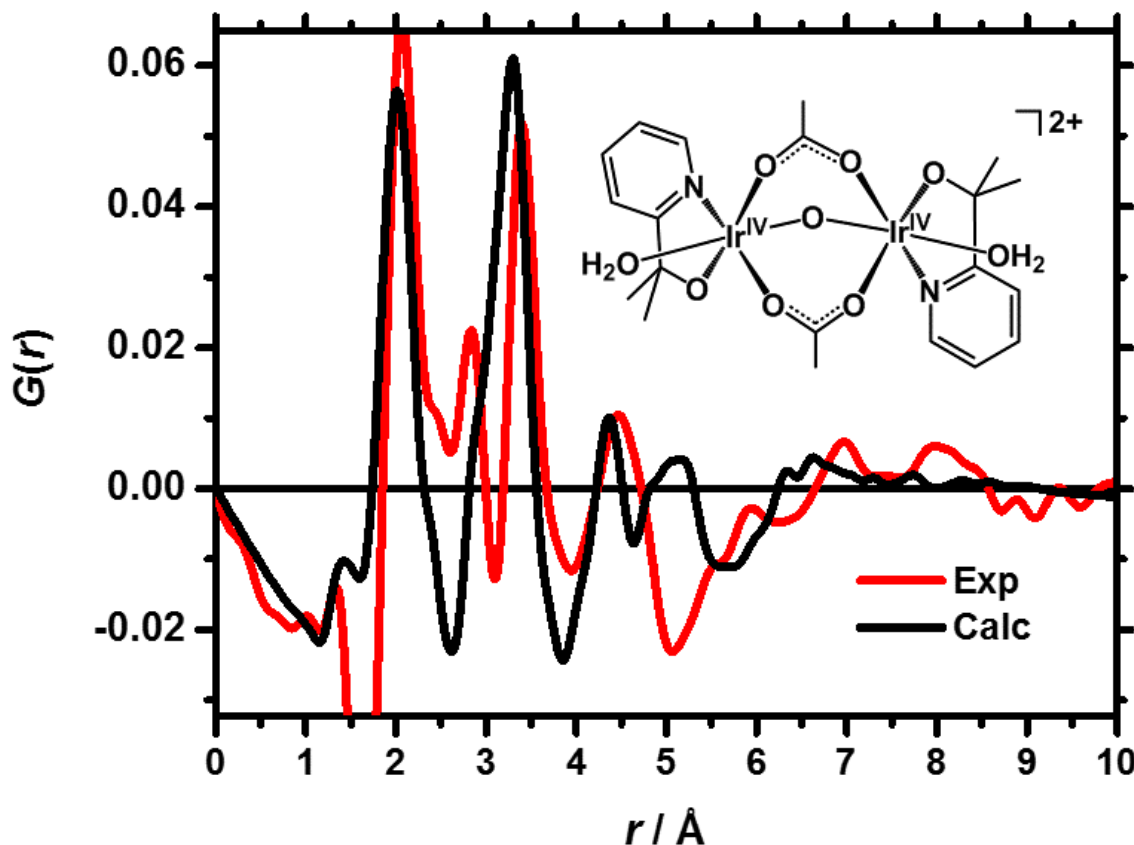


Figure S13. Calculated  $G(r)$  of the mono- $\mu$ -O Ir dimer with  $AcO^-$  bridging to Ir centers (S10ab) and experimental  $G(r)$  of the chemically activated Ir blue species.

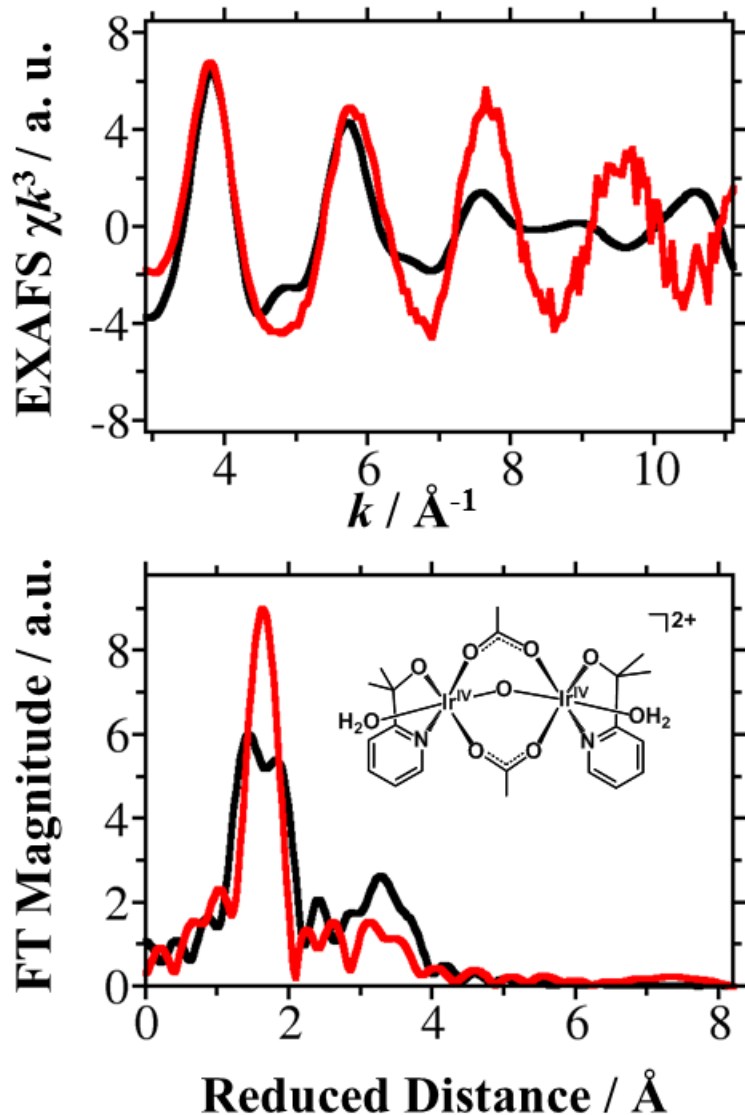


Figure S14. Simulated (black) EXAFS spectra of the mono- $\mu$ -O Ir dimer with  $\text{AcO}^-$  bridging to Ir centers (S10bb) and experimental (red) EXAFS spectra of the chemically activated Ir blue species in  $k$  space (top) and reduced distance  $R$  space (bottom).

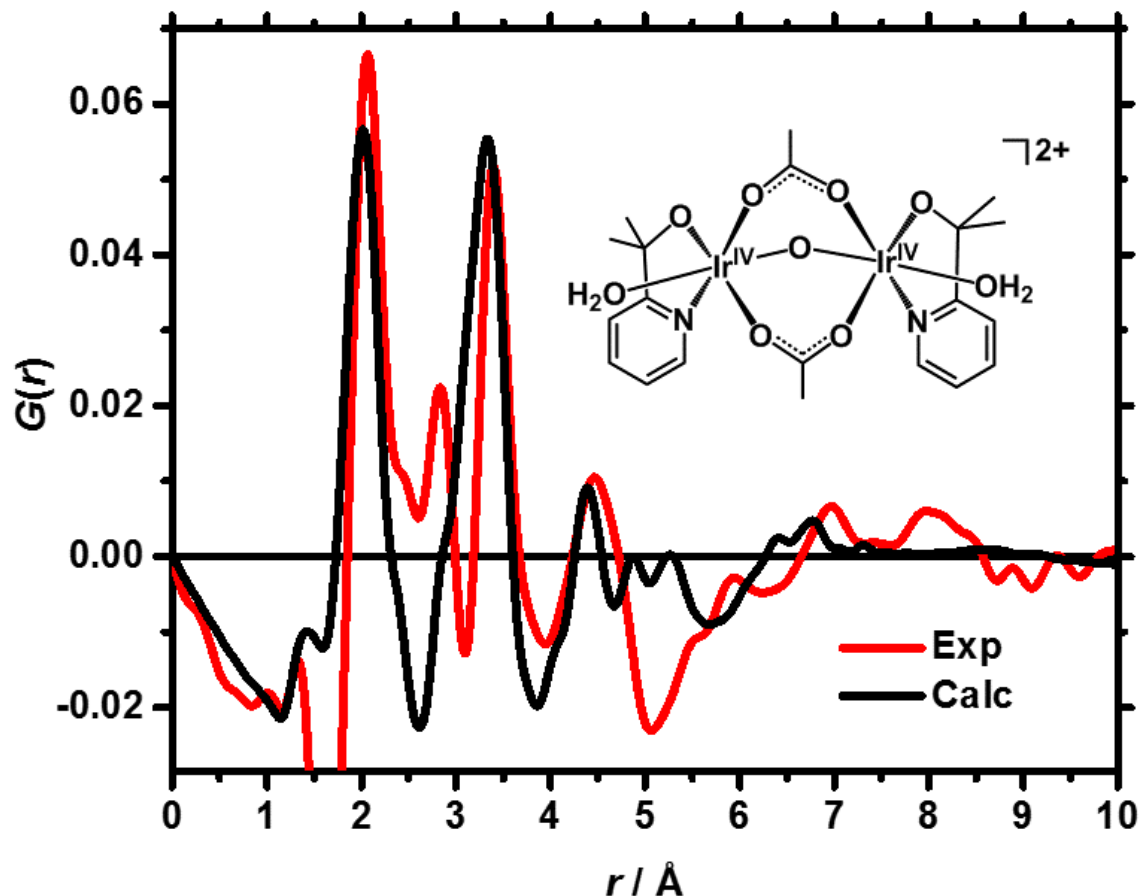


Figure S15. Calculated  $G(r)$  of the mono- $\mu$ -O Ir dimer with AcO<sup>-</sup> bridging to Ir centers (S10bb) and experimental  $G(r)$  of the chemically activated Ir blue species.

### 3.2 Bi-dentate Binding of Macac

The chelating and bridging bi-dentate binding of 2-methyl-2-acetyl acetonate (macac) was also considered. The most stable S5bb chelating isomer and the three bridging binding isomers (S10aa, S10ab, and S10bb) were considered. Their relative energetics are shown in Table S7. The three bridging isomers are much less stable than the chelating S5bb isomer since macac is a good chelating ligand. The EXAFS and HEXS spectra of S5bb, S10aa, S10ab, and S10bb isomers were simulated and are shown in Figures S16-S22.

The simulated EXAFS and HEXS spectra of mono- $\mu$ -O Ir dimer with macac chelating to Ir centers (S5bb) agree with experimental EXAFS and HEXS (Figures S16-S18). The  $^1\text{H}$  NMR spectrum of the chemically activated Ir blue species from precursor **1** has peaks around 1.7 ppm which have not been assigned.<sup>31</sup> Previously study<sup>33</sup> has shown that the protons in the methyl group in Ir(acac) complexes have peaks around 1.7 ppm (Scheme S4), so the peaks around 1.7 ppm could be assigned to the protons in the methyl groups in the macac ligands in the chemically activated Ir blue species (Figure S23). This is more clear when analyzing the  $^1\text{H}$  NMR spectra of the chemically activation of precursor  $[\text{Ir}(\text{OH})(\text{bipy})(\text{Cp}^*)]^+$  (bipy = 2,2'-bipyridine). A peak at 2.09 ppm which could be assigned to acetic acid evolves and the Cp\* peaks at 1.67 ppm quickly disappear when  $[\text{Ir}(\text{OH})(\text{bipy})(\text{Cp}^*)]^+$  is activated by sodium periodate (Figure S24). A broad peak (or several peaks) around 1.7 ppm evolves which could be assigned to the methyl groups in macac.

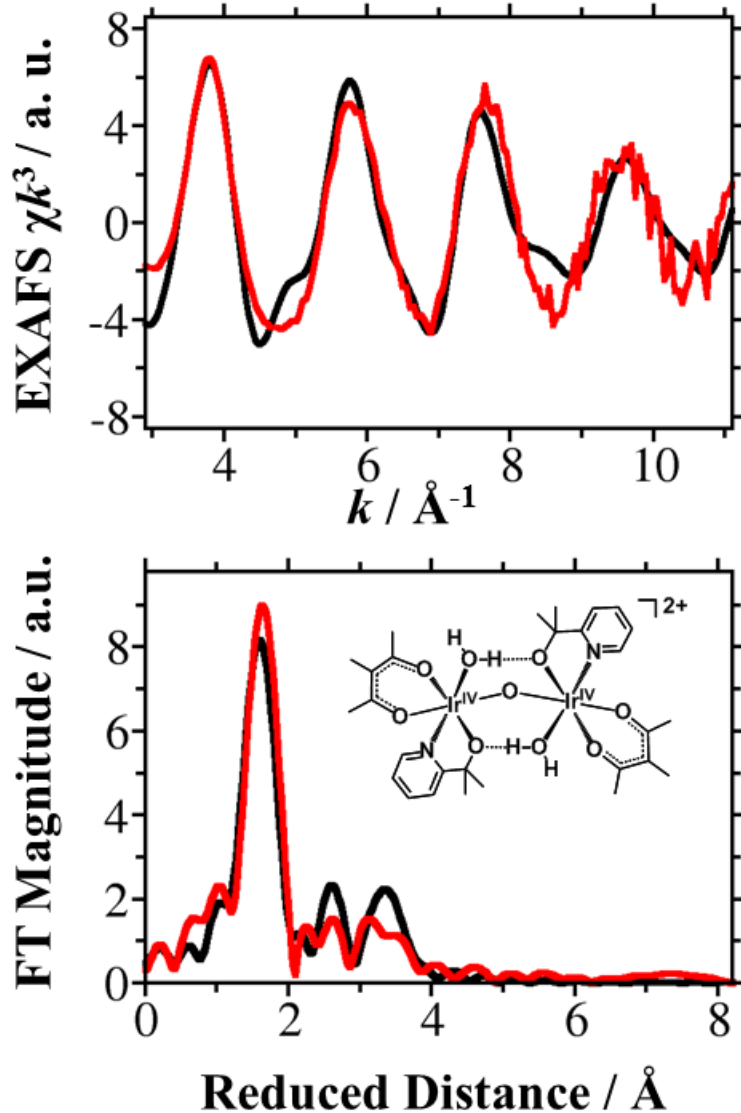


Figure S16. Simulated (black) EXAFS spectra of the most stable mono- $\mu$ -O Ir dimer with macac chelating to Ir centers (S5bb) and experimental (red) EXAFS spectra of the chemically activated Ir blue species in  $k$  space (top) and reduced distance  $R$  space (bottom).

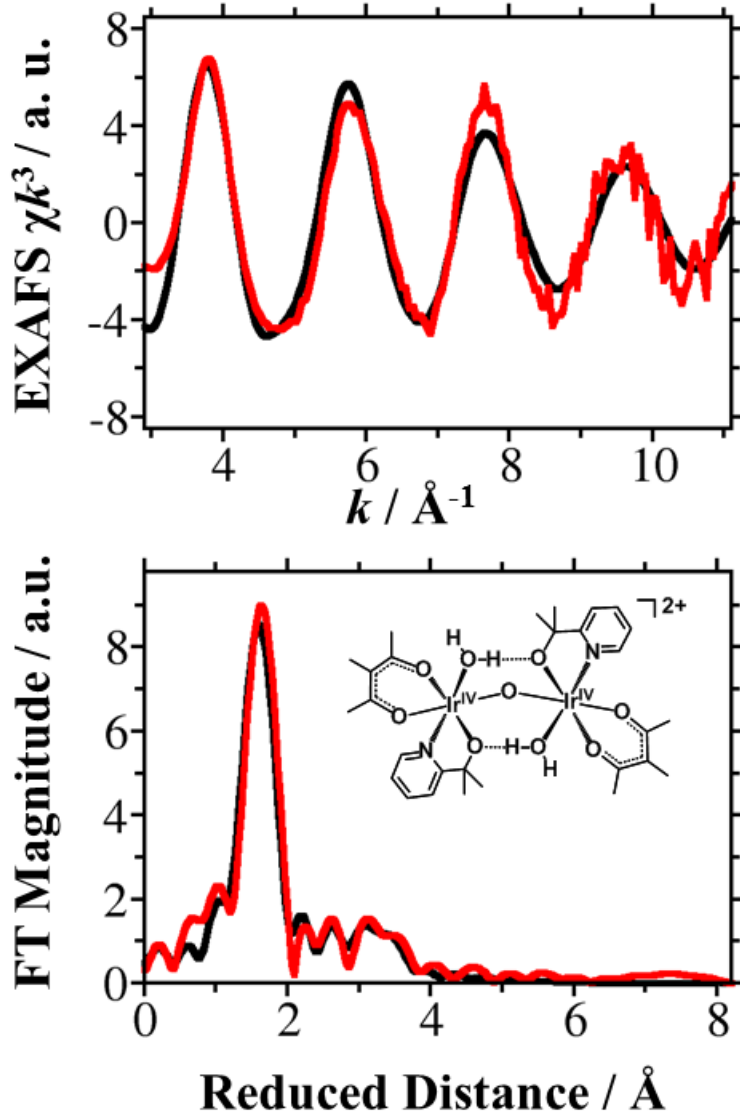


Figure S17. Refined (black) EXAFS spectra of the most stable mono- $\mu$ -O Ir dimer with macac chelating to Ir centers (S5bb) and experimental (red) EXAFS spectra of the chemically activated Ir blue species in  $k$  space (top) and reduced distance  $R$  space (bottom). The  $\sigma^2$  values for different scattering paths are given in Table S4.

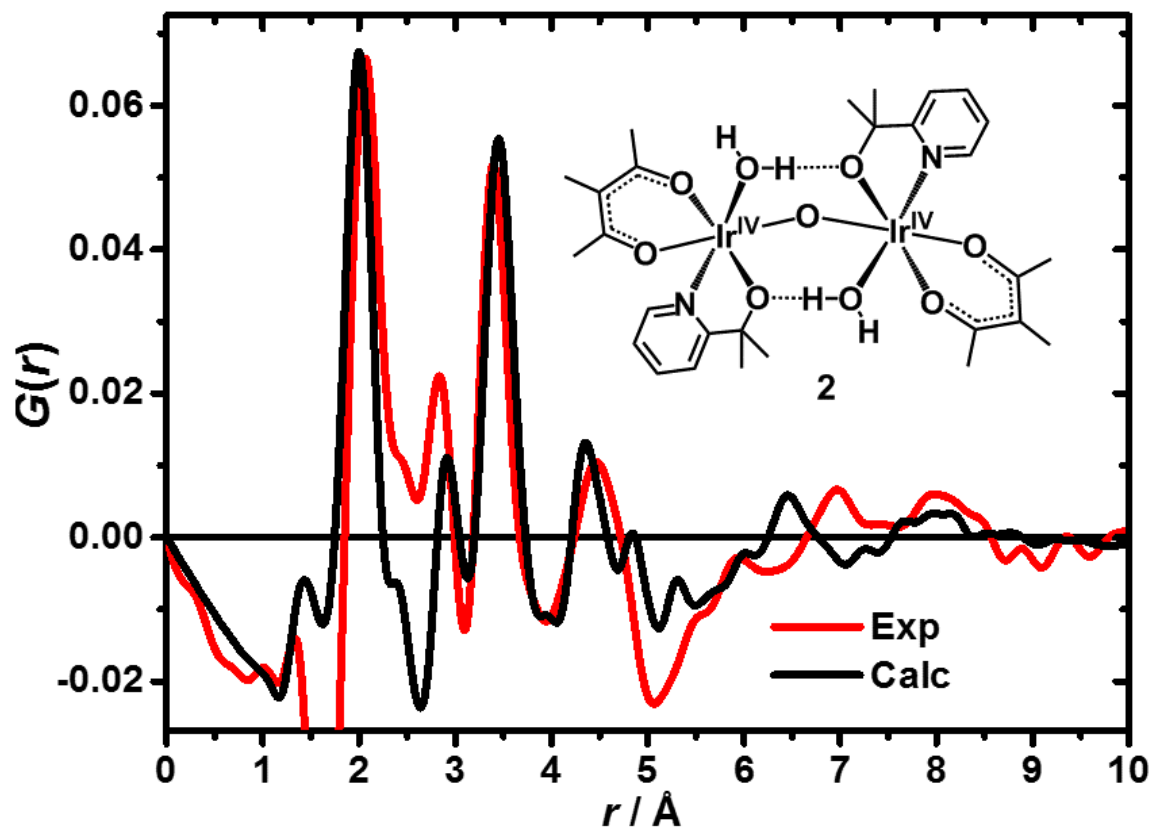


Figure S18. Calculated  $G(r)$  of the most stable mono- $\mu$ -O Ir dimer with macac chelating to Ir centers (S5bb) and experimental  $G(r)$  of the chemically activated Ir blue species.

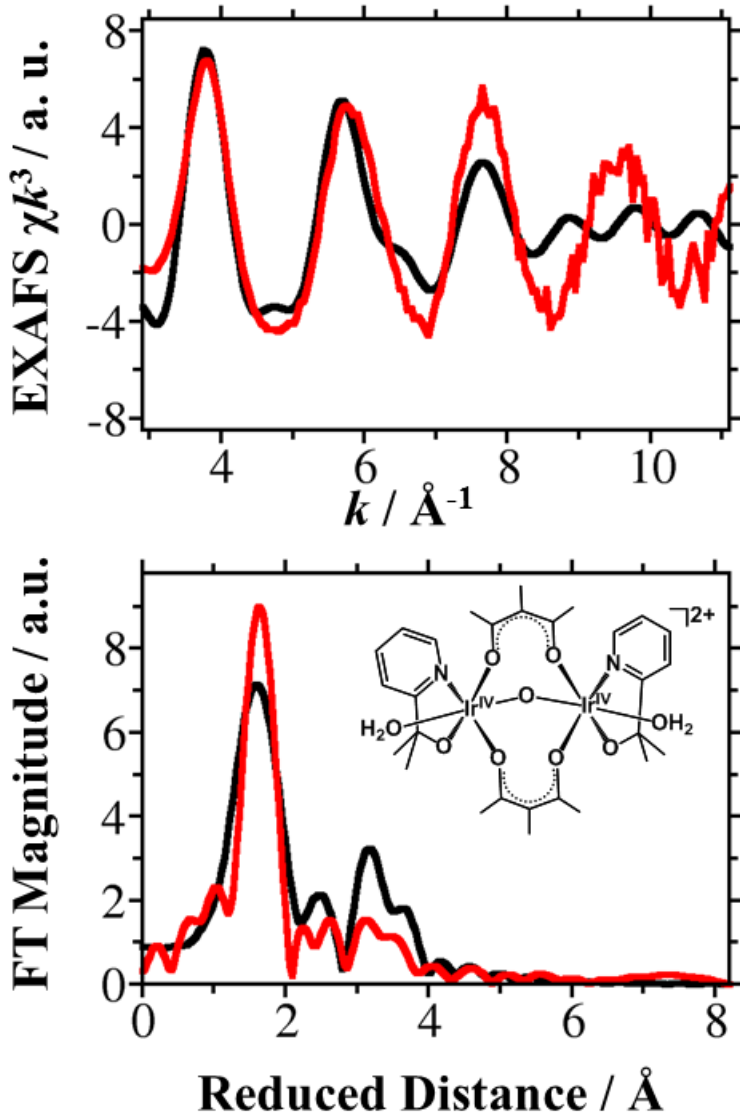


Figure S19. Simulated (black) EXAFS spectra of the mono-\(\mu\)-O Ir dimer with macac bridging to Ir centers (S10aa) and experimental (red) EXAFS spectra of the chemically activated Ir blue species in  $k$  space (top) and reduced distance  $R$  space (bottom).

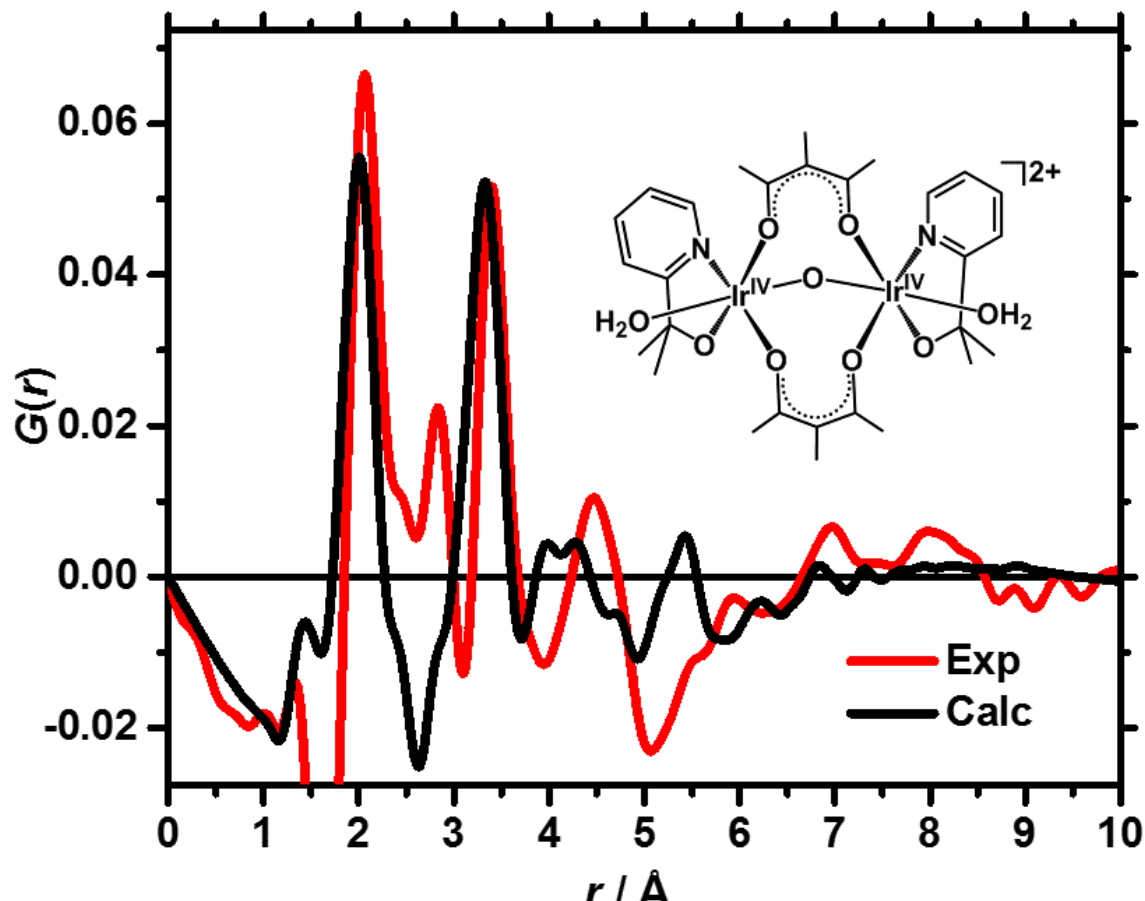


Figure S20. Calculated  $G(r)$  of the mono- $\mu$ -O Ir dimer with macac bridging to Ir centers (S10aa) and experimental  $G(r)$  of the chemically activated Ir blue species.

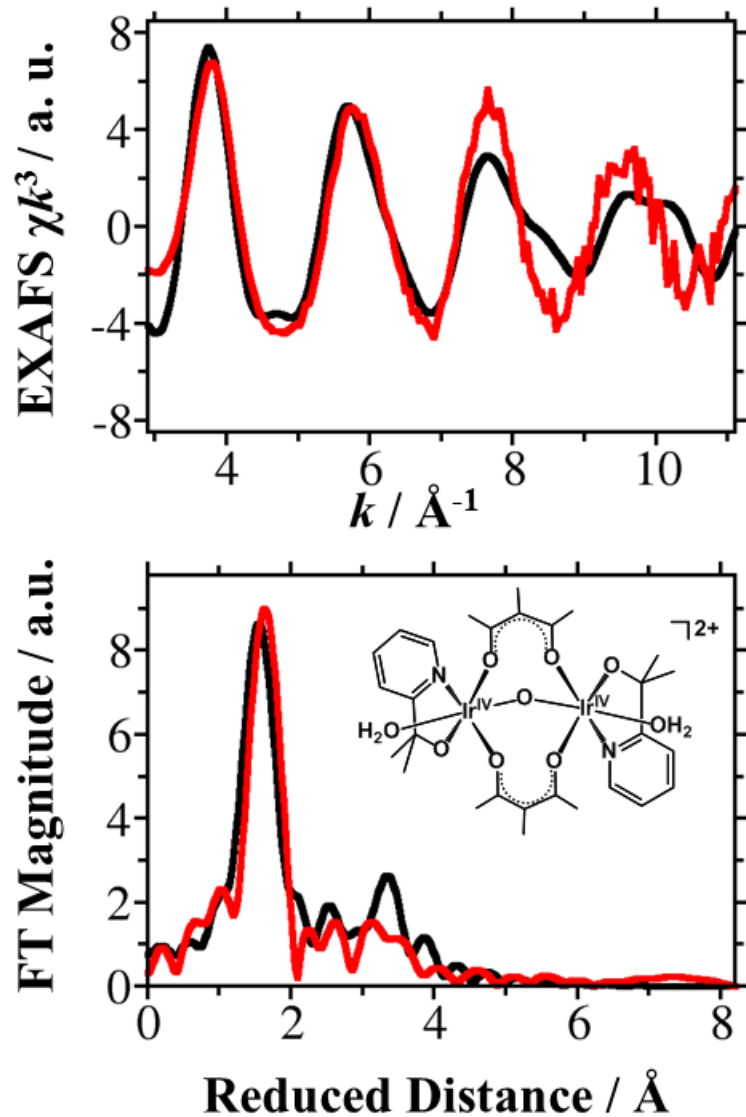


Figure S21. Simulated (black) EXAFS spectra of the mono- $\mu$ -O Ir dimer with macac bridging to Ir centers (S10ab) and experimental (red) EXAFS spectra of the chemically activated Ir blue species in  $k$  space (top) and reduced distance  $R$  space (bottom).

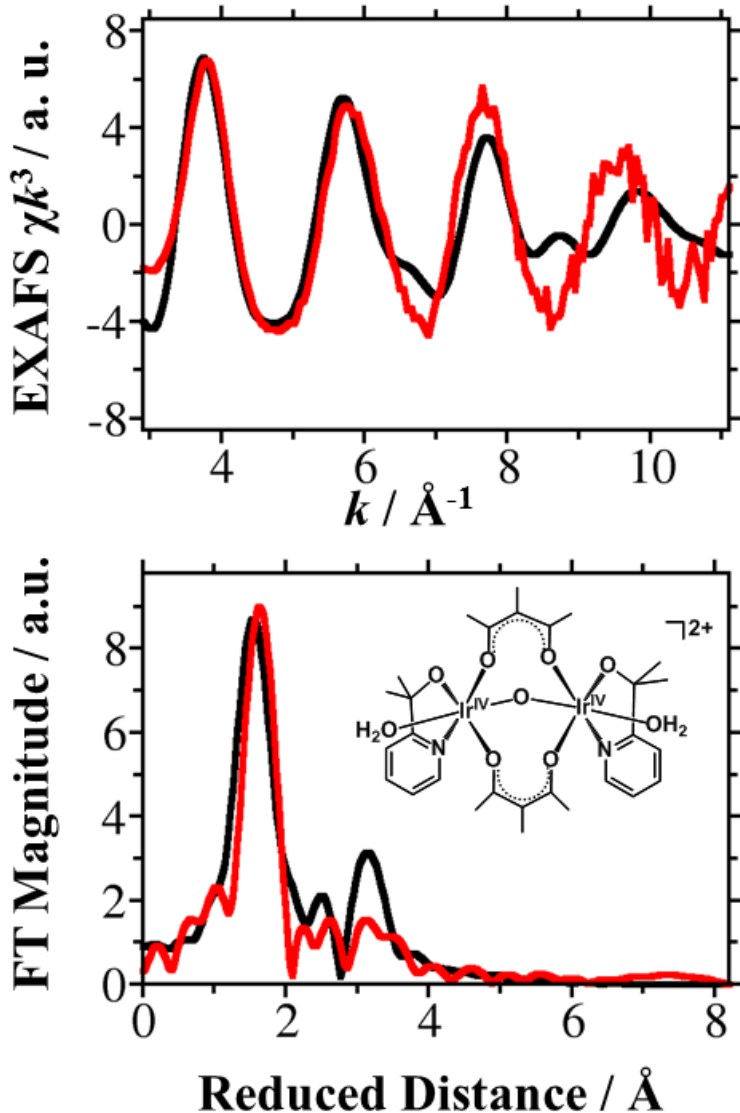
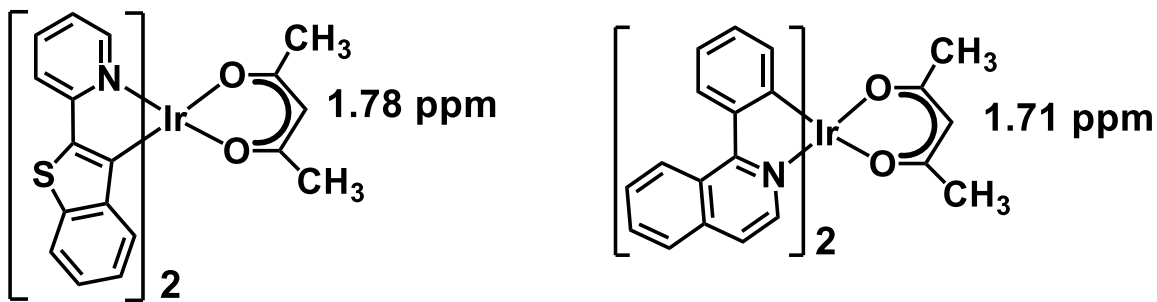


Figure S22. Simulated (black) EXAFS spectra of the mono- $\mu$ -O Ir dimer with macac bridging to Ir centers (S10bb) and experimental (red) EXAFS spectra of the chemically activated Ir blue species in  $k$  space (top) and reduced distance  $R$  space (bottom).

Table S7. Energetics and Ir–Ir Distances of Mono- $\mu$ -O Ir Dimers with macac Chelating and Bridging to Ir Centers.

	$\Delta E$ (kcal/mol)	$\Delta G$ (kcal/mol)	$d_{\text{Ir-Ir}}$ ( $\text{\AA}$ )
S5bb	<b>0.0</b>	<b>0.0</b>	<b>3.45</b>
S10aa	42.0	41.5	3.43
S10ab	43.4	43.5	3.44
S10bb	54.6	55.0	3.34

**Scheme S4.**  $^1\text{H}$  NMR data of methyl group in two acac complexes. (Experimental chemical shifts taken from Ref. 33)



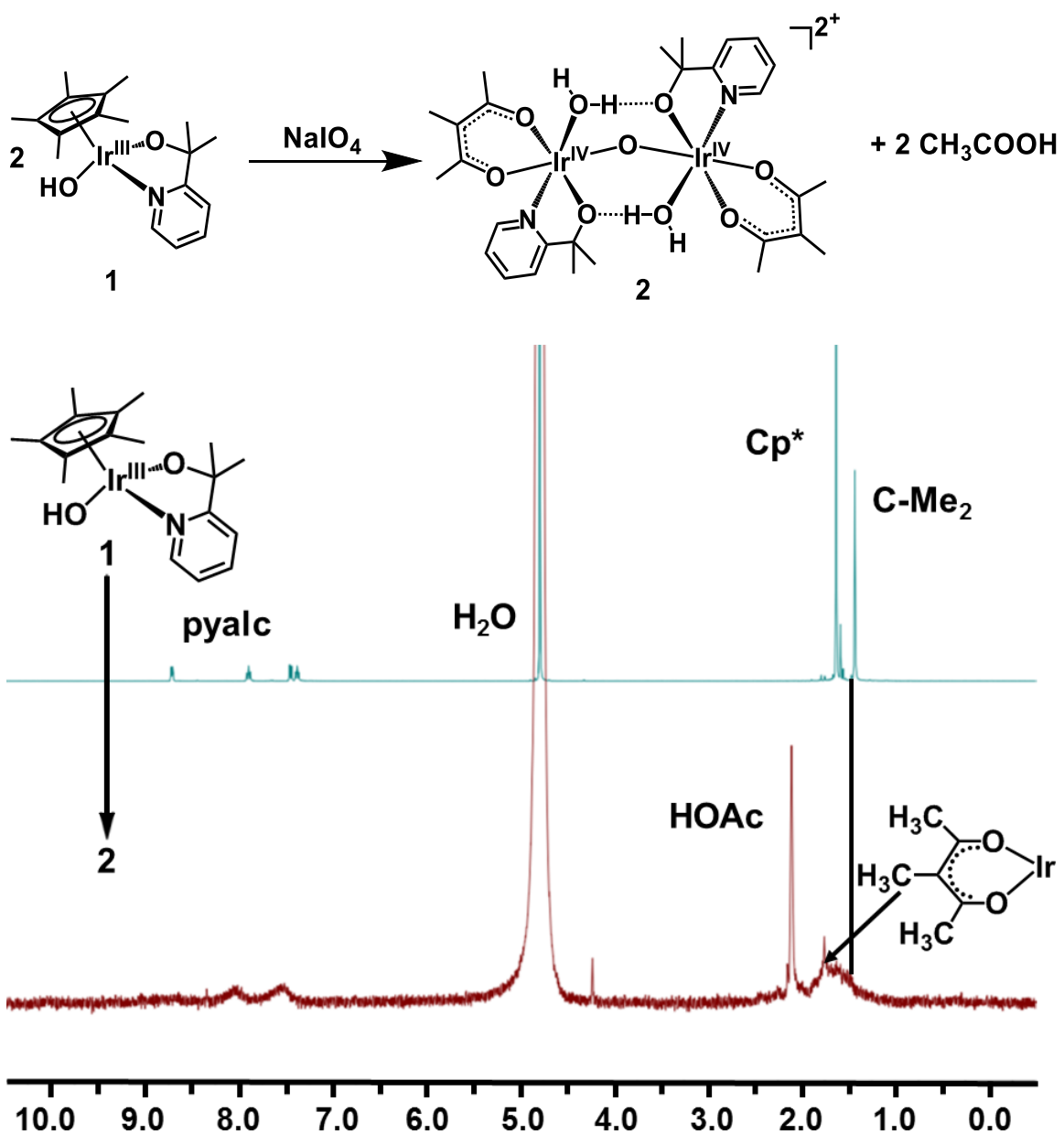


Figure S23. Assignment of peaks in <sup>1</sup>H-NMR spectra of the precursor **1** and the chemically activated Ir blue species **2** (experimental spectra taken from Ref. 31).

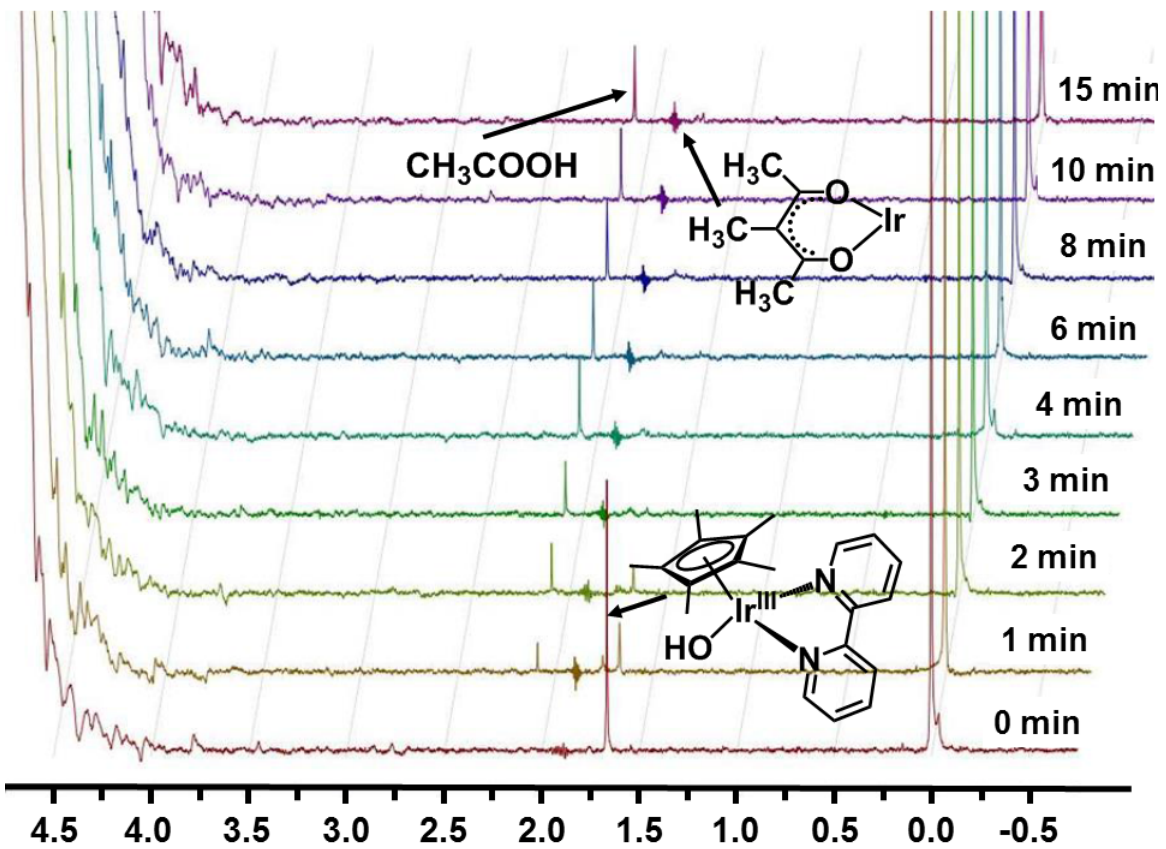
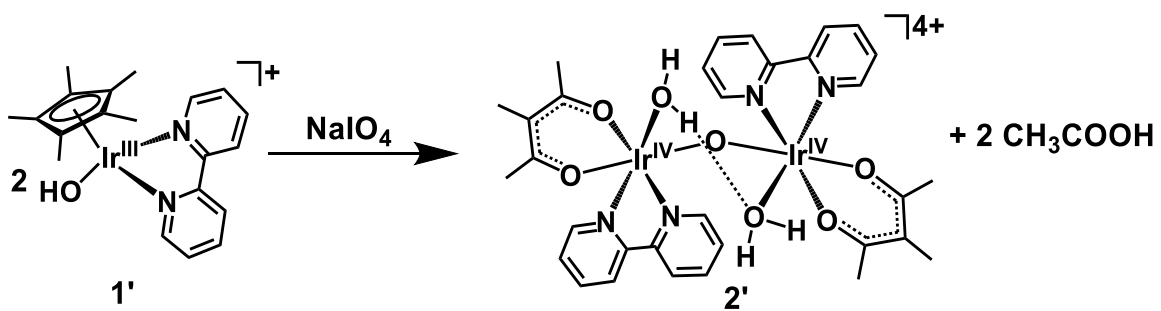


Figure S24. Assignment of peaks in  $^1\text{H}$ -NMR spectra of the precursor

$[\text{Ir}(\text{OH})(\text{bipy})(\text{Cp}^*)]^+$  (bipy = 2,2'-bipyridine) and the chemically activated Ir blue species (spectra of time-course experiment taken from Ref. 31).

### **3.3 Bi-dentate Binding of Iodate**

The chelating and bridging bi-dentate binding of iodates were also considered. Since from section 3.1 we knew that the S5bb isomer of chelating binding is much more stable than other isomers, only the S5bb chelating isomer was considered, and the three bridging binding isomers (S10aa, S10ab, and S10bb) were considered. Their relative energetics are shown in Table S8. Again, all three bridging isomers are more stable than the chelating S5bb isomer. The EXAFS spectra of S5bb, S10aa, S10ab, and S10bb isomers were simulated and are shown in Figures S25-S28. The simulated EXAFS spectra with iodates binding to Ir centers disagree with the experimental EXAFS spectra. It is worth pointing out that our simulated spectra in reduced distance space show an intense peak corresponding to an Ir–I distance which is not present in the experimental spectra, indicating there are no iodates in the active species in the chemically activated Ir blue species. The electron density pair distribution function (PDF),  $G(r)$ , of S5bb and S10aa isomers were calculated and compared with experimental  $G(r)$  in Figures S29-S30. As for EXAFS, the calculated  $G(r)$  has intense peaks corresponding to Ir–I distances which is not present in the experimental  $G(r)$ , suggesting no iodates in the chemically activated Ir blue species.

Table S8. Energetics and Ir–Ir Distances of Mono- $\mu$ -O Ir Dimers with  $\text{IO}_3^-$  Chelating and Bridging to Ir Centers.

	$\Delta E$ (kcal/mol)	$\Delta G$ (kcal/mol)	$d_{\text{Ir-Ir}}$ ( $\text{\AA}$ )
S5bb	<b>0.0</b>	<b>0.0</b>	<b>3.42</b>
S10aa	-11.7	-13.7	3.49
S10ab	-14.6	-16.3	3.42
S10bb	-13.3	-14.8	3.49

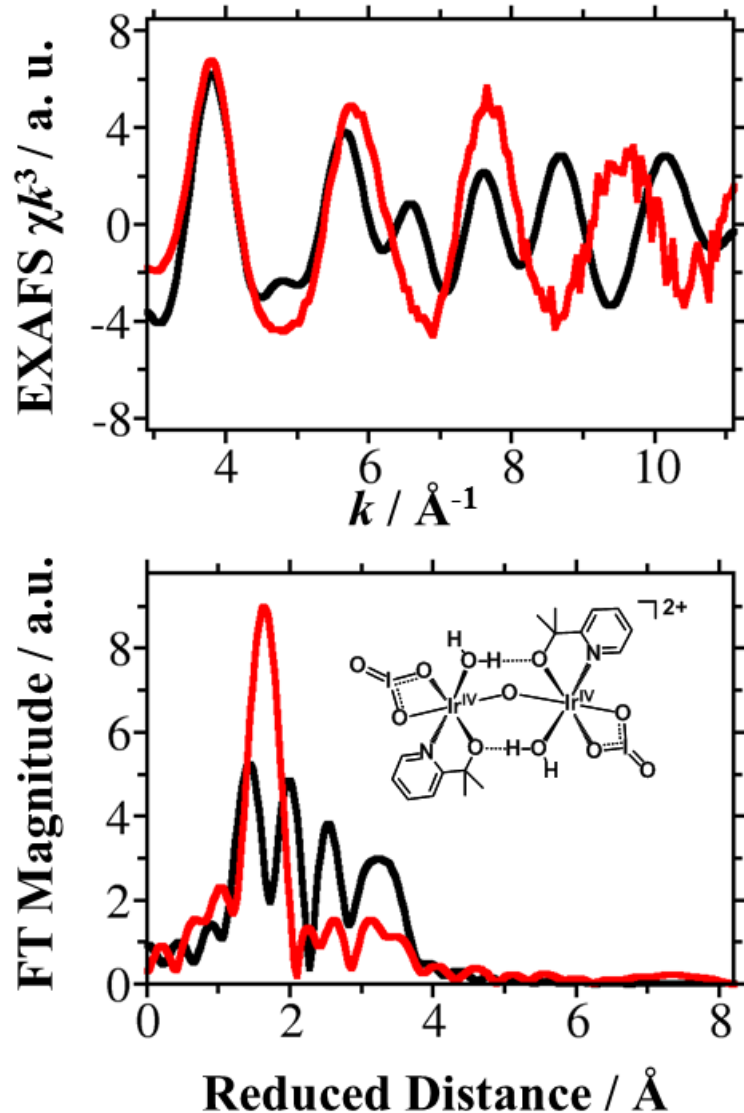


Figure S25. Simulated (black) EXAFS spectra of the most stable mono- $\mu$ -O Ir dimer with  $\text{IO}_3^-$  chelating to Ir centers (S5bb) and experimental (red) EXAFS spectra of the chemically activated Ir blue species in  $k$  space (top) and reduced distance  $R$  space (bottom).

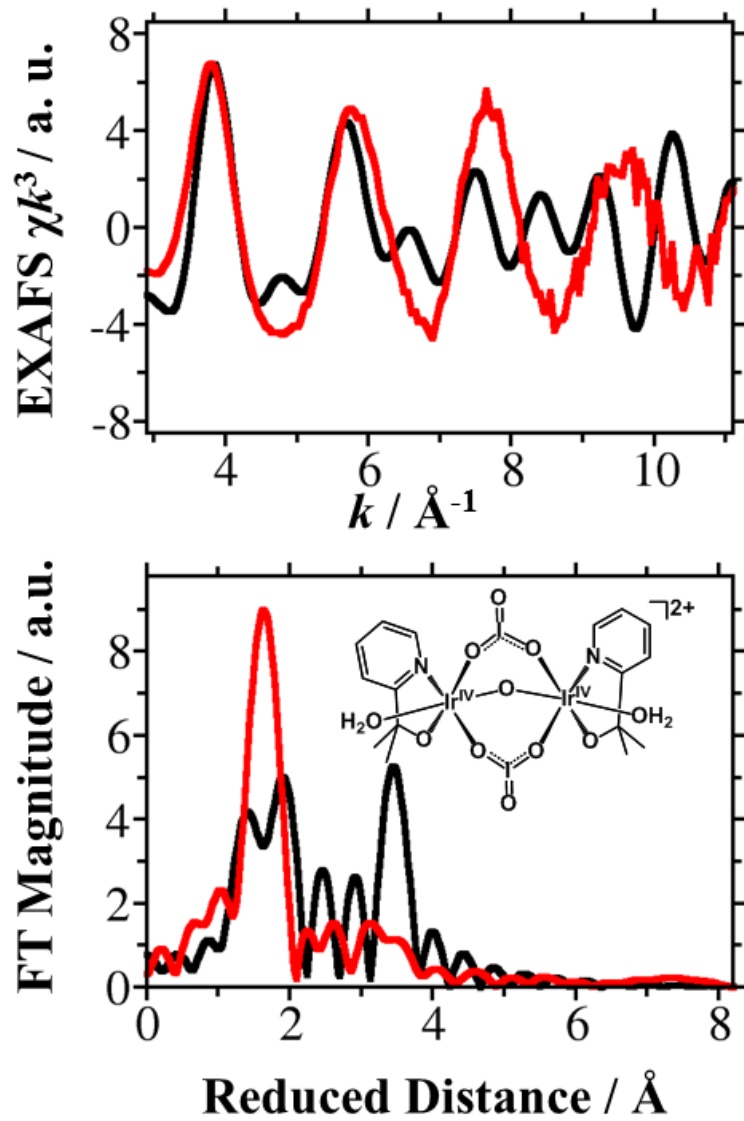


Figure S26. Simulated (black) EXAFS spectra of the mono- $\mu$ -O Ir dimer with  $\text{IO}_3^-$  bridging to Ir centers (S10aa) and experimental (red) EXAFS spectra of the chemically activated Ir blue species in  $k$  space (top) and reduced distance  $R$  space (bottom).

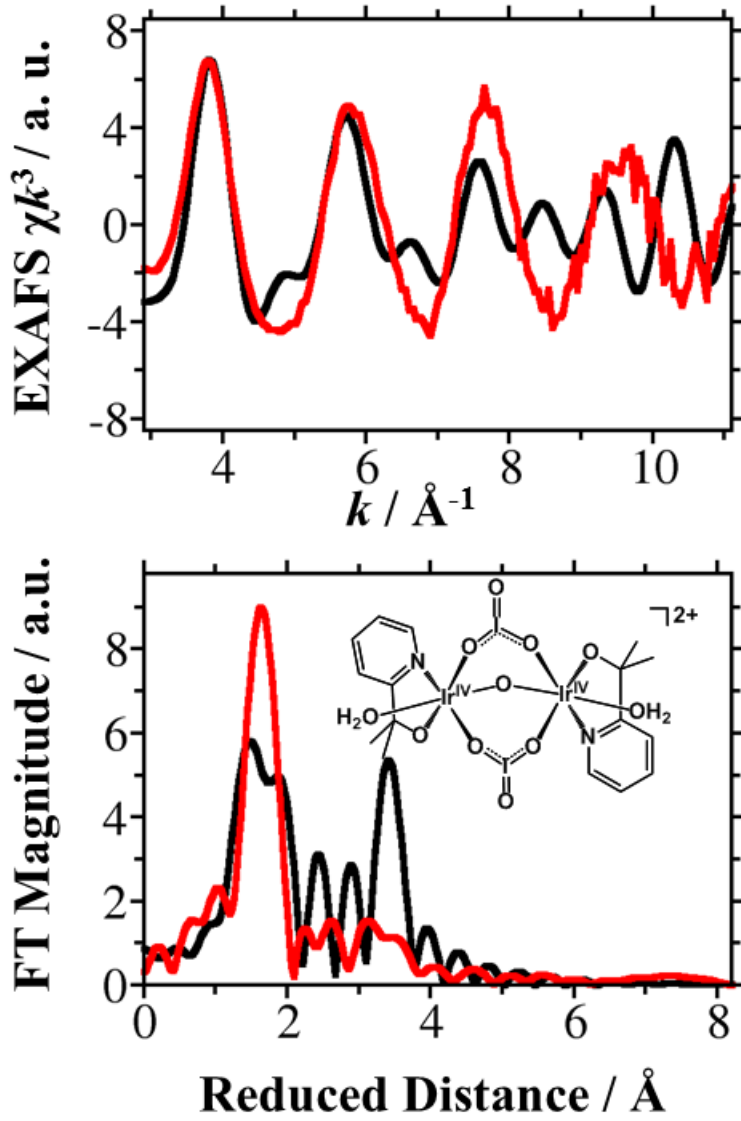


Figure S27. Simulated (black) EXAFS spectra of the mono- $\mu$ -O Ir dimer with  $\text{IO}_3^-$  bridging to Ir centers (S10ab) and experimental (red) EXAFS spectra of the chemically activated Ir blue species in  $k$  space (top) and reduced distance  $R$  space (bottom).

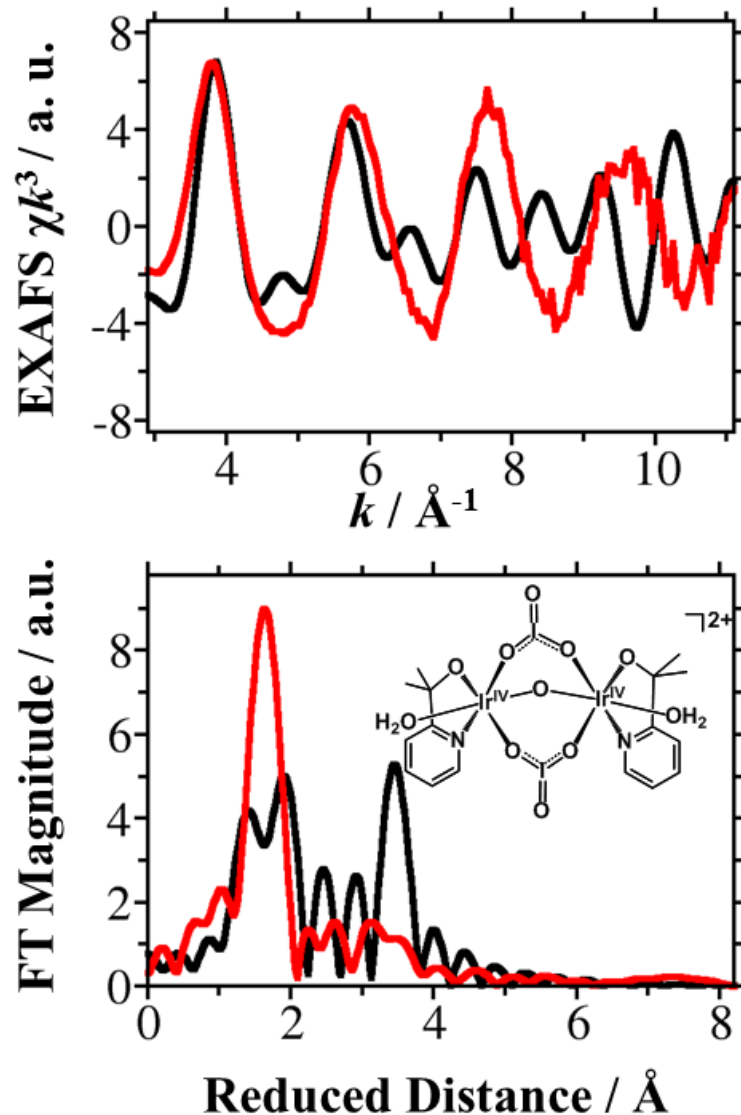


Figure S28. Simulated (black) EXAFS spectra of the mono- $\mu$ -O Ir dimers with  $\text{IO}_3^-$  bridging to Ir centers (S10bb) and experimental (red) EXAFS spectra of the chemically activated Ir blue species in  $k$  space (top) and reduced distance  $R$  space (bottom).

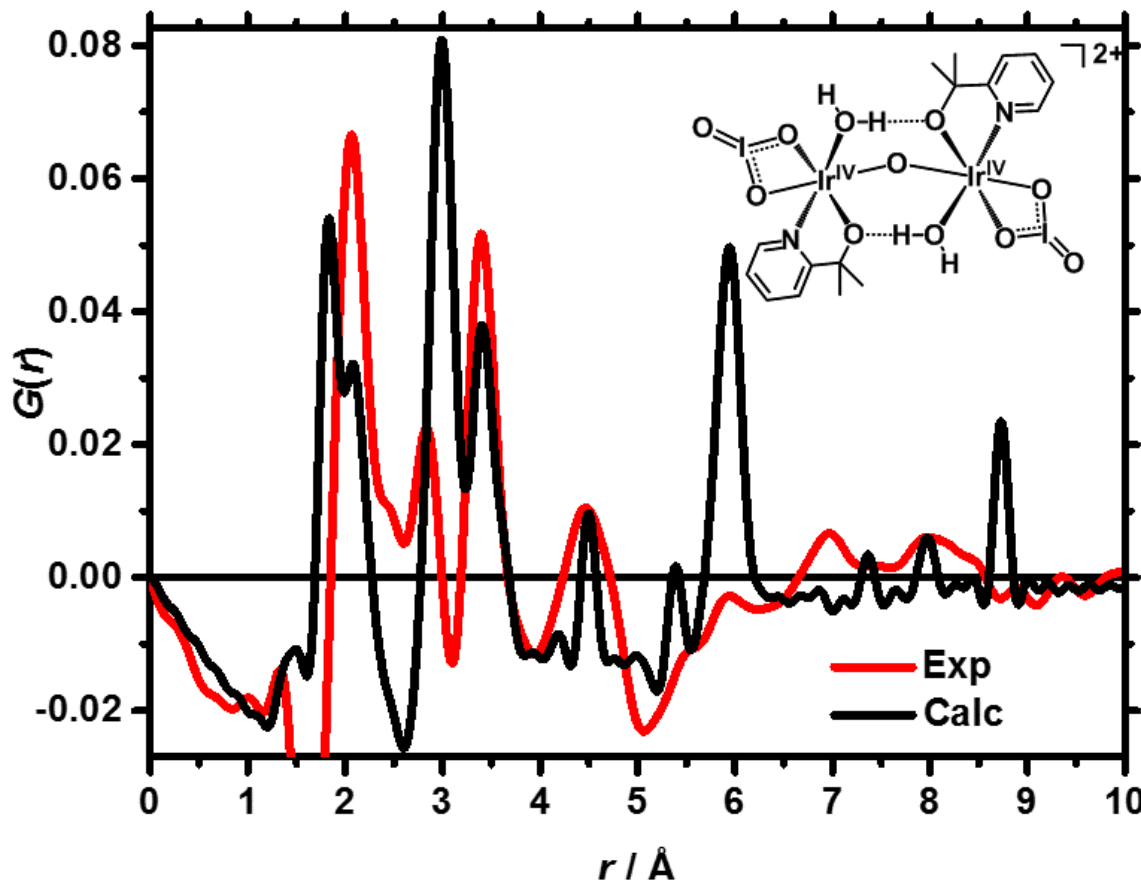


Figure S29. Calculated  $G(r)$  of the mono- $\mu$ -O Ir dimer with  $\text{IO}_3^-$  chelating to Ir centers (S5bb) and experimental  $G(r)$  of the chemically activated Ir blue species.

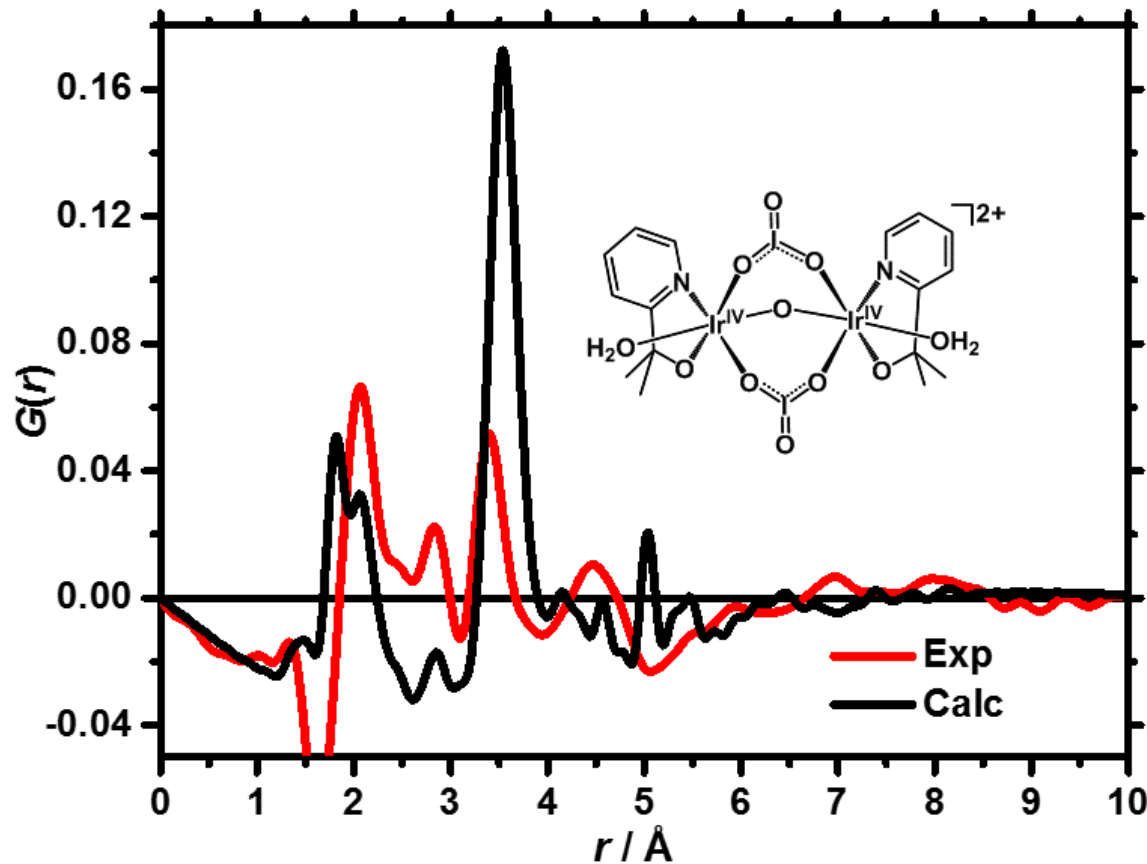


Figure S30. Calculated  $G(r)$  of the mono- $\mu$ -O Ir dimer with  $\text{IO}_3^-$  bridging to Ir centers (S10aa) and experimental  $G(r)$  of the chemically activated Ir blue species.

### **3.4 Mono-dentate and Bi-dentate Binding of Acetate**

For electrochemically activated Ir blue solution, there are several possible ligands in the solution, including acetate and sulfate. Only EXAFS spectra of the electrochemically activated Ir blue solution were studied experimentally. We considered bidentate and mono-dentate binding of  $\text{AcO}^-$  and bidentate binding of sulfate. Relative Energetics of mono-dentate binding of  $\text{AcO}^-$  are giving in Table S9. The most stable isomer is labeled as 4AcO\_NN\_S1. The simulated EXAFS spectra with a global  $\sigma^2$  are shown in Figure S31 and the simulated EXAFS spectra with different  $\sigma^2$  for different scattering paths are given in Figure S32. The calculated PDF  $G(r)$  of the most stable isomer with  $\text{AcO}^-$  mono-dentate binding to Ir centers is shown in Figure S33, as well as the experimental  $G(r)$  of chemically activate Ir blue solution. The poor agreement between the calculated and experimental  $G(r)$  in Figure S33 suggests complexes **3** could not the dominant species in chemically activated blue solution. The EXAFS spectra of Ir dimers with  $\text{AcO}^-$  bidentate binding to Ir centers are shown in Figure S34-S37.

**Scheme S5. Possible isomers of  $\text{AcO}^-$  with mono-dentate binding mode**

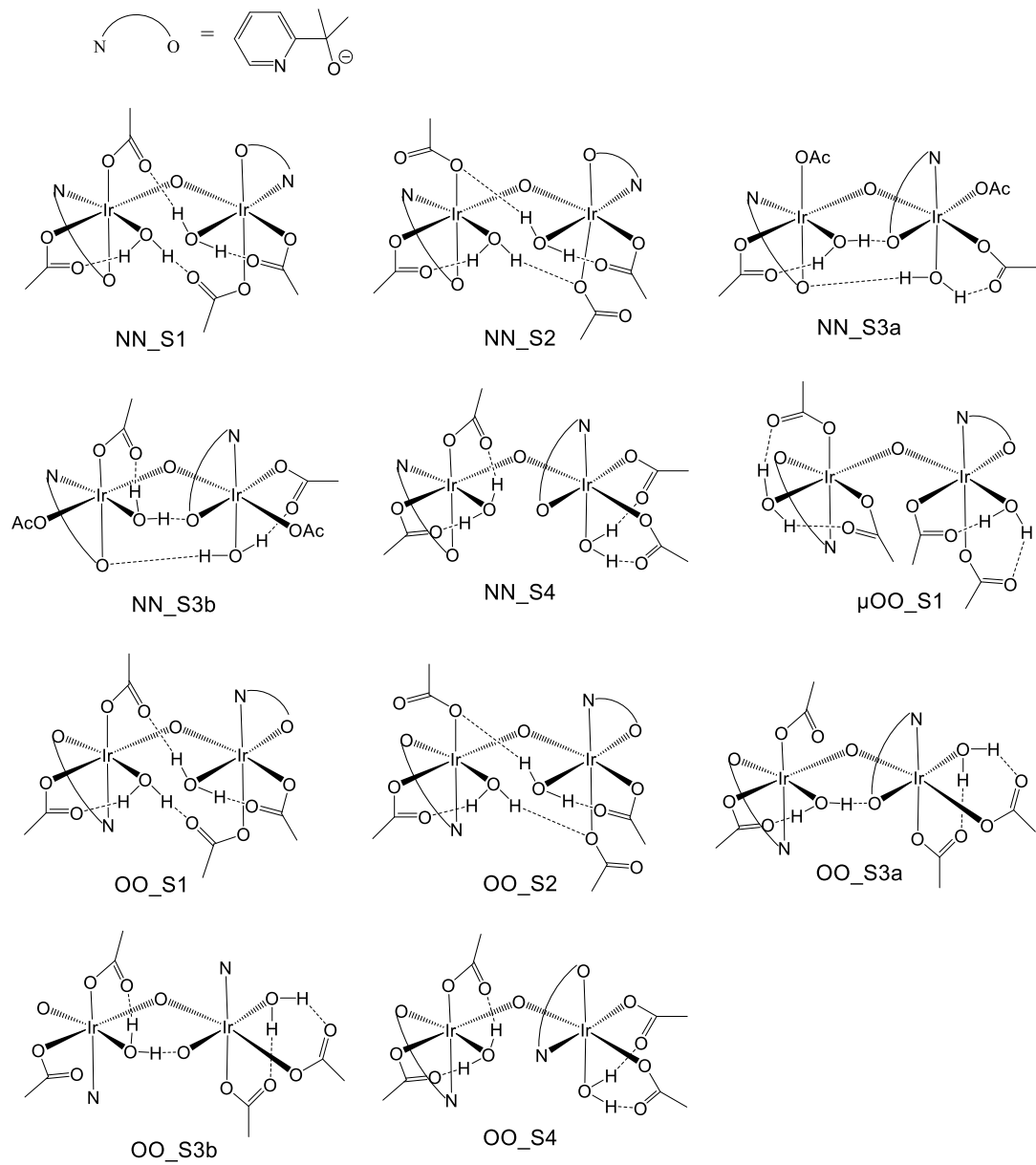


Table S9. Energetics and Ir–Ir Distances of Mono- $\mu$ -O Ir Dimers with AcO<sup>−</sup> Mono-dentate Binding to Ir Centers.

	$\Delta E$ (kcal/mol)	$\Delta G$ (kcal/mol)	$d_{\text{Ir-Ir}}$ (Å)
NN_S1	<b>0.0</b>	<b>0.0</b>	<b>3.57</b>
NN_S2	7.4	8.7	3.48
NN_S3a	5.9	4.7	3.45
NN_S3b	3.9	2.1	3.51
NN_S4	4.0	3.0	3.54
OO_S1	3.2	2.6	3.57
OO_S2	5.4	3.8	3.50
OO_S3a	10.3	9.0	3.62
OO_S3b	6.9	6.3	3.59
OO_S4	1.6	1.8	3.59
$\mu$ OO_S1	8.1	9.4	3.50

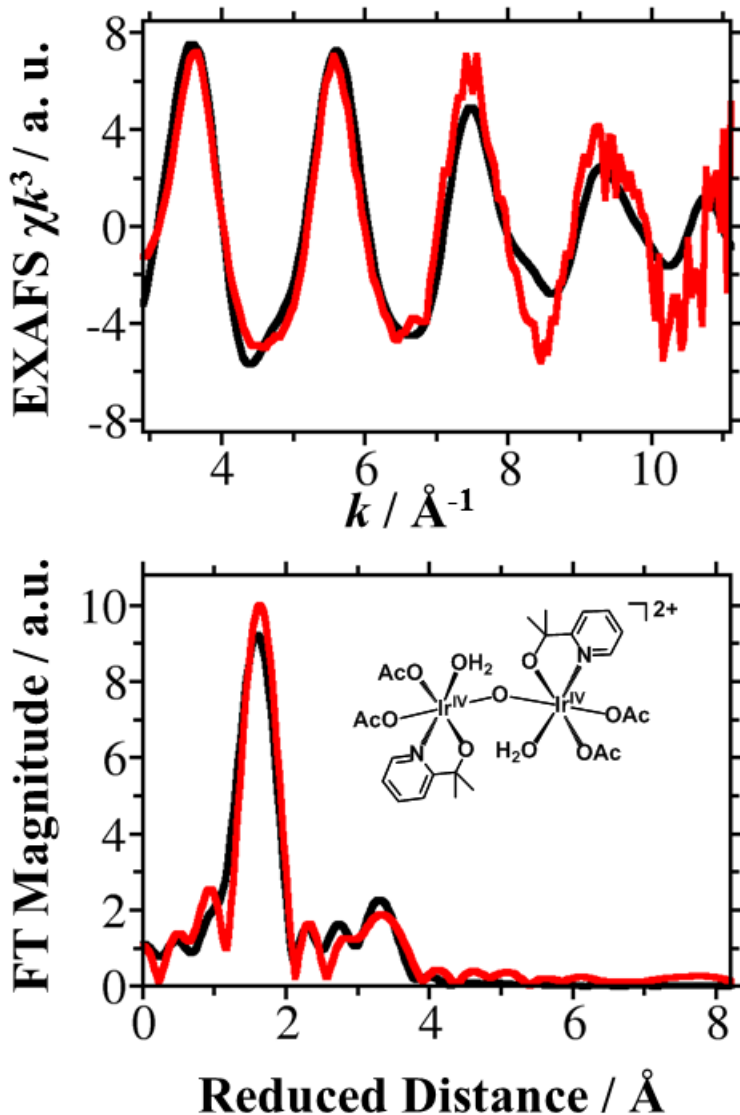


Figure S31. Simulated (black) EXAFS spectra of the most stable mono- $\mu$ -O Ir dimers with  $\text{AcO}^-$  mono-dentate bridging to Ir centers (4AcO\_NN\_S1) and experimental (red) EXAFS spectra of the electrochemically activated Ir blue species in  $k$  space (top) and reduced distance  $R$  space (bottom).

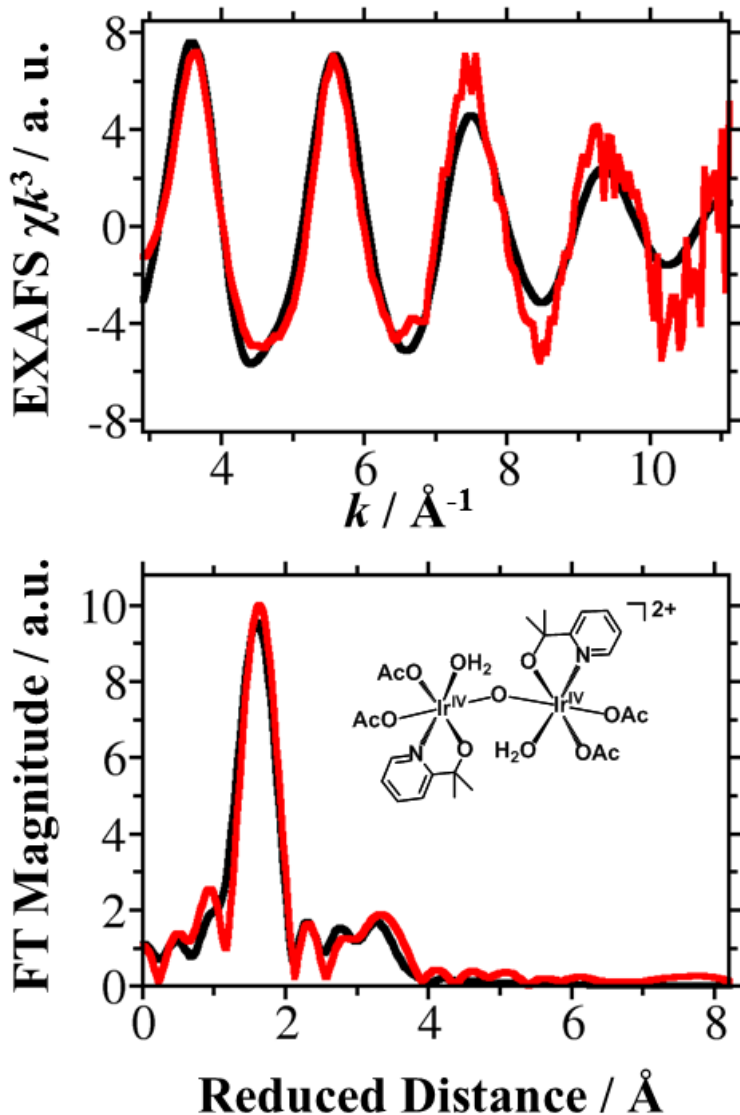


Figure S32. Refined (black) EXAFS spectra of the most stable mono- $\mu$ -O Ir dimer with  $\text{AcO}^-$  mono-dentate bridging to Ir centers (4AcO\_NN\_S1) and experimental (red) EXAFS spectra of the electrochemically activated Ir blue species in  $k$  space (top) and reduced distance  $R$  space (bottom). The  $\sigma^2$  values for different scattering paths are given in Table S4.

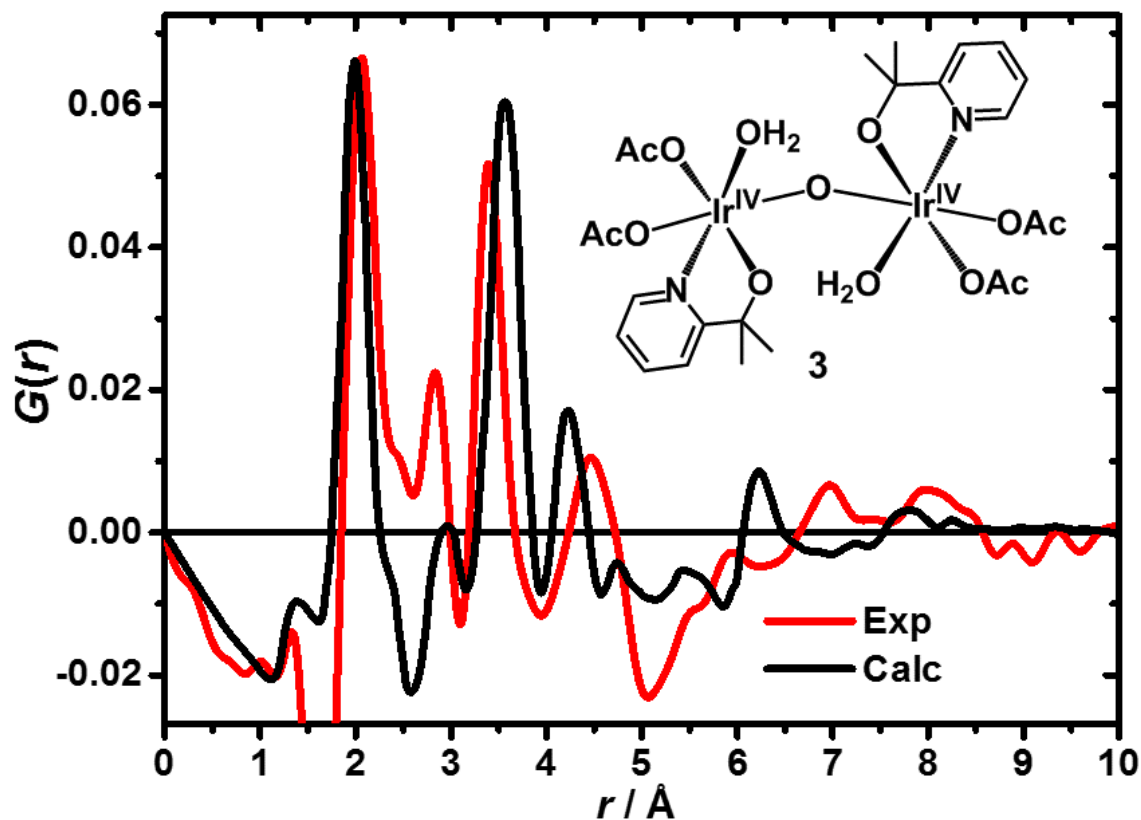


Figure S33. Calculated  $G(r)$  of the mono- $\mu$ -O Ir dimer with  $\text{AcO}^-$  mono-dentate binding to Ir centers (4 $\text{AcO}^-$ \_NN\_S1) and experimental  $G(r)$  of the chemically activated Ir blue species.

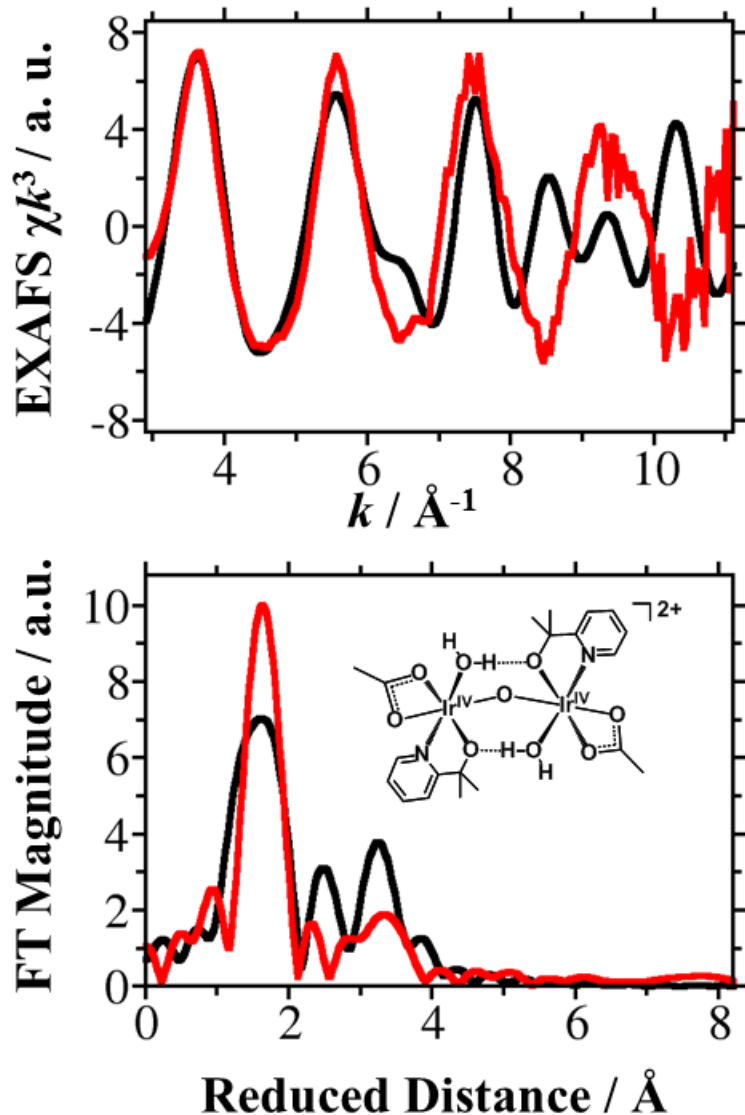


Figure S34. Simulated (black) EXAFS spectra of the most stable mono- $\mu$ -O Ir dimer with AcO<sup>-</sup> chelating to Ir centers (2AcO\_S5bb) and experimental (red) EXAFS spectra of the electrochemically activated Ir blue species in  $k$  space (top) and reduced distance  $R$  space (bottom).

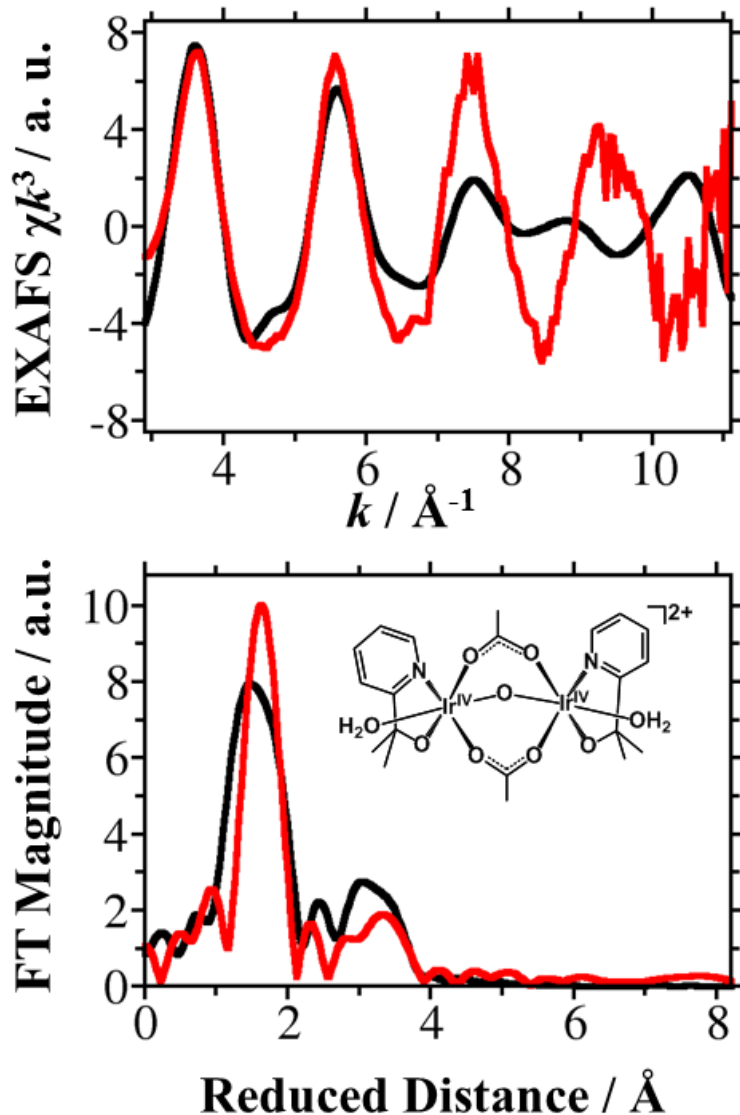


Figure S35. Simulated (black) EXAFS spectra of the mono- $\mu$ -O Ir dimer with AcO<sup>-</sup> bridging to Ir centers (2AcO\_S10aa) and experimental (red) EXAFS spectra of the electrochemically activated Ir blue species in  $k$  space (top) and reduced distance  $R$  space (bottom).

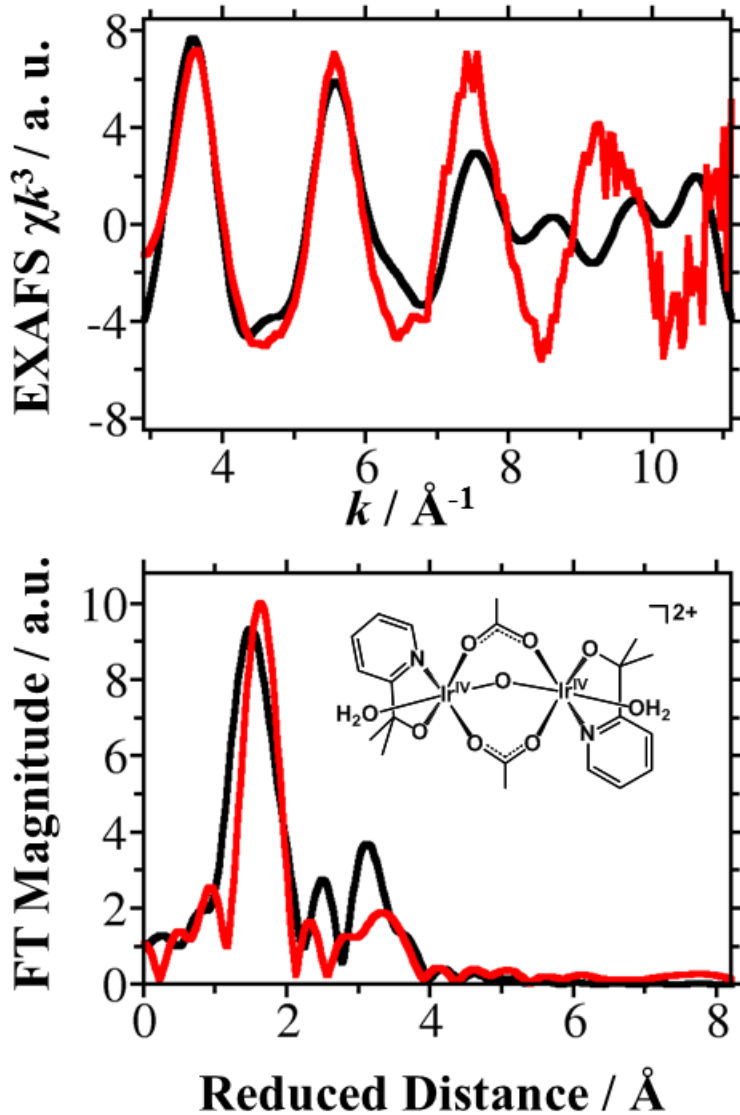


Figure S36. Simulated (black) EXAFS spectra of the mono- $\mu$ -O Ir dimer with AcO<sup>-</sup> bridging to Ir centers (2AcO\_S10ab) and experimental (red) EXAFS spectra of the electrochemically activated Ir blue species in  $k$  space (top) and reduced distance  $R$  space (bottom).

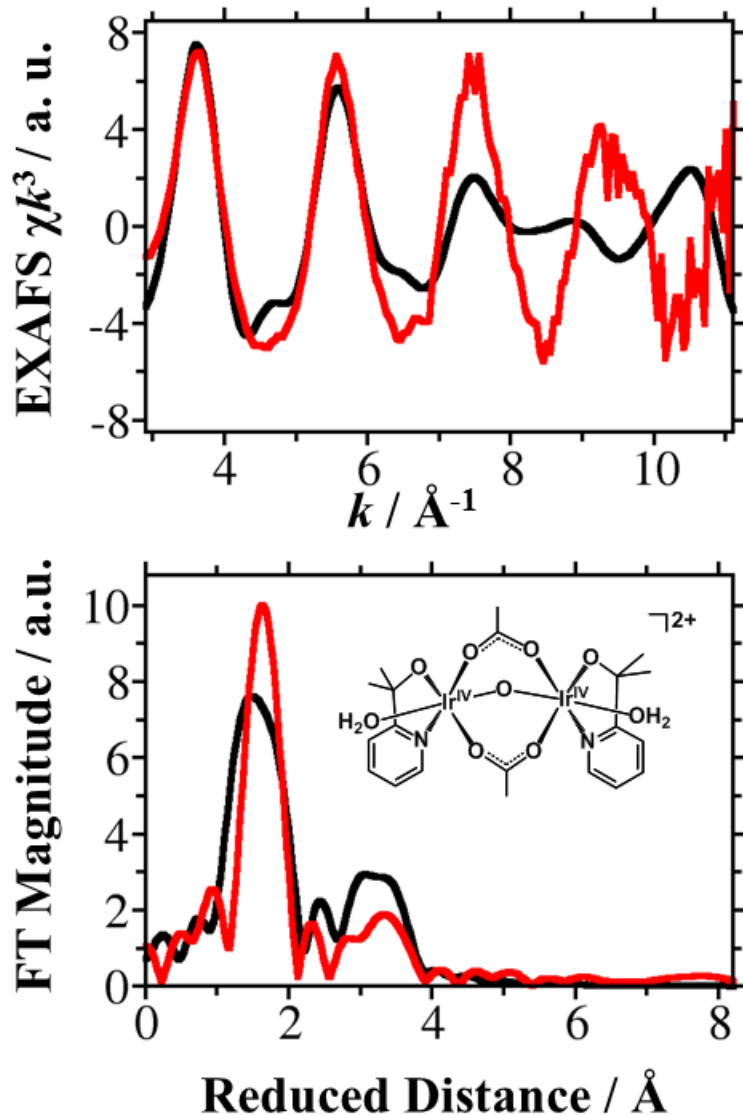


Figure S37. Simulated (black) EXAFS spectra of the mono- $\mu$ -O Ir dimer with AcO<sup>-</sup> bridging to Ir centers (2AcO\_S10bb) and experimental (red) EXAFS spectra of the electrochemically activated Ir blue species in  $k$  space (top) and reduced distance  $R$  space (bottom).

### **3.5 Bi-dentate Binding of Sulfate**

Sulfate is present in the electrochemically activated Ir blue solution as electrolytes. We considered the most stable S5bb isomer and three bridging binding isomers (S10aa, S10ab, and S10bb). Sulfate prefers to bind to Ir as a chelating rather than bridging ligand (Table S10), possible due to the negative charges on sulfates that prefer to avoid each other. The simulated EXAFS spectra of sulfate binding to Ir centers are shown in Figures S38-S41.

Table S10. Energetics and Ir–Ir Distances of Mono- $\mu$ -O Ir Dimers with  $\text{SO}_4^{2-}$  Chelating and Bridging to Ir Centers.

	$\Delta E$ (kcal/mol)	$\Delta G$ (kcal/mol)	$d_{\text{Ir-Ir}}$ (Å)
S5bb	<b>0.0</b>	<b>0.0</b>	<b>3.41</b>
S10aa	6.9	4.9	3.49
S10ab	7.5	5.0	3.51
S10bb	10.0	7.9	3.42

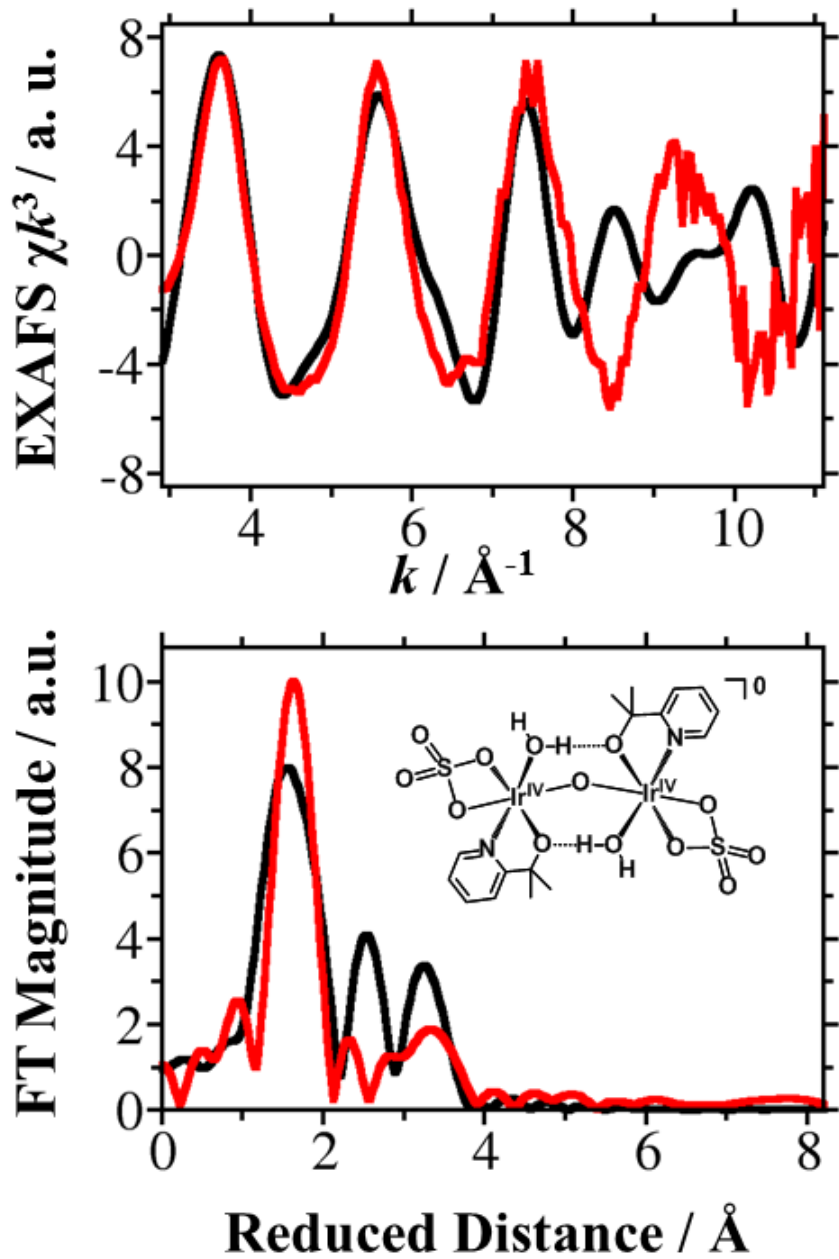


Figure S38. Simulated (black) EXAFS spectra of the most stable mono- $\mu$ -O Ir dimer with  $\text{SO}_4^{2-}$  chelating to Ir centers ( $2\text{SO}_4^{2-}\text{-S5bb}$ ) and experimental (red) EXAFS spectra of the electrochemically activated Ir blue species in  $k$  space (top) and reduced distance  $R$  space (bottom).

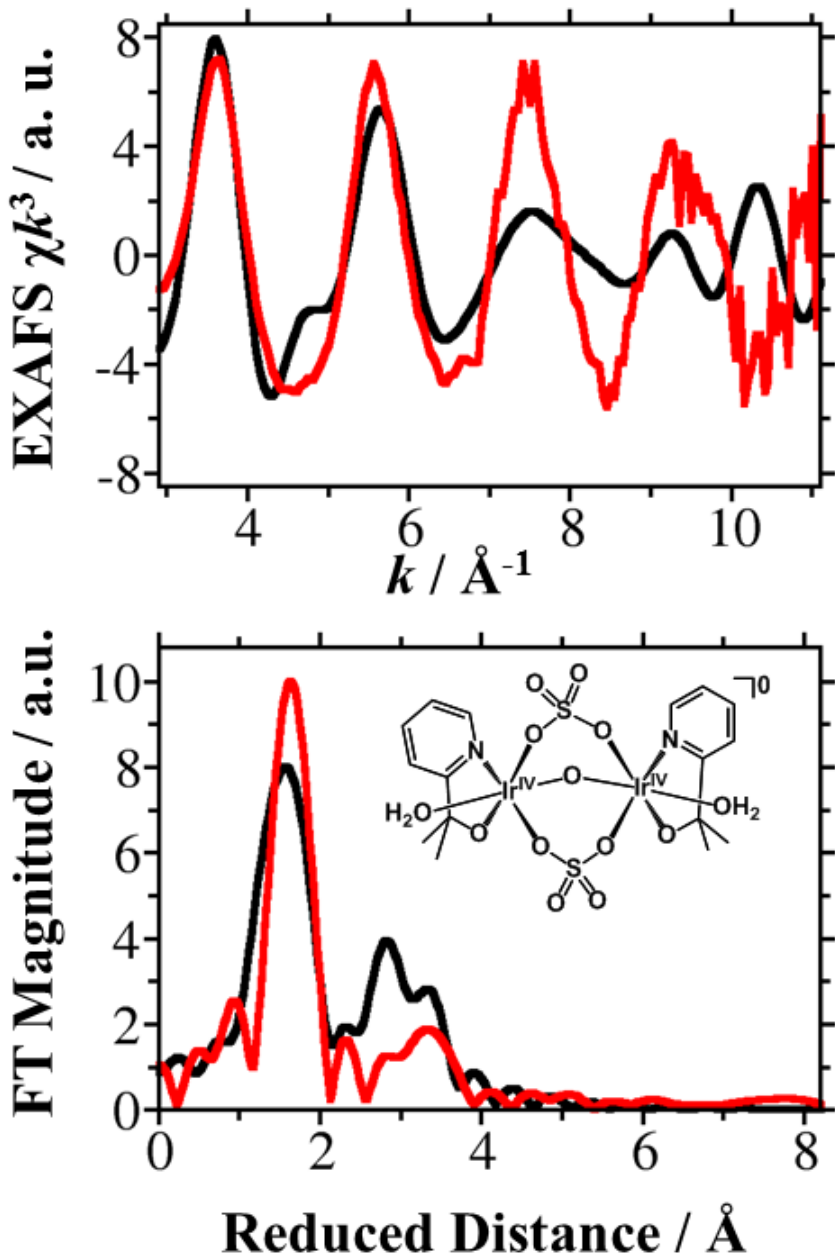


Figure S39. Simulated (black) EXAFS spectra of the mono- $\mu$ -O Ir dimer with  $\text{SO}_4^{2-}$  bridging to Ir centers ( $2\text{SO}_4^{2-}\text{-S10aa}$ ) and experimental (red) EXAFS spectra of the electrochemically activated Ir blue species in  $k$  space (top) and reduced distance  $R$  space (bottom).

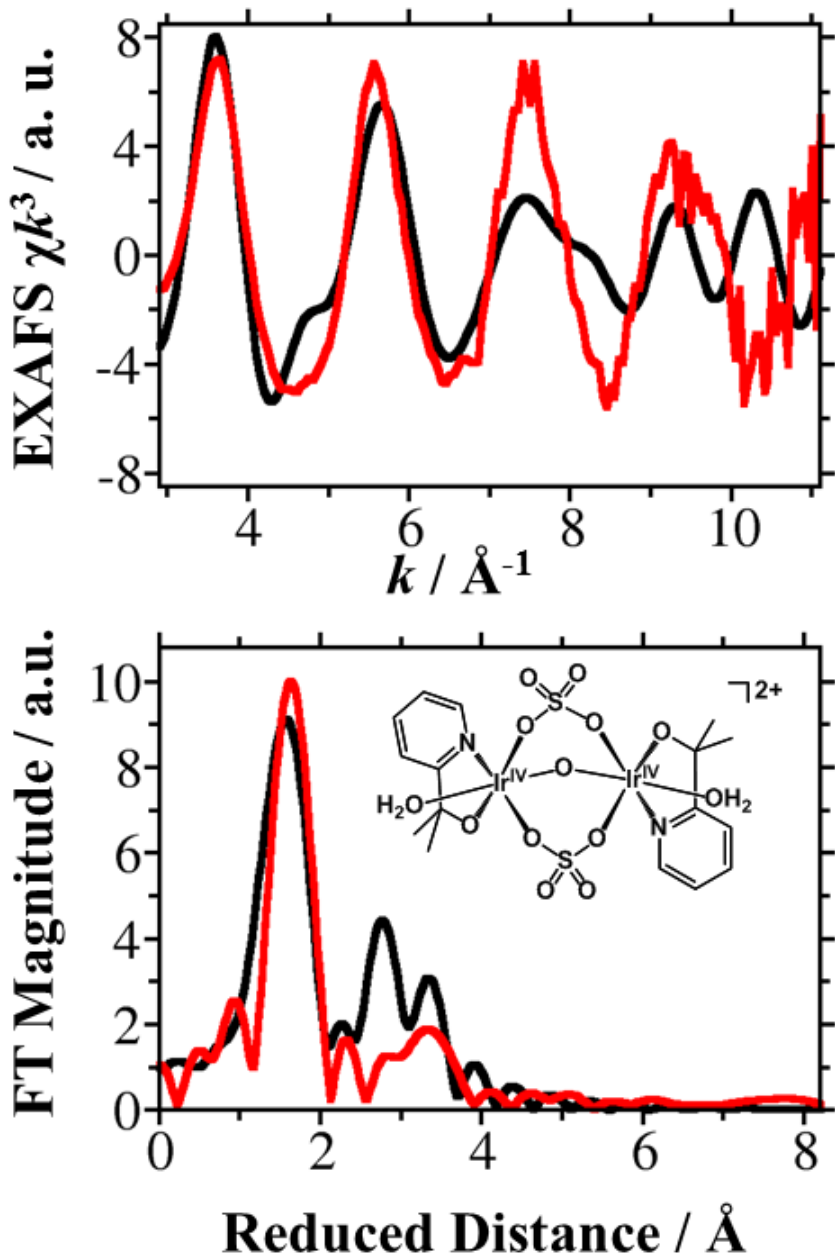


Figure S40. Simulated (black) EXAFS spectra of the mono- $\mu$ -O Ir dimer with  $\text{SO}_4^{2-}$  bridging to Ir centers ( $2\text{SO}_4^{2-}\text{-S10ab}$ ) and experimental (red) EXAFS spectra of the electrochemically activated Ir blue species in  $k$  space (top) and reduced distance  $R$  space (bottom).

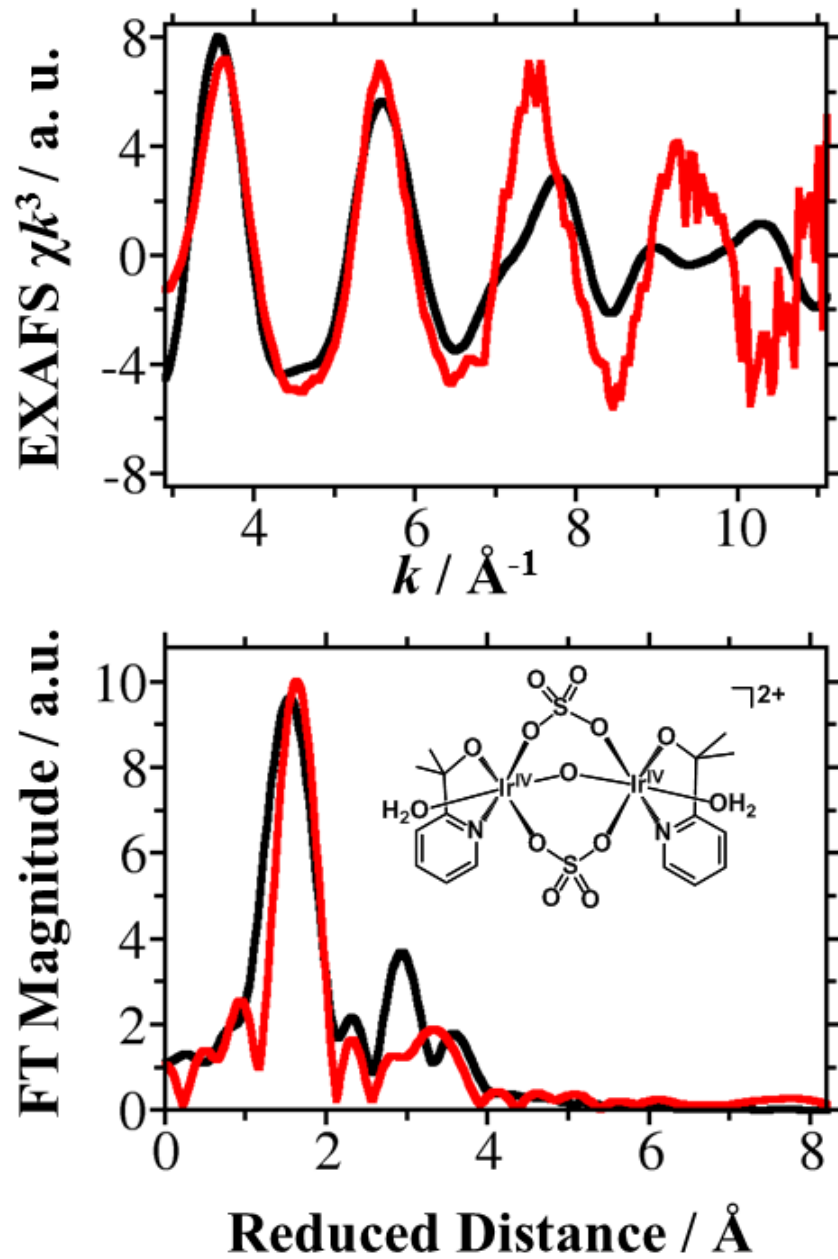


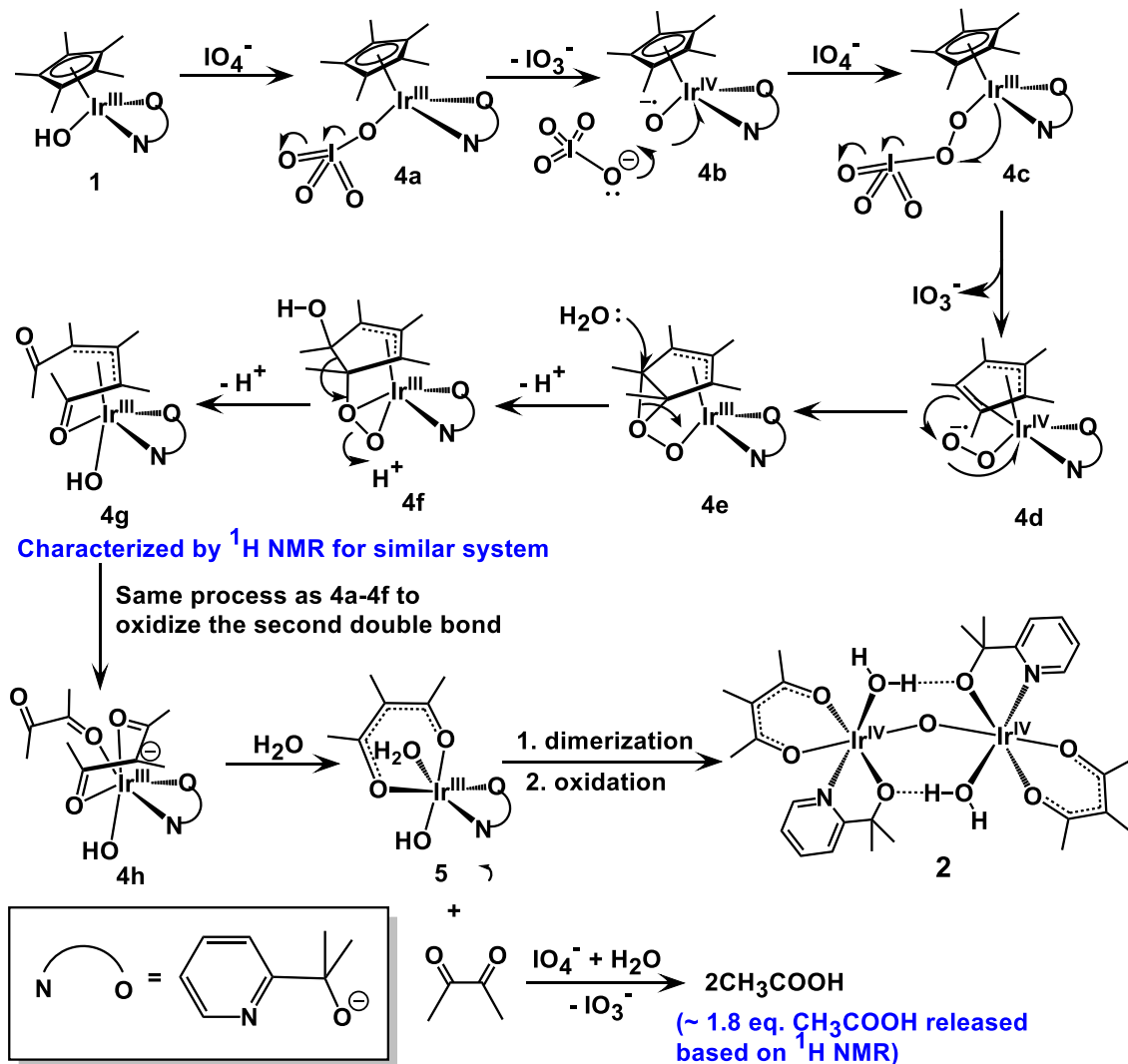
Figure S41. Simulated (black) EXAFS spectra of the mono- $\mu$ -O Ir dimer with  $\text{SO}_4^{2-}$  bridging to Ir centers ( $2\text{SO}_4^{2-}\text{-S10bb}$ ) and experimental (red) EXAFS spectra of the electrochemically activated Ir blue species in  $k$  space (top) and reduced distance  $R$  space (bottom).

### **3.6 Possible Degradation Pathways of Cp\***

It is of great interest to rationalize why different complexes are formed in chemically and electrochemically activated Ir blue solutions. Intermediate 4g was characterized by two-dimensional  $^1\text{H}$  NMR spectroscopy with the oxidation of diol to di-ketone and breaking of the Cp\* ring for a similar system.<sup>36</sup> Those intermediates enable us to propose the oxidation path of Cp\* as shown in Scheme S6. Degradation of Cp\* in complex **1** first involves the exchange of OH<sup>-</sup> by IO<sub>4</sub><sup>-</sup> to form intermediate 4a. Intermediate 4a can undergo O–I bond cleavage to form oxidized intermediate 4b through a 2-electron oxidation process. The electron deficient intermediate 4b could undergo nucleophilic attack by IO<sub>4</sub><sup>-</sup>, OH<sub>2</sub>, or the CH<sub>3</sub> group in the Cp\*. The nucleophilic attack of Ir<sup>IV</sup>–O<sup>•</sup> radical by IO<sub>4</sub><sup>-</sup> is likely to have a lower barrier than that by OH<sub>2</sub> or CH<sub>3</sub> since the substrate IO<sub>4</sub><sup>-</sup> is negative charged. Thus, the dominant path at the initial stage might be the nucleophilic attack of IO<sub>4</sub><sup>-</sup> to intermediate 4b to form intermediate 4c. The intermediate 4c could undergo O–I bond cleavage to form a superoxo intermediate 4d. Intermediate 4d then undergoes intramolecular epoxidation to form intermediate 4e, which has been confirmed by  $^1\text{H}$  NMR for similar systems.<sup>36</sup>

**Scheme S6. Proposed Reaction Path for the Oxidation of Cp\* by Sodium Periodate during the Chemical Activation of the Catalyst Precursor**

**Chemical Activation:**



The hydrolysis of epoxide 4e yields a diol-like intermediate 4f, for which the X-ray crystal structure has been obtained for the similar system of  $[\text{Cp}^*\text{Ir}(\text{bzpy})\text{NO}_3]$  (bzpy = 2-benzoylphyridine). The diol then undergoes diol cleavage to form the di-ketone intermediate 4g. The same procedure could happen again to oxidize another double bond in the  $\text{Cp}^*$  ring, resulting in 2-methyl-2-acetyl acetonate (macac) and diacetyl. The in situ

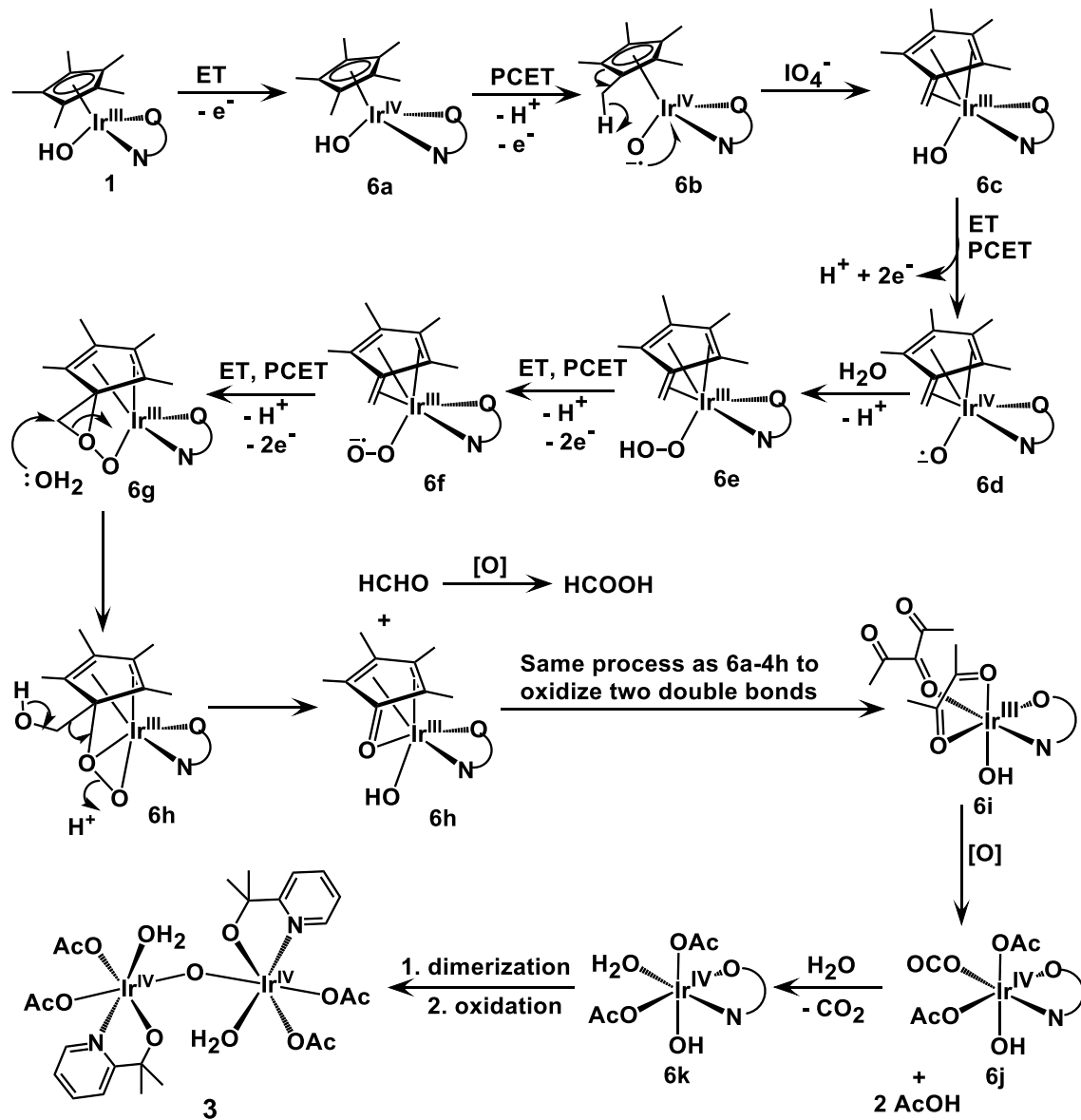
generated macac is a good chelating group that could chelate to Ir centers. The released diacetyl is known to be oxidized to 2 equivalents of acetic acid by periodate.<sup>37</sup> During the initial oxidation of complex **1**, two C=C double bonds are oxidized, to yield macac chelating to the Ir center and release 2 equivalence acetic acid to the solutions. Overall, the 6-electron donor Cp\* has been replaced by the 4-electron donor macac, leaving an open site that is occupied by a water molecule. The intermediate **5** could dimerize to form mono- $\mu$ -O Ir dimer **6**, which could further be oxidized to complex **2**.

The possible reaction path for degradation of Cp\* is proposed in Scheme S7 for the electrochemically activation of complex **1**. Since the OH<sub>2</sub> is not a good nucleophile without the aid of a base and Cp\*Ir<sup>III</sup> precatalysts are known to generate good catalysts for C–H oxidation,<sup>38–40</sup> we propose that C–H oxidation would be the dominant path. Thus, three double bonds would be generated in the Cp\* ring. The intermediate can be oxidized to generate 4 eq. of AcOH and HCOOH (ultimately CO<sub>2</sub>). Which is consistent with the experimental fact that 4 out of the 5 –C–CH<sub>3</sub> groups in the Cp\* are oxidized when a similar half-sandwich complex is reacted with cerium(IV) ammonium nitrate (CAN) as sacrificial oxidant.<sup>41</sup>

The degradation paths of Cp\* proposed in Scheme S6 and S7 needs to be confirmed either experimentally or computationally. A computational study of the degradation of Cp\* is currently being performed.

**Scheme S7. Proposed Reaction Path for the Oxidation of  $\text{Cp}^*$  by Electrochemical Activation of the Catalyst Precursor**

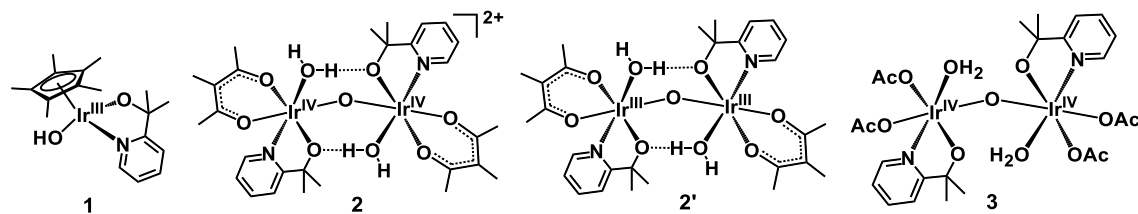
**Electrochemical Activation:**



### 3.7 Ligand Bond Lengths in Ir<sup>III</sup> and Ir<sup>IV</sup> Complexes

In this section, we discuss the ligand bond lengths in Ir<sup>III</sup> and Ir<sup>IV</sup> complexes. Four complexes are shown in Scheme S8. The structures of catalytic precursor **1**, and active species obtained from the present study in the chemically (**2**) and electrochemically (**3**) activated Ir blue solution, as well as complex **2** in lower oxidation states (**2'**) are shown in Scheme S8. For Ir<sup>III</sup> complexes, the metal center has 6 5d electrons, which would form a close shell electronic configuration in octahedral complexes. For Ir<sup>IV</sup> complexes, the metal center has 5 5d electrons, forming an open-shell electronic configuration in octahedral complexes, which has smaller HOMO-LUMO gap, which would be much easier to excite the electrons from HOMO orbital to LUMO orbitals. In our study, the chemically and electrochemically activated Ir solutions have intense blue color, consistent with our analysis of electronic structures of Ir<sup>IV</sup> complexes, as well as previous study on molecular Ir dimers which showed Ir<sup>III</sup> and Ir<sup>IV</sup> solutions are pale yellow and blue, respectively.<sup>35</sup>

**Scheme S8. Catalytic Precursor (1) and Active Species in Chemically (2) and Electrochemically (3) Activated Ir Blue Solutions, as well as 2 in Lower Oxidation State (2')**



DFT optimized ligand bond lengths of complexes **1**, **2**, **2'**, and **3** are given in Table S11. All ligand bond lengths shrink when go from the precursor **1** to either chemically (**2**) or electrochemically (**3**) activated Ir blue dimer. The  $\mu$ -oxo atom and the O atom in pyalc

group are good  $\pi$  donors. When the Ir center is oxidized from Ir<sup>III</sup> to Ir<sup>IV</sup>, the lone pairs on  $\mu$ -oxo atom and the O atom in pyalc group donate to metal center, forming partially Ir–O double bond, as shown by the shrinking of Ir–O bond lengths from 2.01 to 1.92 Å for Ir-oxo and from 2.05 to 1.95 Å for Ir–O bond length in pyalc group. The strong donating nature of O atoms in both  $\mu$ -oxo and pyalc groups stabilizes the Ir<sup>IV</sup> oxidation state, consistent with recent study on the high-valent Ir-pyalc model complexes.<sup>42</sup>

Table S11. Optimized ligand bond lengths (in Å) of complexes 1, 2, 2', and 3

complex 1	complex 2 (IV-IV)	complex 2' (III-III)	complex 3 (IV-IV)
Ir-OH	2.03	Ir-O	1.92
Ir-O(pyalc)	2.06	Ir-O(pyalc)	1.95
Ir-N(pyalc)	2.09	Ir-N(pyalc)	2.01
Ir-C1	2.21	Ir-OH <sub>2</sub>	2.13
Ir-C2	2.17	Ir-O(macac) <sup>a</sup>	2.03
Ir-C3	2.22	Ir-O(macac) <sup>b</sup>	2.02
Ir-C4	2.21		
Ir-C5	2.23		

<sup>a</sup> O atom in the trans-position of O atom in the pyalc group (O(pyalc))

<sup>b</sup> O atom in the trans-position of  $\mu$ -oxo atom

### **3.8 Comparison of Experimental Derived and DFT Optimized Structural Parameters**

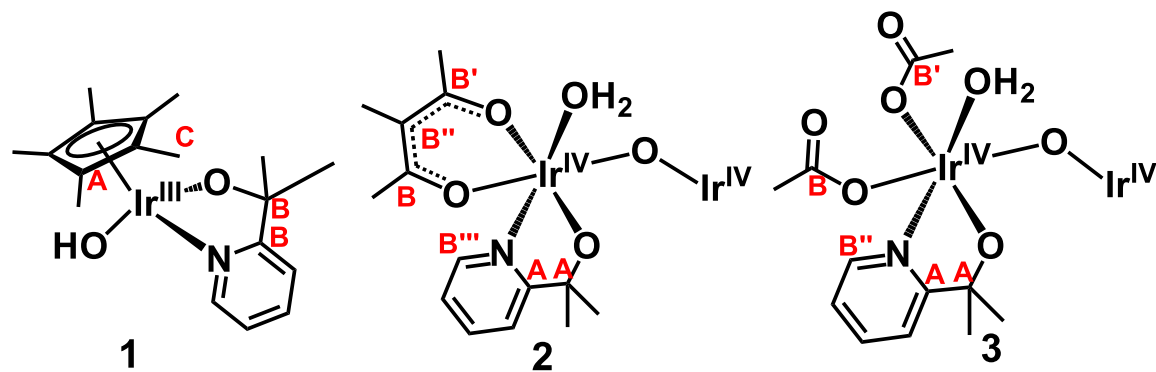
Among all complexes considered in sections 3.1 to 3.5, complexes **2** and **3** are most promising candidates as the active species in chemically and electrochemically activated Ir blue solutions, respectively. In section 1.2 and 1.3, we have extracted structural parameters from experimental HEXS and EXAFS data. It would be of great interest to see whether structural parameters from our DFT optimization are consistent with those derived from experimental HEXS and EXAFS data.

In our analysis of experimental EXAFS data, the structural parameters were derived with shell-model. To make a direct comparison of experimentally derived and DFT optimized structural parameters, we tentatively assign the coordination shells based on coordination numbers from the analysis of EXAFS data and our DFT optimized structures of **1**, **2**, and **3**. The assignments are shown in Scheme S9. The structural parameters derived from experimental EXAFS data and from DFT optimization, as well as their differences are shown in Table S12-S14 for complexes **1**, **2**, and **3**. In all cases, the DFT optimized bond distances agree well with the bond distances extracted from experimental EXAFS data, further confirming the reliability of complexes **2** and **3** as the candidates for the active species in chemically and electrochemically activated Ir blue solutions.

The pair distribution function (PDF), obtained from HEXS experiment of the chemically activated Ir blue solution, has four peaks at 2.06, 2.84, 3.40, and 4.47 Å, which corresponds to Ir–N/O (first-coordination shell), Ir–C, Ir–Ir, and Ir–C/N/O distances. The HEXS derived bond lengths and our DFT calculated bond lengths are

given in Table S15. The Ir–N/O and Ir–Ir distances agree well, while the agreement of Ir–C and Ir–C/N/O distance is slightly worse possible due to these two peaks corresponding to the average of many bond distances which may depend on different conformations.

**Scheme S9. Assignment of the Coordination Shells to Facilitate the Comparison of EXAFS derived and DFT Optimized Structural Parameters based on Coordination Numbers<sup>a</sup>**



<sup>a</sup>The ligands of only one Ir center are shown in Complexes **2** and **3**.

Table S12. Comparison Bond Distances (in Å) Obtained from Experimental EXAFS Spectrum of Precursor **1** and from DFT Optimization of Complex **1**

	EXAFS	DFT	DFT - EXAFS
Ir–O	2.01	2.08	0.07
Ir–N	2.05	2.10	0.05
Ir–C <sub>A</sub>	2.15	2.20	0.05
Ir–C <sub>B</sub>	2.93	2.95	0.02
Ir–C <sub>C</sub>	3.29	3.31	0.02

Table S13. Comparison Bond Distances (in Å) Obtained from Experimental EXAFS Spectrum of Chemically Activated Ir Blue Solution and from DFT Optimization of Complex 2

	EXAFS	DFT	DFT - EXAFS
Ir–O/N	2.00	2.01	0.01
Ir–C <sub>A</sub>	2.93	2.88	-0.05
Ir–C <sub>B</sub>	3.11	3.07	-0.04
Ir–Ir	3.36	3.45	0.09

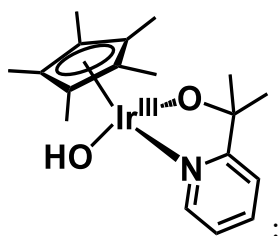
Table S14. Comparison Bond Distances (in Å) Obtained from Experimental EXAFS Spectrum of Electrochemically Activated Ir Blue Solution and from DFT Optimization of Complex 3

	EXAFS	DFT	DFT - EXAFS
Ir–O/N	2.04	2.01	-0.03
Ir–C <sub>A</sub>	2.81	2.84	0.03
Ir–C <sub>B</sub>	2.97	3.03	0.06
Ir–Ir	3.56	3.58	0.02

Table S15. Comparison Bond Distances (in Å) Obtained from Experimental EXAFS Spectrum of Chemically Activated Ir Blue Solution and from DFT Optimization of Complex 2

	HEXS	DFT	DFT - HEXS
Ir–O/N	2.06	2.01	-0.05
Ir–C	2.84	2.92	0.08
Ir–Ir	3.40	3.44	0.04
Ir–C/N/O	4.47	4.35	-0.12

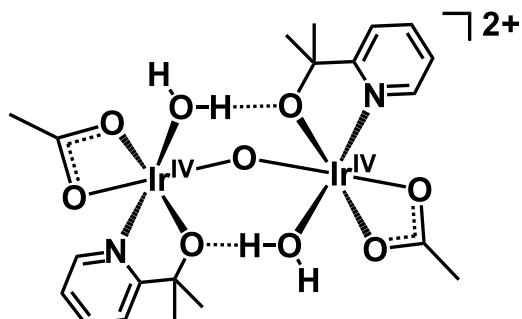
#### 4. Cartesian Coordinates



$E = -1011.15922049$  hartree

C	1.747509000	-0.929684000	1.175274000
C	2.474783000	-0.695991000	-0.072639000
C	2.500393000	0.740933000	-0.296559000
C	1.742621000	1.376938000	0.745794000
C	1.282886000	0.334427000	1.672459000
Ir	0.419013000	-0.021306000	-0.338904000
O	-0.794789000	-1.646409000	-0.773700000
N	-1.521390000	0.765365000	-0.129574000
C	-2.528489000	-0.144227000	-0.077294000
C	-1.804770000	2.087771000	-0.084381000
C	-3.858366000	0.267733000	0.047110000
C	-3.108987000	2.559092000	0.042051000
H	-0.955293000	2.753812000	-0.155477000
C	-4.156538000	1.631541000	0.110160000
H	-4.644681000	-0.474955000	0.092707000
H	-3.295376000	3.625289000	0.078427000
H	-5.183612000	1.965116000	0.206987000
C	-2.055943000	-1.593916000	-0.104806000
C	-1.907535000	-2.067238000	1.361169000
H	-2.867567000	-2.033221000	1.890894000
H	-1.528223000	-3.094916000	1.365172000
H	-1.187656000	-1.422793000	1.873648000
C	-3.035484000	-2.500503000	-0.864905000
H	-2.619400000	-3.513284000	-0.894212000
H	-4.013841000	-2.543136000	-0.372327000
H	-3.166590000	-2.139160000	-1.890991000
O	0.103017000	0.316473000	-2.347120000
H	-0.595544000	-0.338685000	-2.530822000
C	1.548763000	-2.278017000	1.794082000
H	2.491817000	-2.643460000	2.221881000
H	0.798588000	-2.244772000	2.587581000
H	1.212905000	-2.997196000	1.039631000
C	3.211136000	-1.734937000	-0.862217000
H	4.233215000	-1.874547000	-0.481810000
H	2.695323000	-2.699569000	-0.803307000
H	3.280156000	-1.445540000	-1.916307000

C	3.174191000	1.426365000	-1.442834000
H	3.127387000	0.806885000	-2.343629000
H	2.696573000	2.386813000	-1.660025000
H	4.231397000	1.613406000	-1.210355000
C	1.546985000	2.849260000	0.938853000
H	0.598471000	3.052267000	1.447071000
H	2.351713000	3.273374000	1.555408000
H	1.544895000	3.375887000	-0.021392000
C	0.518933000	0.593652000	2.934828000
H	1.181557000	0.983959000	3.719368000
H	-0.271379000	1.333656000	2.764525000
H	0.052524000	-0.321972000	3.309683000

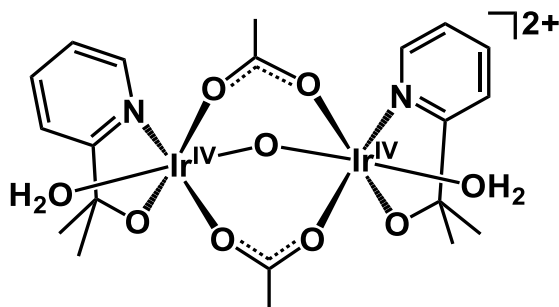


2AcO<sup>-</sup>\_S5bb:

$E = -1775.28249074$  hartree

Ir	-1.612159000	-0.566819000	-0.394518000
Ir	1.612234000	0.566790000	-0.394362000
O	-0.000012000	0.000015000	0.450504000
O	-1.725003000	-2.508139000	0.424318000
O	-3.230078000	-1.790766000	-0.959383000
O	-0.583090000	-1.322510000	-2.096288000
O	1.724959000	2.508169000	0.424333000
O	3.230207000	1.790714000	-0.959139000
O	0.583332000	1.322342000	-2.096295000
H	-0.942562000	-2.140568000	-2.487682000
H	-0.403692000	1.431681000	-1.974693000
C	-2.823024000	-2.763130000	-0.209584000
C	-3.565362000	-4.038752000	-0.062064000
H	-4.268305000	-3.947766000	0.776977000
H	-4.137512000	-4.251909000	-0.967836000
H	-2.873980000	-4.855809000	0.156761000
O	1.960539000	-1.078410000	-1.328221000
C	2.823087000	2.763103000	-0.209412000
C	3.565336000	4.038784000	-0.061952000
H	2.873797000	4.855934000	0.156058000
H	4.267689000	3.948170000	0.777620000
H	4.138079000	4.251566000	-0.967433000
N	2.651571000	-0.301554000	1.076947000
C	2.963641000	0.286885000	2.259133000
C	3.046966000	-1.572742000	0.796777000
C	3.705094000	-0.393949000	3.216823000
H	2.603638000	1.296436000	2.401642000
C	3.794411000	-2.293677000	1.726775000
C	4.129458000	-1.702055000	2.946934000
H	3.941703000	0.093831000	4.153082000
H	4.102585000	-3.304468000	1.493554000
H	4.709311000	-2.252200000	3.677808000
C	2.592374000	-2.147260000	-0.531444000
C	3.767987000	-2.668527000	-1.362870000
H	4.259383000	-3.499498000	-0.846831000

H	3.390598000	-3.027542000	-2.325070000
H	4.496167000	-1.869631000	-1.533024000
C	1.519507000	-3.223427000	-0.294279000
H	1.198533000	-3.634661000	-1.256684000
H	1.935708000	-4.038428000	0.306511000
H	0.660349000	-2.800968000	0.232976000
O	-1.960337000	1.078308000	-1.328556000
N	-2.651679000	0.301644000	1.076595000
C	-2.963871000	-0.286686000	2.258802000
C	-3.047083000	1.572791000	0.796253000
C	-3.705447000	0.394223000	3.216343000
H	-2.603860000	-1.296215000	2.401453000
C	-3.794654000	2.293797000	1.726095000
C	-4.129816000	1.702290000	2.946276000
H	-3.942147000	-0.093470000	4.152624000
H	-4.102828000	3.304557000	1.492737000
H	-4.709765000	2.252494000	3.677031000
C	-2.592365000	2.147193000	-0.531976000
C	-3.767913000	2.668274000	-1.363611000
H	-4.259451000	3.499256000	-0.847724000
H	-3.390429000	3.027221000	-2.325799000
H	-4.496001000	1.869296000	-1.533776000
C	-1.519627000	3.223481000	-0.294784000
H	-1.198625000	3.634703000	-1.257184000
H	-1.935960000	4.038468000	0.305933000
H	-0.660465000	2.801139000	0.232558000
H	0.403914000	-1.431924000	-1.974576000
H	0.942783000	2.140431000	-2.487644000

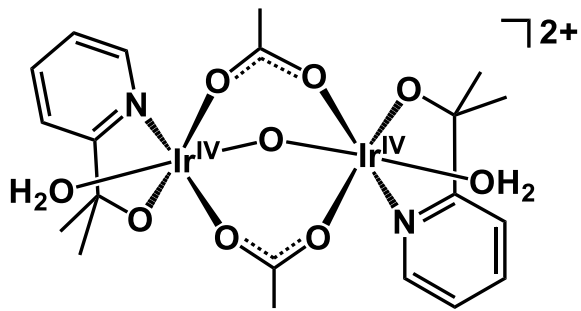


2AcO<sup>-</sup>\_S10aa:

*E* = -1775.29665672 hartree

Ir	1.695914000	-0.619362000	0.089424000
Ir	-1.609350000	-0.597194000	-0.075988000
O	0.047246000	0.312934000	0.016210000
O	2.285843000	0.049611000	1.770942000
O	3.565375000	-1.675525000	-0.094178000
O	1.125592000	-2.399566000	0.969349000
O	-2.351477000	-0.034663000	1.582611000
O	-3.472737000	-1.595124000	-0.503720000
O	-1.140659000	-2.434701000	0.745780000
O	1.260899000	-1.454647000	-1.768663000
O	-1.022904000	-1.337747000	-1.930191000
C	-0.024303000	-2.943862000	1.111398000
C	-0.070915000	-4.283126000	1.792947000
H	-0.174731000	-4.123419000	2.874052000
H	-0.933105000	-4.855953000	1.445128000
H	0.854817000	-4.833647000	1.612945000
C	0.146086000	-1.619211000	-2.383011000
C	0.216397000	-2.152188000	-3.787305000
H	-0.682434000	-2.727082000	-4.020580000
H	1.110652000	-2.765033000	-3.917159000
H	0.273020000	-1.303715000	-4.482021000
N	2.510565000	1.094324000	-0.609202000
C	2.910344000	1.940684000	0.376973000
C	2.652939000	1.424743000	-1.915395000
C	3.486623000	3.168972000	0.057618000
C	3.219472000	2.639462000	-2.285465000
H	2.306334000	0.692595000	-2.632233000
C	3.644474000	3.523857000	-1.284940000
H	3.801046000	3.833437000	0.851847000
H	3.323743000	2.883458000	-3.334486000
H	4.089648000	4.475832000	-1.547890000
C	2.626880000	1.475629000	1.793902000
C	1.377071000	2.198730000	2.336687000
H	1.179283000	1.849277000	3.354660000
H	1.541194000	3.281616000	2.351805000
H	0.516422000	1.972968000	1.699803000

C	3.839694000	1.631005000	2.713091000
H	4.110575000	2.686803000	2.816806000
H	3.587140000	1.236965000	3.702185000
H	4.695440000	1.079823000	2.310551000
N	-2.341627000	1.160905000	-0.744076000
C	-3.003883000	1.869696000	0.207213000
C	-2.151852000	1.662795000	-1.988219000
C	-3.519744000	3.130597000	-0.089880000
C	-2.646306000	2.915350000	-2.333346000
H	-1.604856000	1.033254000	-2.676814000
C	-3.341338000	3.660161000	-1.370515000
H	-4.048256000	3.684444000	0.675246000
H	-2.488109000	3.296341000	-3.333657000
H	-3.735358000	4.639295000	-1.614556000
C	-3.146990000	1.196990000	1.560308000
C	-2.598892000	2.081773000	2.688454000
H	-3.169579000	3.014104000	2.752825000
H	-2.692808000	1.544847000	3.637195000
H	-1.545826000	2.317644000	2.508742000
C	-4.609563000	0.786950000	1.803088000
H	-4.680282000	0.280406000	2.770712000
H	-5.253193000	1.673028000	1.816507000
H	-4.943167000	0.108066000	1.012560000
H	3.998690000	-1.633762000	-0.968738000
H	3.455375000	-2.623863000	0.121102000
H	-3.713886000	-1.595428000	-1.450836000
H	-3.440335000	-2.532738000	-0.224104000

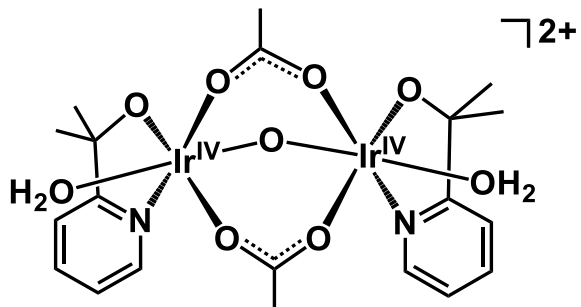


2AcO<sup>-</sup>\_S10ab:

*E* = -1775.29589835 hartree

Ir	-0.901819000	1.372033000	-0.601388000
Ir	0.901819000	-1.372033000	-0.601388000
O	0.000000000	0.000000000	0.348822000
O	0.000000000	2.811825000	0.266414000
O	-2.043986000	2.852530000	-1.694771000
O	0.405011000	1.501920000	-2.214456000
O	0.000000000	-2.811825000	0.266414000
O	2.043986000	-2.852530000	-1.694771000
O	2.021930000	-0.007094000	-1.666189000
O	-2.021930000	0.007094000	-1.666189000
O	-0.405011000	-1.501920000	-2.214456000
C	1.567617000	0.982965000	-2.353519000
C	2.489418000	1.585254000	-3.373580000
H	3.256726000	2.172451000	-2.852732000
H	2.995306000	0.794847000	-3.934995000
H	1.938191000	2.242371000	-4.047827000
C	-1.567617000	-0.982965000	-2.353519000
C	-2.489418000	-1.585254000	-3.373580000
H	-1.938191000	-2.242371000	-4.047827000
H	-2.995306000	-0.794847000	-3.934995000
H	-3.256726000	-2.172451000	-2.852732000
N	-2.156814000	1.514098000	0.967786000
C	-1.735823000	2.390583000	1.918394000
C	-3.308897000	0.816279000	1.116163000
C	-2.496637000	2.594203000	3.068396000
C	-4.100619000	0.983333000	2.246816000
H	-3.561532000	0.138202000	0.311951000
C	-3.690037000	1.886559000	3.236470000
H	-2.152405000	3.293810000	3.818717000
H	-5.016795000	0.416288000	2.346445000
H	-4.289748000	2.034694000	4.126434000
C	-0.392910000	3.050048000	1.658434000
C	0.691482000	2.374224000	2.523451000
H	1.655883000	2.847290000	2.313754000
H	0.455589000	2.495411000	3.586379000
H	0.747283000	1.308712000	2.281596000

C	-0.438496000	4.565792000	1.863039000
H	-0.664928000	4.804949000	2.907356000
H	0.541179000	4.985189000	1.614354000
H	-1.200058000	5.016341000	1.218747000
N	2.156814000	-1.514098000	0.967786000
C	1.735823000	-2.390583000	1.918394000
C	3.308897000	-0.816279000	1.116163000
C	2.496637000	-2.594203000	3.068396000
C	4.100619000	-0.983333000	2.246816000
H	3.561532000	-0.138202000	0.311951000
C	3.690037000	-1.886559000	3.236470000
H	2.152405000	-3.293810000	3.818717000
H	5.016795000	-0.416288000	2.346445000
H	4.289748000	-2.034694000	4.126434000
C	0.392910000	-3.050048000	1.658434000
C	0.438496000	-4.565792000	1.863039000
H	0.664928000	-4.804949000	2.907356000
H	-0.541179000	-4.985189000	1.614354000
H	1.200058000	-5.016341000	1.218747000
C	-0.691482000	-2.374224000	2.523451000
H	-1.655883000	-2.847290000	2.313754000
H	-0.455589000	-2.495411000	3.586379000
H	-0.747283000	-1.308712000	2.281596000
H	-2.902103000	2.509106000	-2.014030000
H	-1.556693000	3.145548000	-2.491455000
H	1.556693000	-3.145548000	-2.491455000
H	2.902103000	-2.509106000	-2.014030000

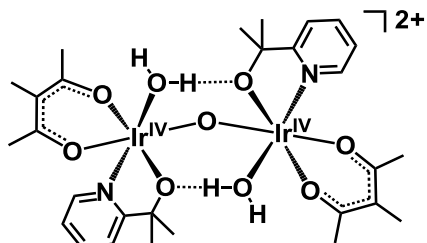


2AcO<sup>-</sup>\_S10bb:

*E* = -1775.29658856 hartree

Ir	-1.609088000	-0.594977000	-0.071795000
Ir	1.696494000	-0.616569000	0.090704000
O	0.047847000	0.315314000	0.012957000
O	-2.349636000	-0.019752000	1.583145000
O	-3.473072000	-1.595472000	-0.490377000
O	-1.023276000	-1.349483000	-1.920756000
O	2.287492000	0.062702000	1.767723000
O	3.565892000	-1.673903000	-0.088089000
O	1.260574000	-1.464782000	-1.761640000
O	-1.140188000	-2.426881000	0.762513000
O	1.126584000	-2.391443000	0.981607000
C	0.144681000	-1.643748000	-2.369029000
C	0.199452000	-2.272594000	-3.734073000
H	-0.494454000	-1.762146000	-4.407798000
H	1.214168000	-2.237559000	-4.133190000
H	-0.119094000	-3.319729000	-3.654010000
C	-0.023448000	-2.933828000	1.130096000
C	-0.069684000	-4.267800000	1.821949000
H	0.857202000	-4.818418000	1.648448000
H	-0.930286000	-4.844536000	1.476585000
H	-0.176541000	-4.099756000	2.901492000
N	-2.339924000	1.159033000	-0.751953000
C	-3.001426000	1.875114000	0.194413000
C	-2.148504000	1.652476000	-1.999173000
C	-3.515286000	3.134769000	-0.111286000
C	-2.640943000	2.903456000	-2.352828000
H	-1.601795000	1.017657000	-2.683145000
C	-3.335487000	3.655554000	-1.395346000
H	-4.043167000	3.694604000	0.649894000
H	-2.481489000	3.277638000	-3.355518000
H	-3.727938000	4.633642000	-1.646041000
C	-3.145362000	1.211650000	1.552007000
C	-4.607985000	0.802978000	1.796885000
H	-4.678939000	0.302823000	2.767814000
H	-5.251753000	1.689025000	1.804306000
H	-4.941209000	0.118789000	1.010797000

C	-2.598191000	2.104229000	2.674425000
H	-3.169328000	3.036727000	2.732129000
H	-2.692450000	1.573730000	3.626739000
H	-1.545117000	2.339334000	2.493748000
N	2.509647000	1.093486000	-0.618605000
C	2.909348000	1.946042000	0.362221000
C	2.650014000	1.416601000	-1.926810000
C	3.483805000	3.173160000	0.035183000
C	3.214659000	2.629860000	-2.304509000
H	2.302979000	0.680170000	-2.639000000
C	3.639775000	3.520481000	-1.309569000
H	3.798177000	3.842591000	0.825262000
H	3.317317000	2.868036000	-3.355027000
H	4.083467000	4.471475000	-1.578504000
C	2.627555000	1.489062000	1.782071000
C	3.841159000	1.650725000	2.699108000
H	4.111345000	2.707335000	2.796160000
H	3.589899000	1.262464000	3.690812000
H	4.696886000	1.097760000	2.298987000
C	1.377776000	2.214455000	2.321851000
H	1.181434000	1.871100000	3.342175000
H	1.541048000	3.297544000	2.330133000
H	0.516594000	1.984073000	1.687346000
H	-3.439316000	-2.532384000	-0.208649000
H	-3.718953000	-1.597862000	-1.436255000
H	3.455991000	-2.620756000	0.133702000
H	3.997741000	-1.638206000	-0.963658000

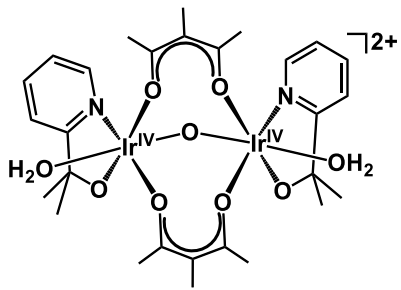


2macac\_S5bb:

$E = -2087.35359901$  hartree

Ir	1.722979000	0.044299000	-0.459800000
Ir	-1.723106000	-0.044518000	-0.459715000
O	-0.000035000	-0.000221000	0.378879000
O	2.094738000	1.822295000	0.436051000
O	3.575504000	0.190894000	-1.252804000
O	1.011732000	1.148771000	-2.130657000
O	-2.095273000	-1.822272000	0.436415000
O	-3.575609000	-0.190811000	-1.252773000
O	-1.011637000	-1.148632000	-2.130656000
H	1.596333000	1.893139000	-2.366235000
H	-0.084048000	-1.519540000	-1.951349000
O	-1.425937000	1.633075000	-1.408421000
N	-2.374797000	1.167043000	0.999241000
C	-2.762687000	0.759445000	2.233139000
C	-2.357990000	2.487282000	0.673180000
C	-3.185784000	1.673259000	3.189541000
H	-2.716595000	-0.302162000	2.423408000
C	-2.777751000	3.442994000	1.599301000
C	-3.199931000	3.037140000	2.866434000
H	-3.493683000	1.321087000	4.165241000
H	-2.765649000	4.489500000	1.323614000
H	-3.527496000	3.770232000	3.593540000
C	-1.867698000	2.846064000	-0.719294000
C	-3.013829000	3.441282000	-1.551539000
H	-3.386894000	4.362064000	-1.090686000
H	-2.640462000	3.670746000	-2.554497000
H	-3.831224000	2.716926000	-1.626793000
C	-0.652141000	3.782866000	-0.640105000
H	-0.321815000	4.020928000	-1.656923000
H	-0.918621000	4.718502000	-0.137850000
H	0.163713000	3.301447000	-0.091154000
O	1.426100000	-1.633405000	-1.408439000
N	2.375081000	-1.167134000	0.999082000
C	2.763406000	-0.759377000	2.232806000
C	2.358671000	-2.487365000	0.673031000
C	3.187304000	-1.673032000	3.188997000
H	2.717009000	0.302215000	2.423088000
C	2.779249000	-3.442927000	1.598943000

C	3.201858000	-3.036912000	2.865875000
H	3.495532000	-1.320753000	4.164556000
H	2.767434000	-4.489431000	1.323230000
H	3.530078000	-3.769865000	3.592825000
C	1.867714000	-2.846346000	-0.719139000
C	3.013194000	-3.442296000	-1.551727000
H	3.386118000	-4.363074000	-1.090751000
H	2.639265000	-3.671951000	-2.554431000
H	3.830866000	-2.718318000	-1.627612000
C	0.651809000	-3.782651000	-0.639076000
H	0.321108000	-4.021168000	-1.655666000
H	0.918066000	-4.718092000	-0.136333000
H	-0.163723000	-3.300602000	-0.090201000
H	0.083685000	1.518807000	-1.951617000
H	-1.596697000	-1.892126000	-2.367855000
C	3.275080000	2.273905000	0.768661000
C	4.507795000	1.708964000	0.375422000
C	3.227594000	3.509538000	1.626406000
C	4.597015000	0.755391000	-0.660554000
C	5.790058000	2.280159000	0.952234000
H	3.500579000	3.257825000	2.660665000
H	3.940490000	4.262659000	1.276466000
H	2.216581000	3.922277000	1.623411000
C	5.931069000	0.354597000	-1.228528000
H	6.572346000	1.517211000	0.994021000
H	6.173412000	3.117447000	0.351595000
H	5.635060000	2.644961000	1.970885000
H	6.545452000	1.232024000	-1.456620000
H	6.482990000	-0.244974000	-0.491883000
H	5.785865000	-0.242172000	-2.131161000
C	-4.597264000	-0.755078000	-0.660501000
C	-4.508300000	-1.708422000	0.375670000
C	-5.931186000	-0.354168000	-1.228732000
C	-3.275679000	-2.273471000	0.769191000
C	-5.790672000	-2.279458000	0.952403000
H	-6.545747000	-1.231539000	-1.456562000
H	-6.483042000	0.245825000	-0.492391000
H	-5.785742000	0.242221000	-2.131578000
C	-3.228536000	-3.508798000	1.627391000
H	-6.173459000	-3.117422000	0.352337000
H	-5.636055000	-2.643286000	1.971458000
H	-6.573228000	-1.516739000	0.993132000
H	-3.502403000	-3.256815000	2.661344000
H	-3.941051000	-4.262166000	1.277153000
H	-2.217455000	-3.921360000	1.625251000

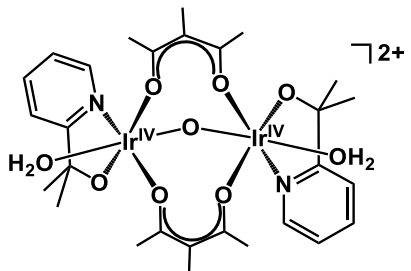


2macac\_S10aa:

$E = -2087.28663177$  hartree

Ir	-1.442952000	-0.999786000	-0.319973000
Ir	1.533862000	0.570506000	0.365199000
O	-0.373582000	0.483717000	0.158083000
O	-2.494615000	-0.142921000	-1.683564000
O	-2.631549000	-2.798636000	-0.693520000
O	0.082575000	-1.701137000	-1.465502000
O	1.902381000	1.485599000	-1.271967000
O	3.631766000	0.894819000	0.866896000
O	2.475115000	-1.159092000	-0.332356000
O	-0.494831000	-1.956432000	1.206584000
O	1.468498000	-0.238246000	2.260736000
N	-2.918238000	-0.308968000	0.893012000
C	-3.870493000	0.417326000	0.252392000
C	-2.988309000	-0.520922000	2.230986000
C	-4.953229000	0.942047000	0.958041000
C	-4.044205000	-0.015208000	2.980942000
H	-2.180152000	-1.098132000	2.659723000
C	-5.045254000	0.723245000	2.334748000
H	-5.703919000	1.517468000	0.431697000
H	-4.078913000	-0.197469000	4.047138000
H	-5.879561000	1.125789000	2.896606000
C	-3.629882000	0.660478000	-1.225239000
C	-3.248747000	2.138755000	-1.431694000
H	-2.995600000	2.300401000	-2.483797000
H	-4.090399000	2.785457000	-1.160758000
H	-2.386500000	2.393865000	-0.809645000
C	-4.838468000	0.260330000	-2.079311000
H	-5.711695000	0.867015000	-1.816930000
H	-4.598084000	0.429323000	-3.133601000
H	-5.082937000	-0.796192000	-1.929387000
N	1.010458000	2.416821000	1.004507000
C	0.946524000	3.327943000	-0.000783000
C	0.655062000	2.739925000	2.269939000
C	0.514411000	4.628279000	0.259686000
C	0.221286000	4.024146000	2.581265000
H	0.729147000	1.943654000	2.998599000
C	0.147615000	4.982166000	1.560761000

H	0.464617000	5.345730000	-0.549275000
H	-0.056983000	4.263328000	3.599438000
H	-0.192984000	5.987865000	1.776343000
C	1.337337000	2.826811000	-1.381526000
C	0.093476000	2.674433000	-2.277169000
H	-0.471494000	3.611514000	-2.328283000
H	0.419549000	2.398415000	-3.285071000
H	-0.548655000	1.886504000	-1.876697000
C	2.406233000	3.721079000	-2.018744000
H	2.695853000	3.291403000	-2.982877000
H	2.014607000	4.729807000	-2.187843000
H	3.286561000	3.782506000	-1.370756000
H	-2.920966000	-2.853610000	-1.625002000
H	-3.442792000	-2.866494000	-0.153468000
H	3.773039000	1.076075000	1.816442000
H	4.101145000	0.057607000	0.668317000
C	0.609347000	-1.244879000	-2.566829000
C	2.837293000	-1.403274000	-1.569998000
C	0.475577000	-2.832697000	1.202462000
C	1.882610000	-1.418430000	2.666118000
C	2.010261000	-1.270224000	-2.701116000
C	1.565148000	-2.660635000	2.082464000
C	-0.273106000	-0.821943000	-3.704522000
H	-0.096158000	0.234775000	-3.943694000
H	-0.028418000	-1.398740000	-4.605367000
H	-1.322707000	-0.956156000	-3.449872000
C	2.608281000	-1.124900000	-4.088568000
H	2.340994000	-1.963909000	-4.745607000
H	2.236173000	-0.208695000	-4.565604000
H	3.697267000	-1.054252000	-4.056818000
C	4.288754000	-1.795471000	-1.698137000
H	4.907262000	-0.897331000	-1.845806000
H	4.612554000	-2.278301000	-0.770869000
H	4.465018000	-2.466868000	-2.541941000
C	0.313146000	-4.068563000	0.364115000
H	1.237239000	-4.290544000	-0.178898000
H	0.090571000	-4.932034000	1.006093000
H	-0.505784000	-3.934336000	-0.340397000
C	2.433599000	-3.850835000	2.455605000
H	2.244214000	-4.174048000	3.488744000
H	2.244313000	-4.705875000	1.804763000
H	3.499304000	-3.603874000	2.382006000
C	2.840864000	-1.363213000	3.827812000
H	3.871071000	-1.497715000	3.464484000
H	2.771904000	-0.388280000	4.316393000
H	2.649884000	-2.161991000	4.551130000

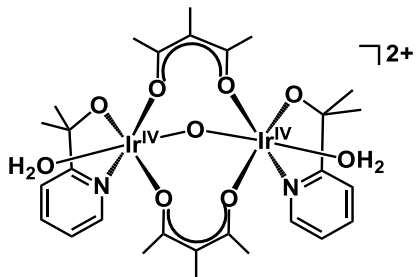


2macac\_S10ab:

$E = -2087.28446324$  hartree

Ir	-1.618017000	-0.415595000	0.130513000
Ir	1.559666000	0.721042000	-0.553240000
O	0.271712000	-0.555677000	0.009542000
O	-1.617826000	-1.065895000	1.955396000
O	-3.795495000	-0.449395000	0.372752000
O	-1.247655000	1.531275000	0.636193000
O	2.119341000	-0.349889000	-2.037994000
O	3.199070000	2.033881000	-1.174111000
O	1.469254000	2.084431000	0.969573000
O	-2.082248000	0.081867000	-1.769006000
O	0.144296000	1.523537000	-1.811988000
N	-1.712248000	-2.398798000	-0.288014000
C	-1.476854000	-3.191444000	0.791320000
C	-1.917790000	-2.932547000	-1.515956000
C	-1.433474000	-4.578024000	0.646968000
C	-1.884983000	-4.308902000	-1.710985000
H	-2.099119000	-2.224030000	-2.312716000
C	-1.635476000	-5.144778000	-0.614137000
H	-1.240785000	-5.197598000	1.513234000
H	-2.046456000	-4.713262000	-2.701718000
H	-1.598931000	-6.220175000	-0.740661000
C	-1.239657000	-2.468768000	2.108638000
C	0.257212000	-2.513352000	2.477126000
H	0.401736000	-1.979101000	3.421934000
H	0.585577000	-3.551695000	2.600493000
H	0.848874000	-2.033830000	1.694868000
C	-2.112242000	-3.044377000	3.230225000
H	-1.840890000	-4.085007000	3.436908000
H	-1.951110000	-2.455065000	4.138400000
H	-3.170771000	-3.000238000	2.953760000
N	2.903423000	-0.398027000	0.464575000
C	3.370851000	-1.448556000	-0.261470000
C	3.288651000	-0.211888000	1.749982000
C	4.259524000	-2.357877000	0.311835000
C	4.172207000	-1.090937000	2.366084000
H	2.865828000	0.648151000	2.249417000
C	4.664287000	-2.181924000	1.637282000

H	4.620354000	-3.191901000	-0.276015000
H	4.461907000	-0.924059000	3.395321000
H	5.349925000	-2.884397000	2.095738000
C	2.831119000	-1.575961000	-1.676278000
C	3.958536000	-1.752185000	-2.698529000
H	4.500667000	-2.686516000	-2.518773000
H	3.522253000	-1.789205000	-3.701647000
H	4.659904000	-0.913664000	-2.639460000
C	1.804037000	-2.724862000	-1.745586000
H	1.426287000	-2.798264000	-2.770316000
H	2.276424000	-3.674237000	-1.469375000
H	0.973613000	-2.520514000	-1.066094000
H	-4.272317000	0.383084000	0.199275000
H	-4.038582000	-0.730603000	1.276315000
H	3.149271000	2.331347000	-2.102503000
H	3.273888000	2.832331000	-0.617008000
C	-1.409862000	2.151270000	1.767335000
C	0.928980000	2.966170000	1.760519000
C	-2.635824000	1.244251000	-2.140209000
C	-0.606289000	2.557831000	-1.720993000
C	-0.413442000	3.048414000	2.202291000
C	-1.975882000	2.465103000	-2.141219000
C	-2.680593000	1.902723000	2.532934000
H	-3.533467000	2.330572000	1.988246000
H	-2.830771000	0.822618000	2.615310000
H	-2.659565000	2.325236000	3.537134000
C	-0.747302000	4.090783000	3.259459000
H	-1.825329000	4.249007000	3.331816000
H	-0.376887000	3.810623000	4.255508000
H	-0.299830000	5.057564000	3.005256000
C	1.940263000	3.936797000	2.332419000
H	2.946062000	3.655219000	2.014384000
H	1.723765000	4.956140000	1.985892000
H	1.896896000	3.954608000	3.427346000
C	-4.093213000	1.121751000	-2.522177000
H	-4.276772000	1.513658000	-3.529376000
H	-4.392940000	0.072317000	-2.486860000
H	-4.728521000	1.702361000	-1.838583000
C	-2.714069000	3.754659000	-2.438538000
H	-2.135652000	4.396588000	-3.113248000
H	-3.682867000	3.570709000	-2.905646000
H	-2.891595000	4.327232000	-1.516772000
C	-0.054936000	3.859609000	-1.224872000
H	1.002331000	3.759209000	-0.983494000
H	-0.182277000	4.639502000	-1.984928000
H	-0.601569000	4.182665000	-0.330982000

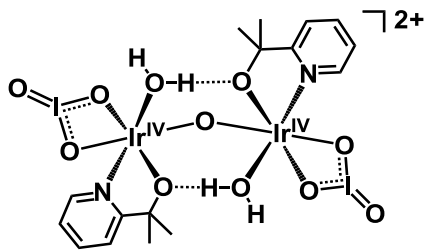


2macac\_S10bb:

$E = -2087.26650863$  hartree

Ir	1.565031000	-0.126527000	0.751148000
Ir	-1.315506000	-0.217649000	-0.929323000
O	-0.108693000	0.614161000	0.237166000
O	2.683984000	0.166391000	-0.773269000
O	3.349204000	-0.892930000	1.742761000
O	0.634432000	-0.369021000	2.549959000
O	-1.499354000	1.286273000	-2.116490000
O	-2.790966000	-1.218770000	-2.188660000
O	-1.295498000	-1.980030000	0.071067000
O	1.280686000	-2.133159000	0.534317000
O	0.215853000	-0.773744000	-2.169177000
N	2.044906000	1.807549000	1.131326000
C	2.691985000	2.424183000	0.109548000
C	1.720351000	2.481012000	2.260704000
C	3.040705000	3.770647000	0.205477000
C	2.046232000	3.824995000	2.406983000
H	1.199013000	1.909179000	3.016029000
C	2.716265000	4.480247000	1.364618000
H	3.553072000	4.249324000	-0.618979000
H	1.777084000	4.345051000	3.317125000
H	2.978471000	5.527660000	1.453880000
C	2.939026000	1.565083000	-1.116685000
C	4.387650000	1.653322000	-1.603829000
H	4.518220000	0.967103000	-2.446331000
H	4.616241000	2.669225000	-1.942574000
H	5.082027000	1.380347000	-0.802563000
C	1.933879000	1.938648000	-2.222833000
H	2.044994000	2.996645000	-2.485417000
H	2.135874000	1.325287000	-3.104885000
H	0.912364000	1.750503000	-1.888988000
N	-2.866919000	0.693827000	0.020310000
C	-3.115942000	1.950436000	-0.443459000
C	-3.638182000	0.162195000	0.999595000
C	-4.142145000	2.718080000	0.105879000
C	-4.675236000	0.884691000	1.578635000
H	-3.399997000	-0.842091000	1.308538000
C	-4.928299000	2.187084000	1.131096000

H	-4.318108000	3.716474000	-0.272554000
H	-5.267345000	0.430731000	2.362403000
H	-5.726839000	2.774350000	1.568209000
C	-2.202263000	2.436265000	-1.553691000
C	-2.986417000	3.082847000	-2.700075000
H	-3.487498000	3.995308000	-2.360679000
H	-2.285357000	3.347107000	-3.497859000
H	-3.736205000	2.388506000	-3.092915000
C	-1.140729000	3.397589000	-0.980229000
H	-0.489552000	3.731738000	-1.793248000
H	-1.628789000	4.269071000	-0.529867000
H	-0.541509000	2.886617000	-0.222361000
H	4.152620000	-0.721458000	1.212825000
H	3.261855000	-1.867358000	1.791982000
H	-3.103980000	-0.623368000	-2.897779000
H	-2.444208000	-2.016229000	-2.633480000
C	-0.480910000	-0.847139000	3.034671000
C	-1.474828000	-2.455966000	1.261180000
C	1.327239000	-3.059150000	-0.384341000
C	0.981664000	-1.757765000	-2.513343000
C	-1.391949000	-1.803701000	2.526967000
C	1.306654000	-2.925241000	-1.781514000
C	-0.694395000	-0.345939000	4.453853000
H	-1.652293000	0.182398000	4.535575000
H	-0.719663000	-1.172515000	5.173413000
H	0.115560000	0.334784000	4.721293000
C	-2.398062000	-2.342114000	3.560931000
H	-3.166389000	-2.962473000	3.097297000
H	-1.915226000	-2.932454000	4.350952000
H	-2.919369000	-1.508916000	4.044222000
C	-1.911398000	-3.906734000	1.203780000
H	-2.987997000	-3.970000000	0.992378000
H	-1.385772000	-4.388357000	0.374602000
H	-1.706375000	-4.440718000	2.133025000
C	1.527442000	-4.432135000	0.223457000
H	0.802485000	-5.153266000	-0.168877000
H	2.526378000	-4.815921000	-0.023384000
H	1.430694000	-4.368782000	1.309211000
C	1.739808000	-4.158206000	-2.577682000
H	2.787652000	-4.426754000	-2.386490000
H	1.127806000	-5.025975000	-2.304369000
H	1.620270000	-4.013989000	-3.651794000
C	1.511649000	-1.579571000	-3.922613000
H	0.843806000	-2.072584000	-4.642845000
H	1.529294000	-0.513134000	-4.158626000
H	2.511383000	-2.004506000	-4.041933000

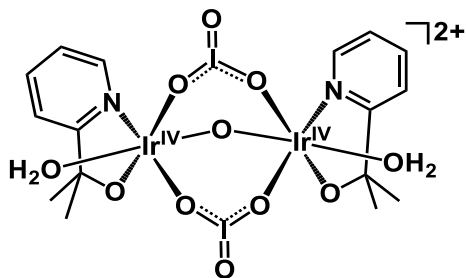


2IO<sub>3</sub><sup>-</sup>\_S5bb:

E = -1792.22053898 hartree

Ir	-1.676535000	0.322106000	-0.218969000
Ir	1.676448000	-0.322037000	-0.218915000
O	-0.000032000	0.000143000	0.619267000
O	-2.633436000	-1.359992000	0.701773000
O	-3.707379000	0.317694000	-0.887101000
O	-1.198402000	-0.873815000	-1.927005000
O	2.633509000	1.360005000	0.701756000
O	3.707276000	-0.317836000	-0.887085000
O	1.198328000	0.873855000	-1.926959000
H	-1.935258000	-1.488898000	-2.165366000
H	0.373711000	1.421465000	-1.810689000
O	1.172141000	-1.903718000	-1.164692000
N	2.113341000	-1.601510000	1.255512000
C	2.621854000	-1.249837000	2.462667000
C	1.846352000	-2.900329000	0.954104000
C	2.898541000	-2.215456000	3.423036000
H	2.792856000	-0.193983000	2.620396000
C	2.111219000	-3.903900000	1.884285000
C	2.643895000	-3.562063000	3.129528000
H	3.304144000	-1.914213000	4.379765000
H	1.896277000	-4.934247000	1.632252000
H	2.853195000	-4.332021000	3.861921000
C	1.219897000	-3.166246000	-0.400335000
C	2.057763000	-4.139079000	-1.235874000
H	2.110124000	-5.113574000	-0.740030000
H	1.586048000	-4.266409000	-2.214810000
H	3.071040000	-3.747455000	-1.367490000
C	-0.234361000	-3.631925000	-0.229220000
H	-0.681197000	-3.796167000	-1.214863000
H	-0.261155000	-4.576640000	0.323227000
H	-0.815581000	-2.885825000	0.319455000
O	-1.172337000	1.903776000	-1.164823000
N	-2.113449000	1.601613000	1.255425000
C	-2.622032000	1.249977000	2.462559000
C	-1.846340000	2.900409000	0.954030000
C	-2.898660000	2.215615000	3.422928000
H	-2.793121000	0.194137000	2.620283000
C	-2.111120000	3.903994000	1.884217000

C	-2.643867000	3.562199000	3.129443000
H	-3.304320000	1.914401000	4.379643000
H	-1.896041000	4.934318000	1.632206000
H	-2.853101000	4.332170000	3.861841000
C	-1.219792000	3.166263000	-0.400378000
C	-2.057340000	4.139397000	-1.235871000
H	-2.109398000	5.113879000	-0.739972000
H	-1.585568000	4.266636000	-2.214791000
H	-3.070740000	3.748105000	-1.367525000
C	0.234595000	3.631497000	-0.229156000
H	0.681440000	3.796015000	-1.214750000
H	0.261667000	4.575982000	0.323675000
H	0.815611000	2.884997000	0.319194000
H	-0.373803000	-1.421440000	-1.810635000
H	1.935192000	1.488907000	-2.165358000
I	-4.144477000	-1.373631000	-0.338922000
I	4.144543000	1.373463000	-0.338959000
O	-3.629600000	-2.319602000	-1.722237000
O	3.629729000	2.319439000	-1.722294000

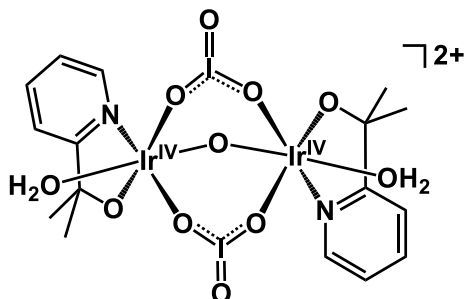


2IO<sub>3</sub><sup>-</sup>\_S10aa:

E = -1792.24172848 hartree

Ir	-1.770749000	-0.391505000	-0.182692000
Ir	1.681219000	-0.187517000	0.253172000
O	-0.057867000	0.451748000	-0.183693000
O	-2.075743000	-0.339233000	-2.057594000
O	-3.742511000	-1.190807000	0.070828000
O	-1.298538000	-2.424238000	-0.231191000
O	2.480485000	-0.205768000	-1.467532000
O	3.602625000	-0.715861000	1.063280000
O	1.436542000	-2.260825000	0.232041000
O	-1.700603000	-0.646985000	1.911203000
O	1.122581000	-0.361054000	2.281911000
N	-2.488949000	1.498731000	-0.265804000
C	-2.627613000	1.963726000	-1.537456000
C	-2.813110000	2.272111000	0.798581000
C	-3.100621000	3.253754000	-1.767646000
C	-3.288718000	3.566780000	0.619691000
H	-2.662678000	1.835735000	1.773485000
C	-3.433413000	4.066606000	-0.680438000
H	-3.206473000	3.609793000	-2.783910000
H	-3.536830000	4.166672000	1.485391000
H	-3.800536000	5.072512000	-0.844298000
C	-2.206876000	1.004643000	-2.634279000
C	-0.807329000	1.375857000	-3.159676000
H	-0.526335000	0.671545000	-3.948430000
H	-0.810493000	2.392720000	-3.566808000
H	-0.082520000	1.315878000	-2.343582000
C	-3.244574000	0.905415000	-3.753537000
H	-3.336163000	1.862806000	-4.276906000
H	-2.917788000	0.146357000	-4.470751000
H	-4.221004000	0.624175000	-3.346273000
N	2.194854000	1.768161000	0.207481000
C	2.923142000	2.110055000	-0.889851000
C	1.805233000	2.705085000	1.106078000
C	3.315475000	3.432170000	-1.090164000
C	2.170729000	4.037712000	0.947632000
H	1.193035000	2.362036000	1.927672000
C	2.941256000	4.407370000	-0.162162000

H	3.899256000	3.686991000	-1.964989000
H	1.852086000	4.767302000	1.680540000
H	3.238661000	5.439140000	-0.305581000
C	3.270088000	0.977823000	-1.834789000
C	2.901396000	1.305311000	-3.287508000
H	3.508245000	2.141124000	-3.650584000
H	3.106512000	0.428191000	-3.908619000
H	1.844497000	1.567792000	-3.369876000
C	4.756408000	0.597421000	-1.707344000
H	4.960383000	-0.253621000	-2.364818000
H	5.381477000	1.442798000	-2.014478000
H	4.993195000	0.325586000	-0.676176000
H	-3.750542000	-2.156439000	-0.089915000
H	-4.437889000	-0.804412000	-0.496497000
H	3.745612000	-0.367752000	1.966235000
H	3.697645000	-1.688744000	1.121460000
I	-0.466084000	-0.087671000	3.120958000
O	-0.633528000	1.651915000	3.088400000
I	0.248996000	-3.218896000	-0.760372000
O	0.486306000	-2.648230000	-2.390757000

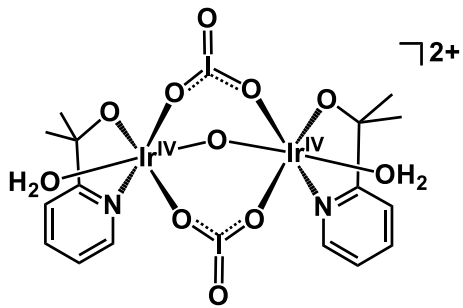


2IO<sub>3</sub><sup>-</sup>\_S10ab:

E = -1792.24375040 hartree

Ir	1.703993000	-0.150338000	-0.124818000
Ir	-1.703956000	-0.150602000	0.124816000
O	-0.000046000	0.682268000	-0.000007000
O	2.388978000	0.627483000	1.475487000
O	3.609803000	-1.066835000	-0.453038000
O	1.240836000	-1.985123000	0.772322000
O	-2.389079000	0.627089000	-1.475495000
O	-3.609619000	-1.067397000	0.453051000
O	-1.142065000	-1.015686000	1.926715000
O	1.142239000	-1.015530000	-1.926706000
O	-1.240512000	-1.985326000	-0.772303000
N	2.310030000	1.585944000	-0.943745000
C	2.692206000	2.513330000	-0.024963000
C	2.305269000	1.865998000	-2.269745000
C	3.093220000	3.782148000	-0.439302000
C	2.697292000	3.117670000	-2.730236000
H	1.976020000	1.069342000	-2.922966000
C	3.096283000	4.089689000	-1.802642000
H	3.393717000	4.513899000	0.299200000
H	2.684452000	3.323951000	-3.792283000
H	3.402742000	5.073241000	-2.137753000
C	2.601299000	2.078354000	1.426567000
C	1.365433000	2.715046000	2.093795000
H	1.311553000	2.374603000	3.132505000
H	1.448870000	3.807261000	2.077264000
H	0.459403000	2.412020000	1.563449000
C	3.890079000	2.367675000	2.199831000
H	4.071648000	3.446264000	2.250763000
H	3.783251000	1.983142000	3.218783000
H	4.744965000	1.882996000	1.717578000
N	-2.310263000	1.585593000	0.943729000
C	-2.692632000	2.512898000	0.024944000
C	-2.305515000	1.865668000	2.269724000
C	-3.093862000	3.781649000	0.439277000
C	-2.697746000	3.117277000	2.730208000
H	-1.976108000	1.069079000	2.922948000

C	-3.096937000	4.089211000	1.802613000
H	-3.394514000	4.513335000	-0.299227000
H	-2.684912000	3.323575000	3.792253000
H	-3.403561000	5.072714000	2.137717000
C	-2.601689000	2.077918000	-1.426583000
C	-3.890556000	2.366966000	-2.199804000
H	-4.072355000	3.445517000	-2.250731000
H	-3.783681000	1.982454000	-3.218759000
H	-4.745322000	1.882105000	-1.717521000
C	-1.365980000	2.714856000	-2.093868000
H	-1.312063000	2.374401000	-3.132571000
H	-1.449646000	3.807054000	-2.077359000
H	-0.459868000	2.412035000	-1.563546000
H	3.716936000	-1.876755000	0.085588000
H	4.388983000	-0.505350000	-0.274585000
H	-4.388886000	-0.506043000	0.274568000
H	-3.716615000	-1.877351000	-0.085551000
I	-0.109625000	-2.332073000	-2.165986000
O	-0.924922000	-1.723851000	-3.579006000
I	0.110006000	-2.332030000	2.166010000
O	0.925210000	-1.723659000	3.579020000

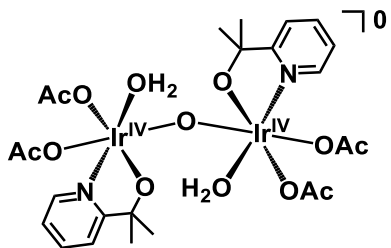


2IO<sub>3</sub><sup>-</sup>\_S10bb:

E = -1792.24172840 hartree

Ir	1.681176000	-0.187664000	0.253185000
Ir	-1.770814000	-0.391385000	-0.182782000
O	-0.057831000	0.451698000	-0.183806000
O	2.480715000	-0.205982000	-1.467405000
O	3.602512000	-0.716065000	1.063520000
O	1.122452000	-0.361199000	2.281895000
O	-2.075714000	-0.339001000	-2.057692000
O	-3.742685000	-1.190337000	0.070785000
O	-1.700743000	-0.646828000	1.911122000
O	1.436171000	-2.260958000	0.232182000
O	-1.298848000	-2.424170000	-0.231361000
N	2.194995000	1.767963000	0.207526000
C	2.923464000	2.109807000	-0.889696000
C	1.805325000	2.704913000	1.106078000
C	3.315957000	3.431887000	-1.089932000
C	2.170959000	4.037509000	0.947697000
H	1.192982000	2.361912000	1.927585000
C	2.941697000	4.407108000	-0.161973000
H	3.899890000	3.686656000	-1.964672000
H	1.852261000	4.767121000	1.680559000
H	3.239215000	5.438853000	-0.305335000
C	3.270387000	0.977561000	-1.834616000
C	4.756690000	0.597092000	-1.707128000
H	4.960650000	-0.253950000	-2.364605000
H	5.381809000	1.442446000	-2.014225000
H	4.993420000	0.325238000	-0.675952000
C	2.901760000	1.305089000	-3.287348000
H	3.508625000	2.140911000	-3.650377000
H	3.106894000	0.427981000	-3.908469000
H	1.844864000	1.567577000	-3.369748000
N	-2.488784000	1.498935000	-0.265820000
C	-2.627304000	1.964021000	-1.537454000
C	-2.812876000	2.272305000	0.798593000
C	-3.100077000	3.254142000	-1.767599000
C	-3.288256000	3.567064000	0.619747000
H	-2.662568000	1.835847000	1.773479000

C	-3.432786000	4.066990000	-0.680362000
H	-3.205810000	3.610259000	-2.783848000
H	-3.536319000	4.166950000	1.485466000
H	-3.799722000	5.072971000	-0.844183000
C	-2.206712000	1.004918000	-2.634318000
C	-3.244472000	0.905844000	-3.753538000
H	-3.335984000	1.863266000	-4.276863000
H	-2.917792000	0.146781000	-4.470795000
H	-4.220912000	0.624681000	-3.346244000
C	-0.807149000	1.375988000	-3.159774000
H	-0.526267000	0.671653000	-3.948546000
H	-0.810237000	2.392853000	-3.566900000
H	-0.082310000	1.315932000	-2.343713000
H	3.697686000	-1.688960000	1.121217000
H	3.745001000	-0.368457000	1.966747000
H	-4.438029000	-0.803763000	-0.496461000
H	-3.750991000	-2.155966000	-0.089958000
I	0.248699000	-3.218884000	-0.760451000
O	0.486213000	-2.648072000	-2.390756000
I	-0.466196000	-0.087744000	3.120949000
O	-0.633490000	1.651858000	3.088541000

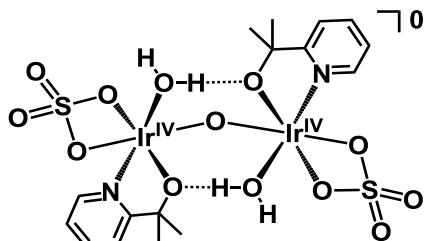


4AcO<sup>-</sup>\_NN\_S1:

*E* = -2232.61015199 hartree

Ir	-1.773843000	-0.394025000	0.208307000
Ir	1.773818000	-0.394039000	-0.208316000
O	0.000005000	0.279827000	0.000086000
O	-2.264109000	-0.099575000	-1.637795000
O	-1.301360000	-2.377694000	-0.243196000
O	2.264151000	-0.099775000	1.637802000
O	1.301326000	-2.377756000	0.242982000
N	-2.304753000	1.543566000	0.421518000
C	-2.534230000	2.161321000	-0.766499000
C	-2.412778000	2.216570000	1.590639000
C	-2.873595000	3.514965000	-0.798813000
C	-2.751403000	3.565552000	1.612605000
H	-2.212325000	1.638104000	2.482194000
C	-2.982004000	4.226608000	0.398639000
H	-3.048003000	3.997401000	-1.752009000
H	-2.828251000	4.083851000	2.559817000
H	-3.242621000	5.278425000	0.386665000
C	-2.362318000	1.302044000	-2.011465000
C	-1.040483000	1.669637000	-2.716368000
H	-0.958137000	1.079770000	-3.634997000
H	-1.019070000	2.735444000	-2.971680000
H	-0.201808000	1.430179000	-2.059802000
C	-3.566401000	1.436813000	-2.951551000
H	-3.661226000	2.462412000	-3.324546000
H	-3.419980000	0.766796000	-3.804878000
H	-4.487798000	1.158364000	-2.429151000
N	2.304757000	1.543569000	-0.421366000
C	2.534315000	2.161197000	0.766697000
C	2.412727000	2.216696000	-1.590421000
C	2.873714000	3.514830000	0.799139000
C	2.751379000	3.565673000	-1.612265000
H	2.212221000	1.638327000	-2.482026000
C	2.982070000	4.226596000	-0.398243000
H	3.048192000	3.997159000	1.752377000
H	2.828180000	4.084071000	-2.559426000
H	3.242721000	5.278404000	-0.386172000
C	2.362435000	1.301809000	2.011583000
C	3.566564000	1.436469000	2.951627000

H	3.661452000	2.462043000	3.324679000
H	3.420151000	0.766407000	3.804921000
H	4.487925000	1.158009000	2.429170000
C	1.040621000	1.669378000	2.716527000
H	0.958316000	1.079507000	3.635153000
H	1.019185000	2.735182000	2.971847000
H	0.201931000	1.429891000	2.059982000
H	0.695181000	-2.373416000	1.051620000
H	2.207871000	-2.731163000	0.504921000
H	-2.207924000	-2.731010000	-0.505192000
H	-0.695223000	-2.373214000	-1.051807000
O	3.751128000	-0.876240000	-0.595036000
C	4.374052000	-1.932245000	-0.125628000
O	3.837998000	-2.866152000	0.512715000
O	1.529313000	-0.596979000	-2.242025000
C	0.804829000	-1.437872000	-2.938924000
O	0.036870000	-2.310410000	-2.488229000
C	5.863184000	-1.935650000	-0.404894000
H	6.301565000	-2.894767000	-0.121687000
H	6.048058000	-1.737494000	-1.466100000
H	6.342412000	-1.132889000	0.169272000
C	0.962158000	-1.247955000	-4.436502000
H	0.431989000	-2.033369000	-4.978874000
H	0.552773000	-0.270465000	-4.720125000
H	2.022918000	-1.252811000	-4.709431000
O	-1.529355000	-0.597225000	2.242010000
C	-0.804901000	-1.438231000	2.938771000
O	-0.037005000	-2.310755000	2.487906000
O	-3.751158000	-0.876254000	0.594942000
C	-4.374005000	-1.932326000	0.125572000
O	-3.837963000	-2.866045000	-0.513058000
C	-0.962258000	-1.248596000	4.436388000
H	-0.431295000	-2.033551000	4.978644000
H	-0.553885000	-0.270715000	4.720091000
H	-2.023004000	-1.254569000	4.709385000
C	-5.863199000	-1.935626000	0.404508000
H	-6.301620000	-2.894630000	0.120980000
H	-6.048261000	-1.737713000	1.465725000
H	-6.342235000	-1.132675000	-0.169554000

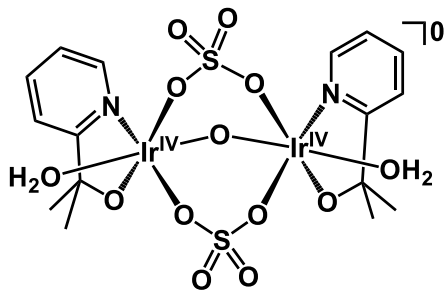


$2\text{SO}_4^{2-}$  S5bb:

$E = -2716.78617782$  hartree

Ir	-1.698385000	-0.206129000	-0.295695000
Ir	1.698188000	0.205984000	-0.295740000
O	-0.000054000	-0.000183000	0.560998000
O	-2.150429000	-2.049749000	0.582790000
O	-3.552938000	-0.924155000	-0.959354000
O	-0.875225000	-1.240222000	-1.975605000
O	2.150354000	2.049796000	0.582761000
O	3.552703000	0.924263000	-0.959386000
O	0.874510000	1.238900000	-1.975846000
H	-1.387057000	-2.082474000	-2.094237000
H	-0.086865000	1.481865000	-1.845308000
O	1.686271000	-1.474425000	-1.252077000
N	2.549570000	-0.882372000	1.148989000
C	3.014533000	-0.380459000	2.319579000
C	2.659728000	-2.206054000	0.857299000
C	3.618302000	-1.209372000	3.258019000
H	2.888263000	0.684114000	2.460517000
C	3.258788000	-3.076115000	1.767501000
C	3.743876000	-2.576863000	2.978643000
H	3.981330000	-0.788553000	4.186510000
H	3.339413000	-4.127750000	1.524822000
H	4.211319000	-3.242615000	3.693979000
C	2.063888000	-2.657865000	-0.463655000
C	3.075384000	-3.438301000	-1.308285000
H	3.374908000	-4.358304000	-0.795929000
H	2.609237000	-3.704185000	-2.262053000
H	3.963038000	-2.826195000	-1.496420000
C	0.776858000	-3.458806000	-0.203689000
H	0.343903000	-3.771182000	-1.159666000
H	1.004710000	-4.355784000	0.381797000
H	0.050340000	-2.852633000	0.342791000
O	-1.686102000	1.474470000	-1.252006000
N	-2.548957000	0.882601000	1.149139000
C	-3.013250000	0.380760000	2.320053000
C	-2.658778000	2.206328000	0.857634000
C	-3.615989000	1.209838000	3.258992000
H	-2.887283000	-0.683871000	2.460824000
C	-3.256806000	3.076562000	1.768368000

C	-3.741201000	2.577413000	2.979817000
H	-3.978494000	0.789106000	4.187725000
H	-3.337162000	4.128252000	1.525830000
H	-4.207832000	3.243295000	3.695564000
C	-2.063893000	2.657939000	-0.463805000
C	-3.076325000	3.437563000	-1.308098000
H	-3.376144000	4.357486000	-0.795773000
H	-2.610881000	3.703514000	-2.262192000
H	-3.963707000	2.824861000	-1.495596000
C	-0.777109000	3.459671000	-0.204996000
H	-0.344869000	3.771681000	-1.161420000
H	-1.005087000	4.356870000	0.380094000
H	-0.049958000	2.854180000	0.341417000
H	0.086665000	-1.481456000	-1.846220000
H	1.387566000	2.080265000	-2.096187000
O	-2.778963000	-3.224960000	-1.529090000
O	2.777068000	3.224171000	-1.530169000
S	-3.327894000	-2.397991000	-0.423525000
S	3.327035000	2.398137000	-0.424249000
O	-4.501281000	-2.921283000	0.271008000
O	4.500489000	2.922539000	0.269333000

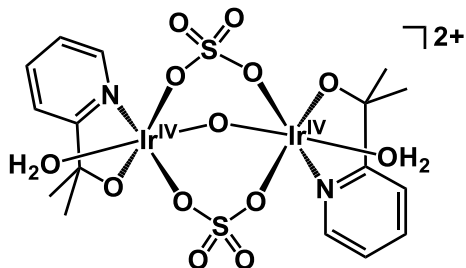


2SO<sub>4</sub><sup>2-</sup>\_S10aa:

E = -2716.77517243 hartree

Ir	-1.748616000	-0.555581000	-0.026103000
Ir	1.643412000	-0.476079000	0.199824000
O	-0.055642000	0.319565000	-0.081810000
O	-2.285043000	-0.187821000	-1.828391000
O	-3.674097000	-1.477768000	0.278339000
O	-1.234827000	-2.504879000	-0.462022000
O	2.430426000	-0.233146000	-1.522547000
O	3.543154000	-1.282962000	0.862635000
O	1.233560000	-2.458652000	-0.186610000
O	-1.391279000	-1.143788000	1.932380000
O	1.107287000	-0.943913000	2.161579000
N	-2.530892000	1.298154000	0.288387000
C	-2.821768000	1.964437000	-0.861994000
C	-2.792775000	1.853563000	1.495424000
C	-3.375010000	3.242889000	-0.818859000
C	-3.351272000	3.124792000	1.592334000
H	-2.513431000	1.265620000	2.356333000
C	-3.642595000	3.832656000	0.419936000
H	-3.593912000	3.761422000	-1.743262000
H	-3.547846000	3.547951000	2.568933000
H	-4.073155000	4.825782000	0.469613000
C	-2.479183000	1.226284000	-2.143619000
C	-1.143478000	1.747196000	-2.712291000
H	-0.909749000	1.195879000	-3.628538000
H	-1.221350000	2.815228000	-2.944364000
H	-0.345982000	1.591918000	-1.980625000
C	-3.608995000	1.301183000	-3.173747000
H	-3.767232000	2.333892000	-3.501553000
H	-3.332212000	0.697948000	-4.043973000
H	-4.540475000	0.914575000	-2.747253000
N	2.305998000	1.419213000	0.504403000
C	3.021826000	1.915860000	-0.538650000
C	2.047514000	2.180226000	1.595692000
C	3.528362000	3.214307000	-0.494143000
C	2.530873000	3.482230000	1.687259000
H	1.433493000	1.720801000	2.359094000

C	3.285448000	4.007120000	0.630477000
H	4.099319000	3.592601000	-1.332365000
H	2.314161000	4.070313000	2.569827000
H	3.672572000	5.018022000	0.679487000
C	3.229795000	0.975543000	-1.711064000
C	2.748712000	1.607553000	-3.025753000
H	3.328908000	2.507783000	-3.254664000
H	2.885273000	0.884560000	-3.835944000
H	1.689455000	1.871549000	-2.952963000
C	4.702914000	0.537517000	-1.791010000
H	4.820282000	-0.160271000	-2.626370000
H	5.349764000	1.405776000	-1.958312000
H	4.993984000	0.041343000	-0.860440000
H	-3.601906000	-2.425279000	0.041741000
H	-4.379723000	-1.106298000	-0.286210000
H	3.598463000	-1.242232000	1.838615000
H	3.568509000	-2.234463000	0.632648000
O	-0.377066000	0.840892000	3.054854000
O	0.229347000	-2.227965000	-2.465880000
S	-0.251787000	-0.622907000	2.875485000
S	0.101780000	-2.923789000	-1.173706000
O	-0.299878000	-1.432248000	4.101018000
O	0.132260000	-4.393702000	-1.202780000

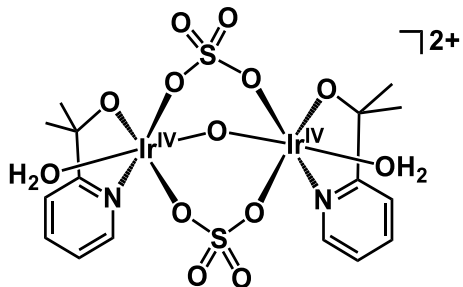


2SO<sub>4</sub><sup>2-</sup>\_S10ab:

E = -2716.77424859 hartree

Ir	1.673893000	-0.540742000	0.354827000
Ir	-1.673780000	-0.540878000	-0.354789000
O	0.000037000	0.289034000	-0.000039000
O	2.114412000	0.576417000	1.858786000
O	3.577904000	-1.489431000	0.713850000
O	0.900239000	-2.076299000	1.501722000
O	-2.114442000	0.576073000	-1.858866000
O	-3.577756000	-1.489691000	-0.713647000
O	-1.574820000	-1.909920000	1.179450000
O	1.574999000	-1.909977000	-1.179269000
O	-0.900063000	-2.076555000	-1.501476000
N	2.542159000	0.980023000	-0.670940000
C	2.768786000	2.088345000	0.085089000
C	2.858988000	0.960580000	-1.987953000
C	3.320324000	3.233011000	-0.488059000
C	3.416804000	2.076005000	-2.604958000
H	2.621218000	0.050327000	-2.517254000
C	3.647998000	3.230530000	-1.846820000
H	3.487921000	4.108857000	0.125319000
H	3.657088000	2.037652000	-3.659564000
H	4.075521000	4.113705000	-2.306555000
C	2.355252000	1.981340000	1.543005000
C	1.030889000	2.736620000	1.777627000
H	0.756367000	2.646911000	2.833439000
H	1.152196000	3.796666000	1.527586000
H	0.240435000	2.304820000	1.159793000
C	3.458911000	2.471111000	2.486305000
H	3.642241000	3.541429000	2.344495000
H	3.136400000	2.306473000	3.519187000
H	4.389622000	1.922854000	2.306710000
N	-2.542077000	0.979924000	0.670876000
C	-2.769039000	2.088085000	-0.085288000
C	-2.858668000	0.960622000	1.987947000
C	-3.320723000	3.232722000	0.487780000
C	-3.416601000	2.076029000	2.604879000
H	-2.620628000	0.050491000	2.517341000
C	-3.648166000	3.230385000	1.846598000

H	-3.488591000	4.108444000	-0.125702000
H	-3.656697000	2.037789000	3.659531000
H	-4.075788000	4.113545000	2.306269000
C	-2.355688000	1.980967000	-1.543252000
C	-3.459654000	2.470212000	-2.486462000
H	-3.643337000	3.540486000	-2.344785000
H	-3.137235000	2.305532000	-3.519366000
H	-4.390144000	1.921649000	-2.306647000
C	-1.031630000	2.736681000	-1.778215000
H	-0.757241000	2.646879000	-2.834054000
H	-1.153287000	3.796730000	-1.528354000
H	-0.240923000	2.305289000	-1.160428000
H	3.428721000	-2.360456000	1.134413000
H	4.108751000	-0.970401000	1.349948000
H	-4.108652000	-0.970738000	-1.349768000
H	-3.428548000	-2.360746000	-1.134139000
O	0.493552000	-0.737322000	-3.094537000
O	-0.493517000	-0.736901000	3.094551000
S	0.455834000	-1.970242000	-2.285865000
S	-0.455677000	-1.969948000	2.286076000
O	0.636621000	-3.239504000	-3.004929000
O	-0.636403000	-3.239114000	3.005325000



2SO<sub>4</sub><sup>2-</sup>\_S10bb:

E = -2716.77028053 hartree

Ir	1.556557000	-0.446953000	-0.418458000
Ir	-1.684574000	-0.318994000	0.279731000
O	-0.027200000	0.548186000	-0.089225000
O	2.162444000	0.543171000	-1.939824000
O	3.364129000	-1.652182000	-0.607414000
O	1.181599000	-1.789555000	1.112066000
O	-2.620911000	0.071428000	-1.345879000
O	-3.474843000	-1.264026000	1.021252000
O	-0.881163000	-0.736829000	2.132508000
O	0.621826000	-1.696372000	-1.761706000
O	-1.298755000	-2.270992000	-0.256748000
N	2.652687000	0.933334000	0.601388000
C	3.190733000	1.890430000	-0.204605000
C	2.929600000	0.918106000	1.928838000
C	4.036588000	2.866938000	0.317612000
C	3.765901000	1.874905000	2.498135000
H	2.456820000	0.138079000	2.512303000
C	4.331940000	2.861962000	1.683558000
H	4.450643000	3.619642000	-0.340467000
H	3.964989000	1.839931000	3.561545000
H	4.987718000	3.615385000	2.103549000
C	2.742542000	1.853296000	-1.653072000
C	3.897316000	2.052004000	-2.637252000
H	3.509791000	1.965383000	-3.657195000
H	4.342292000	3.045300000	-2.517996000
H	4.668675000	1.291763000	-2.477909000
C	1.624260000	2.895728000	-1.851092000
H	2.016682000	3.905080000	-1.685474000
H	1.240995000	2.821508000	-2.873520000
H	0.813448000	2.703005000	-1.143067000
N	-2.310830000	1.534464000	0.800207000
C	-2.900632000	2.212440000	-0.219410000
C	-2.154258000	2.100589000	2.020244000
C	-3.365987000	3.512073000	-0.021384000
C	-2.602139000	3.393905000	2.268611000
H	-1.664361000	1.486279000	2.764041000

C	-3.217532000	4.110210000	1.233003000
H	-3.833470000	4.042313000	-0.841031000
H	-2.468510000	3.827983000	3.250924000
H	-3.573683000	5.119686000	1.400562000
C	-2.963205000	1.478791000	-1.549107000
C	-4.364385000	1.527140000	-2.165128000
H	-4.640070000	2.557326000	-2.414628000
H	-4.364979000	0.933212000	-3.084377000
H	-5.105720000	1.118756000	-1.470676000
C	-1.888852000	2.031642000	-2.504907000
H	-1.981374000	1.525475000	-3.471153000
H	-2.013153000	3.110453000	-2.649870000
H	-0.899067000	1.833355000	-2.087416000
H	3.266233000	-2.247528000	-1.377599000
H	3.429554000	-2.240213000	0.172606000
H	-4.311035000	-0.866669000	0.710683000
H	-3.470375000	-2.190206000	0.701846000
O	-1.311778000	-2.866769000	-2.686776000
O	1.111721000	-1.082352000	3.504492000
S	-0.465930000	-2.793718000	-1.480652000
S	0.321275000	-1.712953000	2.426081000
O	0.162106000	-4.062090000	-1.070126000
O	-0.165988000	-3.069889000	2.711631000

## 5. References

- (1) Hintermair, U.; Hashmi, S. M.; Elimelech, M.; Crabtree, R. H. *J. Am. Chem. Soc.* **2012**, *134*, 9785.
- (2) Chupas, P. J.; Chapman, K. W.; Lee, P. L. *J. Appl. Cryst.* **2007**, *40*, 463.
- (3) Du, P.; Kokhan, O.; Chapman, K. W.; Chupas, P. J.; Tiede, D. M. *J. Am. Chem. Soc.* **2012**, *134*, 11096.
- (4) Blakemore, J. D.; Mara, M. W.; Kushner-Lenhoff, M. N.; Schley, N. D.; Konezny, S. J.; Rivalta, I.; Negre, C. F. A.; Snoeberger, R. C.; Kokhan, O.; Huang, J.; Stickrath, A.; Tran, L. A.; Parr, M. L.; Chen, L. X.; Tiede, D. M.; Batista, V. S.; Crabtree, R. H.; Brudvig, G. W. *Inorg. Chem.* **2013**, *52*, 1860.
- (5) Qiu, X.; Thompson, J. W.; Billinge, S. J. L. *J. Appl. Cryst.* **2004**, *37*, 678.
- (6) Chupas, P. J.; Chapman, K. W.; Chen, H.; Grey, C. P. *Catal. Today* **2009**, *145*, 213.
- (7) Juhás, P.; Cherba, D. M.; Duxbury, P. M.; Punch, W. F.; Billinge, S. J. L. *Nature* **2006**, *440*, 655.
- (8) Billinge, S. J. L.; Kanatzidis, M. G. *Chem. Commun.* **2004**, 749.
- (9) Chung, J. S.; Thorpe, M. F. *Phys. Rev. B* **1997**, *55*, 1545.
- (10) Chung, J. S.; Thorpe, M. F. *Phys. Rev. B* **1999**, *59*, 4807.
- (11) Ravel, B.; Newville, M. *J. Synchrotron Radiat.* **2005**, *12*, 537.
- (12) Stephens, P. J.; Devlin, F. J.; Chabalowski, C. F.; Frisch, M. J. *J. Phys. Chem.* **1994**, *98*, 11623.
- (13) Hehre, W. J.; Ditchfield, R.; Pople, J. A. *J. Chem. Phys.* **1972**, *56*, 2257.
- (14) Hariharan, P. C.; Pople, J. A. *Theor. Chim. Acta* **1973**, *28*, 213.
- (15) Andrae, D.; Häußermann, U.; Dolg, M.; Stoll, H.; Preuß, H. *Theor. Chim. Acta* **1990**, *77*, 123.
- (16) Martin, J. M. L.; Sundermann, A. *J. Chem. Phys.* **2001**, *114*, 3408.
- (17) Wadt, W. R.; Hay, P. J. *J. Chem. Phys.* **1985**, *82*, 284.
- (18) Glukhovtsev, M. N.; Pross, b. A.; Radom, L. *J. Am. Chem. Soc.* **1995**, *117*, 2024.
- (19) Tomasi, J.; Mennucci, B.; Cammi, R. *Chem. Rev.* **2005**, *105*, 2999.
- (20) Grimme, S. *J. Comput. Chem.* **2006**, *27*, 1787.
- (21) Noodleman, L. *J. Chem. Phys.* **1981**, *74*, 5737.
- (22) Chai, J.-D.; Head-Gordon, M. *Phys. Chem. Chem. Phys.* **2008**, *10*, 6615.
- (23) Stratmann, R. E.; Scuseria, G. E.; Frisch, M. J. *J. Chem. Phys.* **1998**, *109*, 8218.
- (24) Clark, T.; Chandrasekhar, J.; Spitznagel, G. W.; Schleyer, P. V. R. *J. Comput. Chem.* **1983**, *4*, 294.
- (25) Warren, B. E. *X-Ray Diffraction*; Dover Publications, Inc: New York, 1990.
- (26) Brown, P. J.; Fox, A. G.; Maslen, E. N.; O'Keeffe, M. A.; Willis, B. T. M.; 2006 ed.; Prince, E., Ed.; John Wiley & Sons Ltd: 2006; Vol. C, p 554.
- (27) Zhang, R.; Thiagarajan, P.; Tiede, D. M. *J. Appl. Cryst.* **2000**, *33*, 565.
- (28) Zuo, X.; Cui, G.; Merz, K. M.; Zhang, L.; Lewis, F. D.; Tiede, D. M. *Proc. Natl. Acad. Sci. U. S. A.* **2006**, *103*, 3534.
- (29) Rehr, J. J.; Albers, R. C. *Rev. Mod. Phys.* **2000**, *72*, 621–654.

- (30) Newville, M. *J. Synchrotron Radiat.* **2001**, *8*, 322–324.
- (31) Hintermair, U.; Sheehan, S. W.; Parent, A. R.; Ess, D. H.; Richens, D. T.; Vaccaro, P. H.; Brudvig, G. W.; Crabtree, R. H. *J. Am. Chem. Soc.* **2013**, *135*, 10837.
- (32) Thomsen, J. M.; Sheehan, S. W.; Hashmi, S. M.; Campos, J.; Hintermair, U.; Crabtree, R. H.; Brudvig, G. W. *J. Am. Chem. Soc.* **2014**, *136*, 13826.
- (33) Li, Y.; Liu, Y.; Zhou, M. *Dalton Trans.* **2012**, *41*, 3807.
- (34) Lou, X.; van Buijtenen, J.; Bastiaansen, J. J. A. M.; de Waal, B. F. M.; Langeveld, B. M. W.; van Dongen, J. L. *J. Mass Spectrom.* **2005**, *40*, 654.
- (35) Castillo-Blum, S. E.; Richens, D. T.; Sykes, A. G. *Inorg. Chem.* **1989**, *28*, 954.
- (36) Zuccaccia, C.; Bellachioma, G.; Bortolini, O.; Bucci, A.; Savini, A.; Macchioni, A. *Chem. Eur. J.* **2014**, *20*, 3446.
- (37) Bunton, C. A.; Shiner, V. J. *J. Chem. Soc. (Resumed)* **1960**, 1593.
- (38) Zhou, M.; Schley, N. D.; Crabtree, R. H. *J. Am. Chem. Soc.* **2010**, *132*, 12550.
- (39) Zhou, M.; Hintermair, U.; Hashiguchi, B. G.; Parent, A. R.; Hashmi, S. M.; Elimelech, M.; Periana, R. A.; Brudvig, G. W.; Crabtree, R. H. *Organometallics* **2013**, *32*, 957.
- (40) Zhou, M.; Balcells, D.; Parent, A. R.; Crabtree, R. H.; Eisenstein, O. *ACS Catal.* **2012**, *2*, 208.
- (41) Savini, A.; Belanzoni, P.; Bellachioma, G.; Zuccaccia, C.; Zuccaccia, D.; Macchioni, A. *Green Chem.* **2011**, *13*, 3360.
- (42) Shopov, D. Y.; Rudshteyn, B.; Campos, J.; Batista, V. S.; Crabtree, R. H.; Brudvig, G. W. *J. Am. Chem. Soc.* **2015**, *137*, 7243.